University of Bath

PHD

Optimal inter-seasonal operation of novel community borehole array heat storage system

Wei, Wei

Award date:
2019

Awarding institution:
University of Bath

Link to publication

Alternative formats
If you require this document in an alternative format, please contact:
openaccess@bath.ac.uk

Copyright of this thesis rests with the author. Access is subject to the above licence, if given. If no licence is specified above, original content in this thesis is licensed under the terms of the Creative Commons Attribution-NonCommercial 4.0 International (CC BY-NC-ND 4.0) Licence (https://creativecommons.org/licenses/by-nc-nd/4.0/). Any third-party copyright material present remains the property of its respective owner(s) and is licensed under its existing terms.

Take down policy
If you consider content within Bath's Research Portal to be in breach of UK law, please contact: openaccess@bath.ac.uk with the details. Your claim will be investigated and, where appropriate, the item will be removed from public view as soon as possible.

Download date: 05. May. 2023

University of Bath

PHD

Optimal inter-seasonal operation of novel community borehole array heat storage system

Wei, Wei

Award date:
2019

Awarding institution:
University of Bath

Link to publication

General rights
Copyright and moral rights for the publications made accessible in the public portal are retained by the authors and/or other copyright owners and it is a condition of accessing publications that users recognise and abide by the legal requirements associated with these rights.

- Users may download and print one copy of any publication from the public portal for the purpose of private study or research.
- You may not further distribute the material or use it for any profit-making activity or commercial gain
- You may freely distribute the URL identifying the publication in the public portal ?

Take down policy
If you believe that this document breaches copyright please contact us providing details, and we will remove access to the work immediately and investigate your claim.

Download date: 13. Jun. 2019

Optimal Operation of Novel Community Inter-seasonal Borehole Array Heat Storage System

By

Wei WEI

Thesis submitted for the degree of

Doctor of Philosophy

in

Department of Electronic and Electrical Engineering

University of Bath

2018

-COPYRIGHT-

Attention is drawn to the fact that copyright of this thesis rests with the author. A copy of this thesis has been supplied on condition that anyone who consults it is understood to recognise that its copyright rests with the author and that they must not copy it or use material from it except as permitted by law or with the consent of the author.

This thesis may be made available for consultation within the University Library and may be photocopied or lent to other libraries for the purposes of consultation.

Signature …… Date ……

Abstract

Methods of increasing energy efficiency and reducing greenhouse gas emission are widely developed across the whole world. Housing energy consumption as a large energy consumption among different energy sectors, such as industry, transportation, needs to be paid more attention. In the UK, gas is still the main fuel used for providing heating in homes and space heating is responsible for over 60% of domestic energy usage.

This work investigates the optimal operation of the low carbon space heating system based on a real-world project providing a community level space heating with low carbon technologies and thermal energy storage system. The proposed space heating system consists of borehole thermal storage and heat pumps. The heat pump has relatively high efficiency compared to boilers and with proper operation, electricity consumption and CO_2 emission can be largely reduced. Borehole thermal storage uses the natural heat source, by coupling with heat pumps the heat pump efficiency can be increased.

The existing research on the borehole mainly focused on the modelling, verification, and optimization on the sizing/material of the system and when it comes to coupling with heat pumps, most research showed the system operation results, temperature behaviour with constant heat injection/extraction and monetary and environmental benefits of the projects. With heat injection/extraction and natural heat replenishment under the ground, the heat energy storage becomes a very complicated problem when coupled with heat pumps especially when the temperature is a key aspect of the system. As a result, how temperature affecting the system efficiency and what is the influence of the operation of the borehole storage coupled with heat pumps have not been studied.

This thesis delivers the researching findings at each stage in each chapter. Starting from the high-level energy chain analysis, borehole temperature behaviour study and borehole charging strategy optimization. For single/multiple charging/discharging cycles, it enables the borehole to store less heat and still retains the performance of the Ground Source Heat Pump (GSHP) during the heating season and for limited available heat flux input- by obtaining the optimized charging strategy, the heat accumulation in the borehole is more efficient. The total GSHP electricity consumption is reduced along with the CO_2 emission reduction and in the long-term operation, borehole thermal energy storage benefit more in the future.

Acknowledgements

First of all, I would like to show my respectful appreciation to my supervisor, Dr. Chenghong Gu and Dr. Simon LeBlond, both of them have supported me with research suggestions, profound knowledge and encouragement throughout the past years of my PhD life. Dr. Simon LeBlond guided me from the start of my research building a good foundation and Dr. Chenghong Gu helped me to deliver the results.

I would like to take this opportunity to express my gratitude to my family and my fiancé Mr Tomasz Crabbs who have supported my decision from the start and encouraged me when I was facing failures and challenges.

I would like to thank Clean Energy Prospector, EUNOMIA, ICAX, Department for Business Energy and Industrial Strategy (Department of Environment and Climate Change) for the help, information and financial support during the CHOICES project.

I am grateful for my colleagues who have collaborated, helped and inspired with me in my projects, researches, and articles. Mrs. Heather Wyman-Pain, Mr. Da Huo, Mr. Xiaohe Yan, Dr. Chen Zhao, Dr. Zhipeng Zhang, Miss Gege Ma, Miss Qiuyang Ma, Miss Chi Zhang, Mr. Yuankai Bian, Mr. Hantao Wang, Dr. Ran Li, Mr. Minghao Xu, Dr. Zhong Zhang, Mr. Xinhe Yang, Miss Wangwei Kong, Mr. Han Wu, Ms. Lanqing Shan, Dr. Ignacio Hernando Gil, Dr. Kang Ma, Dr. Lin Zhou, Dr. Fan Yi, Dr. Shuangyuan Wang, Dr. Jie Yan, Mr. Jiangtao Li. I am sincerely grateful for the efforts and times they devoted to our group.

Besides, I would like to thanks Bath University Kickboxing Club which trained me physically and mentally strong in the past few years.

Last but not least, I would like to appreciate for the Graduate Office, Student Services, IT support in our department and University for providing help when I needed technical instructions and suggestions during my PhD career.

Contents

Abbreviation

ASHP --- Air Source Heat Pump

BTES --- Borehole thermal energy storage

CEPRO --- Clean Energy Prospector

CHP --- Combined Heat and Power

CoP --- Coefficient of Performance

GSHP --- Ground Source Heat Pump

PDE --- Partial Differential Equation

PV --- Photovoltaic

PVGIS --- Photovoltaic Geographical Information System

RHI --- Renewable Heat Incentive

SBRI --- Small Business Research Initiative

List of symbol

Chapter 2

a_b	thermal diffusivity
a_s	thermal diffusivity of soil
erfc(x)	complementary error function
H	borehole length
k_b	conductivity of the backfilling materiel
k_s	thermal conductivity of soil
r_a , r_b	radius coordinates of points A and B
r'	position of the line source
t	time
u	integral variable of the dimension of reciprocal of the length
z'	integral variable along coordinates z

Chapter 3

a, b	constants of heat pump model
$C_{borehole}$	volumetric heat capacity of the borehole (J/m^3/K)
H	heat pump heat output (kWh)
$H_{borehole}$	heat power injection/extraction from the borehole (kWh)
$P_{electricity}$	electricity needed from the heat pump (kWh)
T	evaporator inlet/air temperature (°C)
T_n	temperature in the nth time step (°C)
T_{n+1}	temperature in the (n+1)th time step (°C)
$V_{borehole}$	borehole array storage volume (m^3)

Chapter 4

a, c, f, and d	coefficients in PDE
d	depth of borehole
g	heat flux.
h	weight (equation 4-2)
h	convective heat transfer coefficient.
k	coefficient of heat conduction
q	heat transfer coefficient
Q	heat source
r	temperature (equation 4-2)
r	radius (m)
T_{ext}	external temperature (°C)
u	solution of temperature (°C)
V	borehole volume (m^3)

Chapter 6

CoP	heat pumps' CoP value
E_{HP}	heat pump electricity consumption (kWh)
$Heatflux_{fixed}$	total heat flux injection in the charging season(W/m^3)
H_{HP}	heat energy generated by heat pumps (kWh)
$N_{borehole}$	borehole number
$V_{borehole}$	single borehole volume (m^3)
$x_{(charge)}$, $x_{(discharge)}$	heat flux injection and extraction (W/m^3)

List of figures

List of tables

1 Introduction

1.1 General UK energy consumption

The massive utilization of fossil energy results in air pollution and global warming [1-3]. In order to reduce the damage caused by traditional energy supply, renewable energies and environmentally friendly technologies are being widely introduced worldwide.

1.1.1 Energy consumption and CO_2 emission

In the UK, the Climate Change Act in 2008 requires a specific reduction in greenhouse gas emissions [4]. Annual CO_2 emissions come from different aspects, such as generating electricity using oil, coal, natural gas, etc. As the most important greenhouse gas component, CO_2 is closely related to energy consumption. The total annually used energy fluctuates, for example, between 1970 and 2012, is shown in Figure 1-1. The orange line is the total energy consumption and the blue line is the household energy consumption in the UK. With the development of renewable energies and increasing efficiency of energy supply systems, the total energy consumption and the energy usage per household per year are decreasing. However, total household energy consumption is increasing its share due to people demanding increased comfort levels in houses including heating/cooling houses, population growth, and increasing household appliances [5].

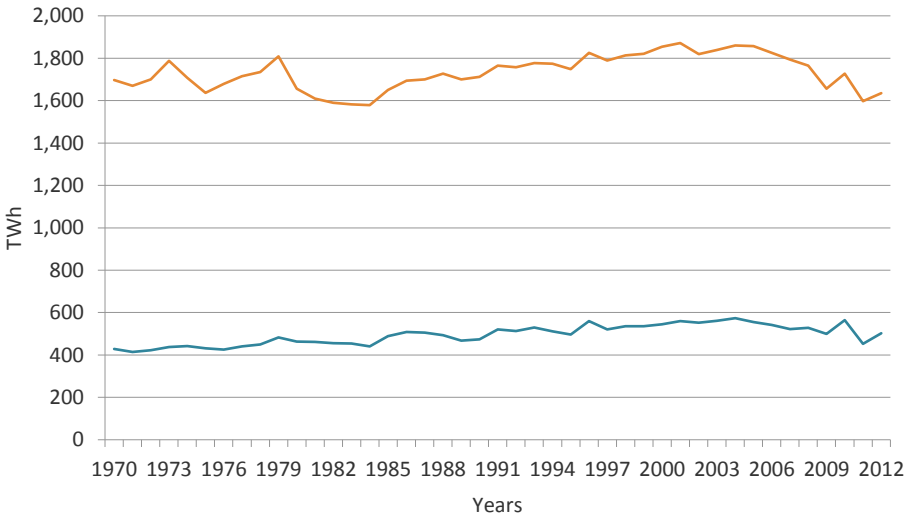

Figure 1-1 UK Household energy and total energy consumptions over 42 years [5]

When analysing different energy sectors from Figure 1-2, the housing sector takes the majority energy consumption compared to other energy users, such as industry, road transport, air transport, commercial buildings, etc. The housing sector consumed 502 TWk energy which has an 11% increase compared with 2011 housing sector energy consumption, 452 TWh [5].

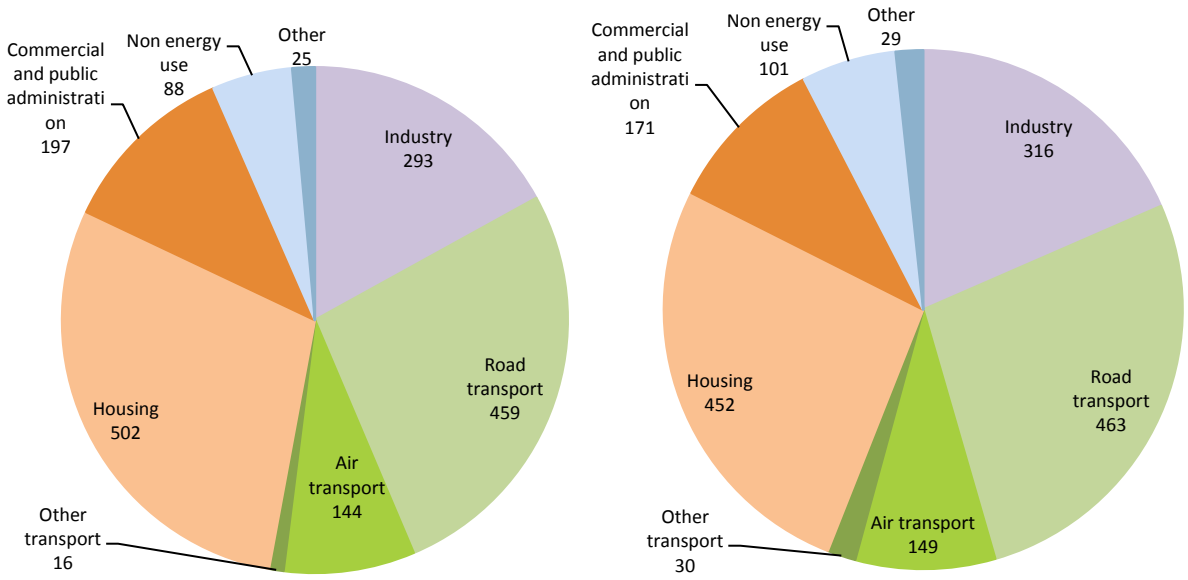

Figure 1-2 Final Energy Consumption by Sector 2012 and 2011(UK, TWh) [5]

Within domestic energy consumption, there are 4 sections that contribute to the total domestic energy usage. From the numbers below, space heating is still the primary energy demand.

- Cooking (3%)
- Lighting and appliances (18%)
- Water (18%)
- Space heating (61%)

With a large amount of space heating consumption, it is important to take a close look at the space heating system. The behaviours of the occupants, the heating systems and house type affect the efficiency of the heating energy consumption such as human behaviours, building materials and characteristics, technologies and weather conditions [6-8]. The effort was made to increase the heating efficiency such as cavity wall insulation, and loft insulation, but they do not always end up saving the energy or reducing CO_2 emission [9]. These methods increase the thermal comfort rather than saving energy.

The UK government also released the United Kingdom housing energy fact file including the CO_2 emission. From the report of energy consumption by the Department of Environment and Climate Change 2012, about 30% of energy consumption is in domestic energy usage and responsible for 38% of greenhouse gas emissions [5]. Because of a large amount of CO_2 emission from the domestic aspect, breakdown of emissions is shown in Figure 1-3. Among the 13 types of housing energy, the electricity and natural gas caused the majority CO_2 emission yearly from 1990 to 2011. During the 22 years, electricity and natural gas accounted for 42.8% and 45.9% CO_2 emission respectively.

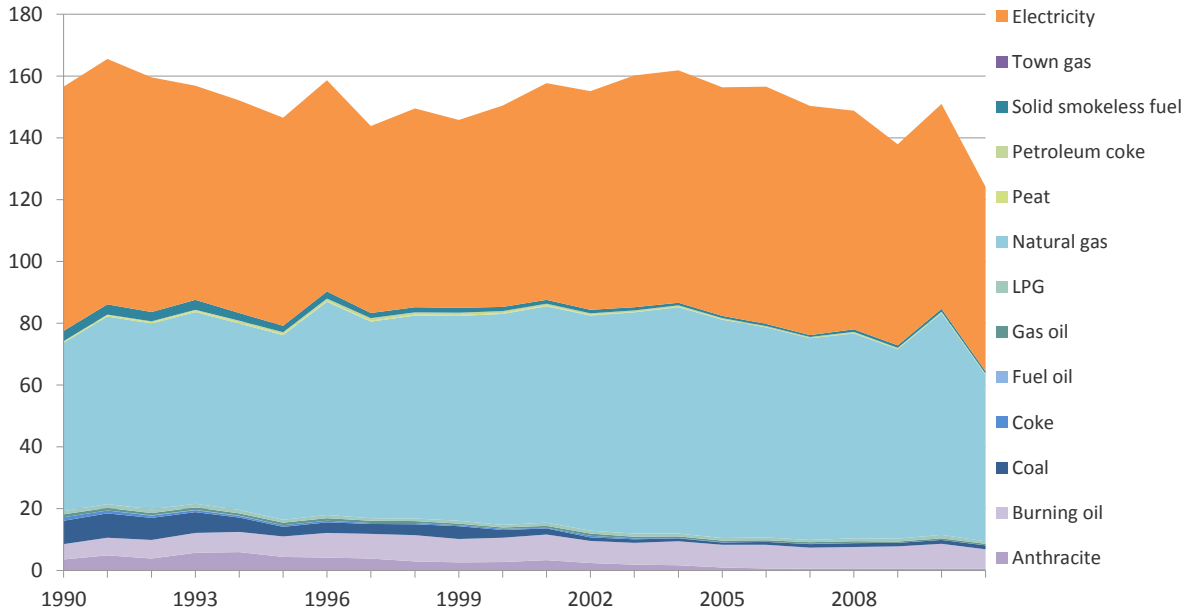

Figure 1-3 Housing energy CO_2 emission in million tonnes [5]

1.1.2 Low carbon heating technologies

To improve the situation, research efforts have focussed on high-efficient heating systems and electricity generation. Nowadays, the Combined Heat and Power (CHP) plant is growing in popularity at the residential level in developed countries [10]. The efficiency of CHP is considered to be high because the consumed gas produces electricity with the waste heat used for a heating system such as domestic hot water and space heating. Research on CHP CO_2 emission shows compared to conventional heat generation from individual boilers, 30% of carbon emissions can be reduced [11] due to gains in efficiency. However, when considering CO_2 emissions, CHP still generates more CO_2 than electric heat pumps run on low carbon

electricity. The installation of electric heat pump was forecasted to lead to reduced CO_2 emissions by more than 90% by the year 2050 [12].

In summary, heat pumps are more convenient to operate than CHP and have better opportunity to reduce the carbon emissions considering the government carbon emission target [13]. The Renewable Heat Incentive (RHI) was launched in November 2011 for non-domestic applicants. Successful applicants to RHI receive payments over 20 years. Several types of heating can claim payment through RHI based on the heat energy generated. As one of the eligible heating types in the RHI program, heat pumps have promising market growth in the future [14]. From the DUKES, in 2017, nearly 26% of renewable sources were used to generate heat and it is due to "the greater contribution of renewable heat from heat pumps".

Heat pumps benefit from low carbon electricity. Instead of using gas, electricity drives a refrigerant cycle to move heat from a low-temperature source to a high-temperature sink. For electricity generation, renewable energies like wind energy and solar energy are now widely applied at both large scale and small scale. The government promotes the "small-scale renewable and low-carbon electricity generation technologies" by making payments on generating and exporting electricity from eligible installations (Feed-in Tariff) [15].

Besides the momentary benefit from the Renewable Heat Incentive and Feed-in-Tariff, heat pumps run more efficiently the warmer the heat source. Electricity consumption of heat pumps is related to the output heat energy and the Coefficient of Performance (CoP) of the heat pumps. The electricity usage can be calculated using the heat energy output divided by CoP. As a result, the higher the CoP, the less electricity required for the same amount of heat demand.

For example, during the summertime, the ambient temperature is high which increases the CoP of an Air Source Heat Pump (ASHP). Since the heating load in temperate climates is usually in the winter, a Ground Source Heat Pump (GSHP) is likely to have higher efficiencies at these times due to more constant ground temperatures. In order to increase the GSHP performance, the borehole is used for storing heat. Inter-seasonal borehole storage which is basically a large underground heat exchanger combines both heat pump technologies to increase overall system efficiency, by storing summer heat in the bedrock until it is required in winter.

1.2 Inter-seasonal borehole heat storage combined heat pump system

1.2.1 Initial design concept

By combining the high efficiency and low carbon emission technologies together, the system provides excellent efficiency during both the heat charging season and heat discharging season and has drawn increasing attention at domestic and community level. This thesis focusses on such a proposed system which consists of heat pumps and borehole and converts electricity to heat, which is initially modelled based on the "energy hub" concept. In the late 2000's, the "energy hub" was firstly described by Geidl and Andersson at ETH Zurich [16, 17]. The idea was "sufficiently general to cover all types of energy flows, but concrete enough to make statements about actual systems" [17]. Energy hubs import energy in different forms into a bounded area, converts and stores it, providing energy to load in the most efficient way over time as is shown in Figure 1-4.

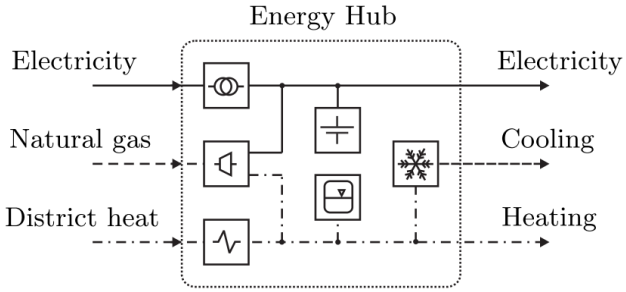

Figure 1-4 Example of a hybrid energy hub with inputs and outputs (multi-input and multi-output with the hub main body converting between different inputs to outputs) [16]

In this proposed system, electricity can be seen as the input and the output is the heat demand. Within the "hub", heat pumps convert electricity and the borehole stores the heat and the whole system is operated efficiently to provide space heating demand. The later chapters will give a detailed explanation and research.

1.2.2 Borehole heating system

In this borehole, inter-seasonal heat storage combined heat pump system, the electricity from the PV and the grid are the inputs and the output is the heat demand. This heat energy hub has relatively high efficiency compared to traditional methods.

Borehole thermal energy storage (BTES) is a ground-based heat storage with a longer asset lifetime compared to other energy storages. The borehole array is buried deep underground which requires less maintenance and minimal heat replenishment. The soil temperature is at a relatively steady temperature. The charged borehole suffers less heat loss to the surrounding mass because of the steady temperature and the good insulating properties of the ground. BTES allows the system to store the heat and use it efficiently in the future. The fluid flowing in the borehole pipe is water with mono-ethylene glycol and the glycol prevent the fluid freezing until the temperature reaches -15 °C so that it is very suitable for operating along with the heat pumps.

The ASHP and the GSHP are the key low carbon devices in this system. In the research [18], Kelly and Cockroft collected the field trial data including the house location, rooms in the house, wall insulation information, roof condition. It is suggested that the houses which are in fuel poverty put 10% of the income to the fuel bills. During the research, the concept of UK carbon intensity was introduced to quantify the relative emissions from grid-based electricity. For the domestic users, the carbon intensity of the grid is around 500g CO_2/kWh.

The study of the performance of the ASHP in the UK suggested that the CO_2 emission was reduced by 12% compared to the gas boiler [19]. When considered the operation cost, there is a 10% increase based on the application parameters [18, 20]. The fan of the ASHP ensures the ambient air passes over the evaporator. The refrigerant absorbs the heat from the summer high-temperature air and the compressor provides high pressure and temperature vapour. After this, the refrigerant releases the heat and returns to liquid. The heat stored or released when the state of the refrigerant changes.

The air temperature varies significantly during a day. As the ASHP absorbs the heat from the ambient air, the ASHP performance is not as steady as the GSHP. If the ASHP is used during winter time, its COP will not be high due to the low ambient air temperature during the heating season.

For the GSHP the heat source is the ground. The evaporator passes the low-pressure cool gas through the compressor which releases the higher pressure hot gas. The condenser facilitates the heat exchange and provides hot water to the heating system. As stated before, the ground has a very steady temperature throughout the whole year even the air temperature drops below

0℃. With a much more stable high temperature source, the GSHP is suitable to operate during the heating season than ASHP. However, the installation of GSHP is much more complicated.

In summary, this borehole inter-seasonal heat storage combined heat pump system is best to operate under the following process:

- In the summer, there is no space heating demand and the temperature is high. The PV can generate enough or surplus electricity to support the ASHP generating heat without spending extra money. The generated heat will be stored in the borehole. The borehole has a base temperature as the ground temperature. The injected heat energy lifts up this base temperature.
- In the winter, it is too cold to operate ASHP and the GSHP supplies the heat demand. The heat is stored in the bedrock during the summer and will be the heat source during the winter time. Instead of providing the GSHP with the ground temperature, the borehole gives the GSHP a higher input temperature depending on the amount of heat energy stored during the summer. The PV electricity generation is low during the winter and the grid electricity takes part in providing the demanded electricity from the GSHP.

1.3 Overview objective, challenge and motivation

The investigation into the low carbon heating system is driven by different policy and programmes from the government. With the previous introduction of energy usage, CO_2 emission and the proposed system, this thesis focuses on the study of borehole modelling, temperature response and its charging strategy. The research aims of this thesis are to:

i) Study the feasibility of the space heating system and modelling it under different time, scales such as single charging/discharging cycle and multi-charging/discharging cycles.

A high-level energy chain analysis using a simple borehole model shows great energy saving potential, which is the feasibility study of the proposed space heating system. Within the high-level energy chain, the model is built on a linear function and the borehole physical layout is not considered, ignoring the heat transfer between the boreholes and surrounding environment. However, the practical operation of the borehole in terms of heat injection and extraction relates to heat transfer between each layer around the borehole and the within the boreholes

themselves. This heat transfer process depends on different parameters, thermal conductivity (W/m/K), thermal capacity (MJ/m^3/K), starting temperature (°C), heat injection, etc. Different media have different parameters, which make the heat transfer a very complex nonlinear process across the whole borehole field.

During the whole process, any heat injection and extraction leads to temperature gradients through each media which in turn affects the heat transfer. So that when considering the system's time domain behaviour, the borehole temperature in each time step is determined by conditions at the previous step. In this thesis, the borehole model will be able to present the temperature/heat relationship and temperature change in each medium.

ii) Optimize the operation of the borehole to increase the system efficiency under different time scales with borehole temperature behaviou study.

Heat transfer is a complex process and when there is a temperature difference, it happens. For the borehole thermal energy storage, less heat loss results in higher temperature. In the past research on the borehole, the focus is always on building the borehole, verifying the model, and optimizing the size. The influence from the borehole temperature within the heating system is not taken seriously [21]. In the proposed heating system, borehole's temperature changing is closely connected to the heat pumps in charging and discharging seasons. During the charging season, the ASHP will carry high-temperature fluid to the borehole and the borehole and adjacent ground will be raised to a higher temperature. However, along with the charging process, the temperature settles down as the heat dissipates to the surrounding area. As a result, the temperature of the fluid to the GSHP is not the same high temperature any more. The borehole wall absorbs the heat from the fluid during the charging season and in the discharging season, the borehole wall is directly related to the performance of the GSHP. The temperature output from the borehole will be a very important aspect. This thesis shows the temperature changing pattern of the borehole due to different heat injection and extraction and chooses the proper temperature point for further analysis on optimizing the borehole charging process. If total low carbon input heat energy is limited, the allocation of charging over time will determine the final borehole temperature and thus the GSHP performance during the discharging season. Early charging tends to lose heat in the early time steps, vice versa. Taking the heat loss into account, this thesis presents that the most efficient borehole charging strategy to increase the heat pump performance.

iii) Illustrate the benefit from this space heating system such as electricity consumption and CO_2 emission and provide a guide for future research.

The efficiency of the heat transfer process between the borehole and the surrounding ground acts on single charging/discharging and multi-charging/discharging cycles and is dependent on all stages of the whole energy chain. Therefore intelligent input of heat energy over time is of critical importance to the system. By studying the borehole coupled heat pump space heating system from a high level energy chain to optimizing the operation, this thesis illustrates the benefit from the proposed space heating system in terms of system efficiency, electricity consumption, and CO_2 emission.

1.4 Outline of the thesis

There are 7 chapters in this thesis:

Chapter 1 --- Introduction of general knowledge on the heat energy consumption, challenges, motivation and thesis outline.

Chapter 2 --- This chapter presents the overview of the existing borehole heat energy storage modelling based on different aspects and types as well as the application of the borehole thermal energy storage coupled with heat pumps. With the overview of the past work, further research needs to be done.

Chapter 3 --- This chapter presents the start stage of this study. A practical borehole project is introduced with the detailed phase one borehole feasibility study and the high-level energy chain analysis brings out the beneficial quantification on the space heating system. With the study on the project, a lumped borehole thermal storage is introduced with initial system knowledge built and the high-level energy chain analysis leads to further system improvement and research.

Chapter 4 --- This chapter presents an accurate borehole modelling in the MATLAB environment. Instead of a lumped borehole model, the borehole accurate temperature behaviour response to the injection/extraction heat flux in long-term and short-term cases are conducted in Chapter 4. The new borehole model considers heat transfer between different layers in within the whole storage volume. With the temperature behaviour study, the useful temperature

information is selected based on this borehole model and initial borehole coupled with heat pumps system performance is studied.

Chapter 5 --- This chapter presents a journal paper on optimizing borehole short-term charging strategy. With the knowledge from the previous chapters, Chapter 5 focused on the operation of the proposed space heating system and the optimized charging strategy of the borehole helps the system to save more consumption and reduce CO_2 emission.

Chapter 6 --- This chapter focuses on the efficient way to charge borehole system with multi-charging/discharging cycle and illustrate how the heat accumulation benefit in the long term operation with limited heat storage in the borehole. The study in this chapter presents a borehole charging guide over long term and with the long term charging strategy, the system reduces more electricity consumption and takes advantage of the high ground storage temperature with heat accumulation with less heat loss in long operation time.

Chapter 7 & 8 --- Conclusions will be drawn in Chapter 7 and the future work in Chapter 8 is based on the current research.

2 Overview of existing borehole research

2.1 Introduction

In this chapter, the historical research on borehole is introduced. The overview of the borehole research is based on different papers. The discussion on each paper includes the borehole model, results, focus and conclusions.

2.2 Thermal storage overview

Energy storage systems, in general, are designed to accumulate different energies for later usage. There are a growing installation and utilization of geothermal energy in the worldwide [22-26]. It helps to store excessive energy and then releases it at the request in a later time. There are several properties that can describe energy storage systems, capacity (the maximum/minimum energy the system can take and remain), efficiency (energy loss during the charging/discharging periods), cost (system capacity and operation), and storage time (the length of energy stored) [27].

Nowadays, the production of renewable energy is increasing [28] and one problem of using renewable energies like wind, solar, is that the generation of electricity or heat energy does not match the peak demand. Electricity storage can be seen as the Holy Grail for the renewable energies and helps to improve the usage of renewable energies [29]. For the heat energy, the majority of heat demand appears during the winter time. The inter-seasonal heat energy storage makes it possible to store the surplus heat in the summer and use it during the winter. For domestic hot water, space heating and air-conditioning in the building sector, thermal energy storage is frequently used.

The first inter-seasonal thermal energy storage was used during the 1960s in the US [30]. Thermal energy storage can be divided into the following types [27, 28]:

- Underground thermal energy storage [27]
  UTES includes borehole storage, aquifer storage, cavern storage and pit storage. The selection of different theologies is based on the geological condition.
  i) The most borehole related projects aim to provide space heating during the winter. The heat exchanger is often used with the heat pumps.

ii) Aquifer storage sees the natural underground water-permeable as the medium and frequently used to store winter cold.

iii) Cavern and pit storage is based on underground water reservoirs. The investment costs are high.

- Sensible (hot water) thermal energy storage [2, 31, 32]

  Sensible heat storage depends on the body mass and heat capacity of the carrying liquid or solid and the change in temperature. There is no phase change within the temperature range.

- Latent heat storage (phase change material) [2, 27]

  Phase change material has higher energy capacity and steady discharging temperature compared to the sensible storage. However, for PCM the thermal conductivity is always in a low range between 0.2 and 0.8 W/mK.

- Thermo-chemical [2]

  A chemical reaction in the thermal energy storage can achieve high energy capacity and it is one of the most novel approaches. Thermo-chemical heat storage does not get limit in time due to the heat loss compared to the sensible thermal energy storage and latent heat storage [32].

The underground energy storage such as borehole thermal energy storage in Figure 2-1 is becoming increasingly popular [28, 33]. The borehole storage is the vertical heat exchanger and transfers the thermal energy to and from the ground layers such as clay, sand and rock. In practice, the borehole thermal energy storage is always used with heat pumps to take advantage of the soil temperature heat [27, 34].

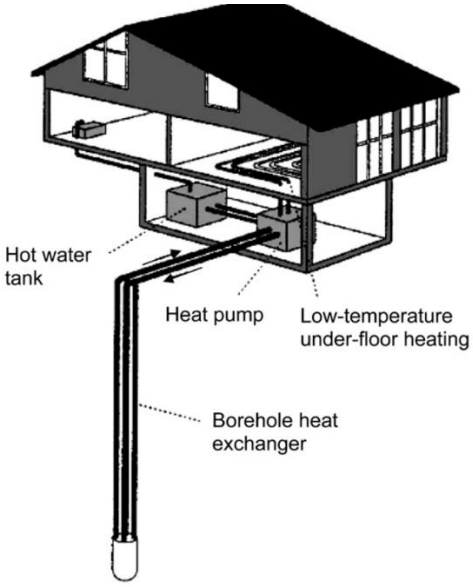

Figure 2-1 Example of usage of borehole thermal storage coupled with heat pump [88]

This chapter includes the introduction of the borehole heat energy storage history and the current research on borehole thermal energy storage.

2.3 Existing key research on the borehole thermal energy storage

The modelling of borehole field response can be conducted in several ways. Borehole thermal energy storage as a commonly used thermal storage has been studied for decades. In 1882 and 1948, "Kelvin's line source theory" first applied the line-source without considering the thermal properties and the axial effect of the borehole. Later on, improvement has been done on the borehole thermal properties and the heat flow effect. However, the new model only considers the temperature response of the borehole for short-term simulation. A lot of current research is based on the famous G-function developed in 1988 by Eskilson. The numerical model always has homogeneous ground with different thermal properties for the fluid, the grout and the ground and the initial temperature so that simulation takes a relatively more time compared to the analytical model and the model is suitable for the long-term temperature response. In the early borehole heat energy storage research, the analysis of the heat transfer of borehole was a great challenge due to the transient heat transfer between different media and the surrounding geometry parameters [35]. Some great work has been done in this area, mainly by analytical [36-41] and numerical [42-45] approaches. In [36] and [38], the borehole is modelled using line-source providing a new way of designing borehole under different property and materials. [37] uses finite line-source solution to calculate the borehole output fluid

temperature response of different configurations of boreholes. In [39] and [40], the focus is on the groundwater advection impact on the borehole modelling and the analytical borehole model provides an efficient way of presenting the influence of the water flow. Angelo in [42], uses the numerical borehole model with different grouting material and compares with the field measurement. Yujin in [43], uses the numerical method to predict the heat exchange rate for designing the system. In [44], Su carried out studies on a single borehole numerical model compared with the analytical model on the fluid temperature and computing time and study shows that the numerical is an efficient way of simulate the ground heat exchanger. [45] studies the temperature effect of different ground layers and finds that the ground layers have little effect on the designing of the borehole coupled GSHP system.

In this section, some important research on the borehole modelling will be selected and presented. Each of the selected research has its own characteristics, focuses and model environments.

2.3.1 Composite-medium line-source model validation

In [35], Min Li studied the borehole temperature short-time response. This research focused on the heat capacity effect and different arrangements of the borehole. In an analytical way, the traditional approach of borehole heat transfer, thermal transfer is divided into steady and unsteady states because of the small dimension and heat capacity. For the short-time borehole temperature study, the U-shaped tube is an equivalent diameter simply tube [46] gives "little insight into the underlying heat transfer mechanism" [35] as is shown in Figure 2-2.

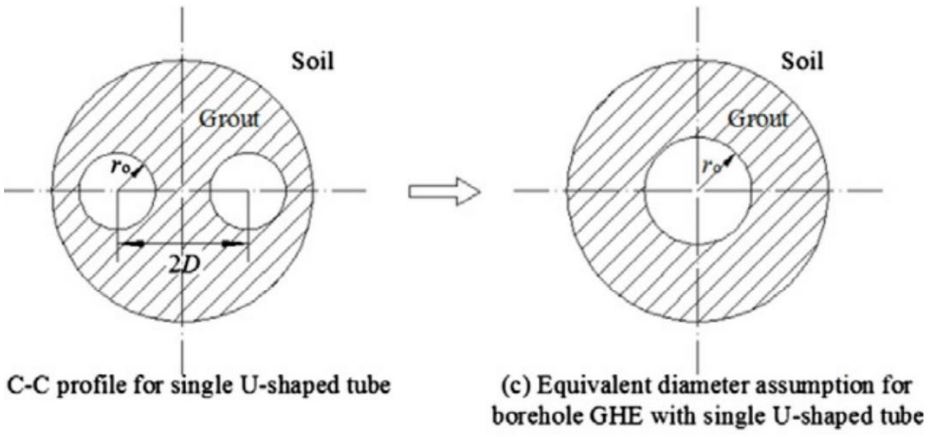

Figure 2-2 equivalent' diameter simplification for U-shaped tube [35]

For the current transient thermal process of the borehole model, L. R. Ingersoll firstly introduced an infinite line-source and cylindrical-source model in 1955. Authors in [35] developed a new line-source model based on their previous wok composite-medium line-source model for analysing the thermal process. The new model turns the original model to a facilitating numerical computation. This approach is different from the traditional one. The method of calculating the average temperature of the borehole wall is simplified. In the traditional method, the heat transfers within and around the borehole are assumed to be steady state and simply represented by thermal resistance.

Besides the borehole modelling, authors also used the experimental data to validate the composite line-source borehole model. Due to the lack of independence thermal parameter measurement of the soil, borehole materials, and the layout of the borehole system in the field, the laboratory data of Beier et al [47] is used to validate the model. This experiment consists of a large sandbox with the borehole model and electric heaters. The initial temperature, borehole size, the sand/ backfilling (grout) thermal parameters and heating power of the heaters were the major control parameters as shown in Figure 2-3. The temperature response at the inlet/outlet and at the different radial positions are comprised.

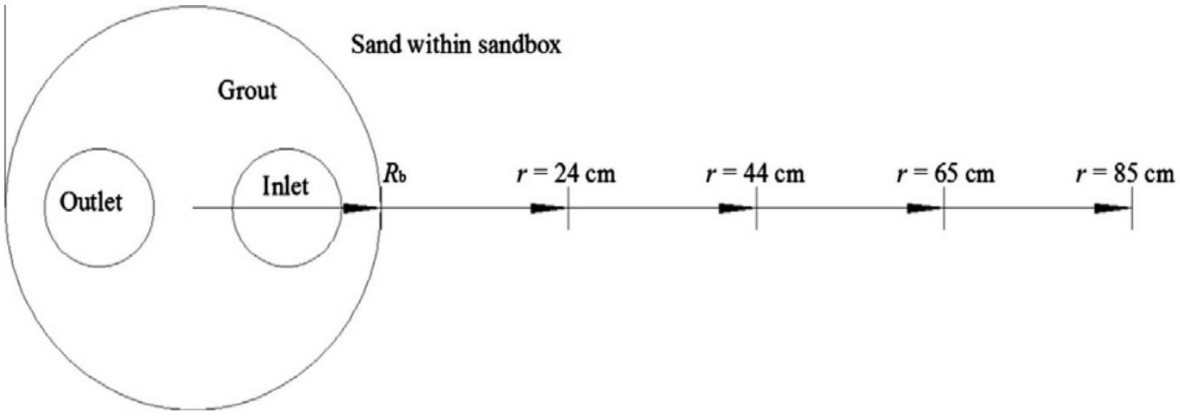

Figure 2-3 Temperature measurement in Beier et al experiment [35]

From the results comparison, the new analytical borehole model, considering the U-shaped tubes as line source heat reducing the calculating time, gives a more accurate reference for predicting the temperature response of in terms of the borehole distance. However, the temperature error between the predicted model and the experimental case is decreasing from 6% at the borehole wall position to 2% at the radius of 24 cm.

From the circulation fluid temperature comparison between the new proposed borehole model and the traditional model, both models produce the same the prediction of the fluid temperature trend. However, the traditional method consumed more time.

The conclusions from this research are described in two aspects. The new composite borehole model was validated by the laboratory experiment. Three factors were analysed to show the influence on the borehole model temperature prediction, heat rate, thermal conductivity and thermal capacity. For the short-term, the borehole temperature response in the new model is more suitable and time-saving for prediction than the traditional method.

2.3.2 Heat transfer based on borehole different geological lays

In the analysis of borehole heat exchanger in [48], the focus was drawn to the heat transfer between different geological layers as shown in Figure 2-3 (a). For an accurate estimation of borehole thermal performance, the heat conductivity and the specific heat capacity are very vital in the heat transfer process [49]. The experimental measurements were taken on 18 boreholes with GSHP in an office building in Germany.

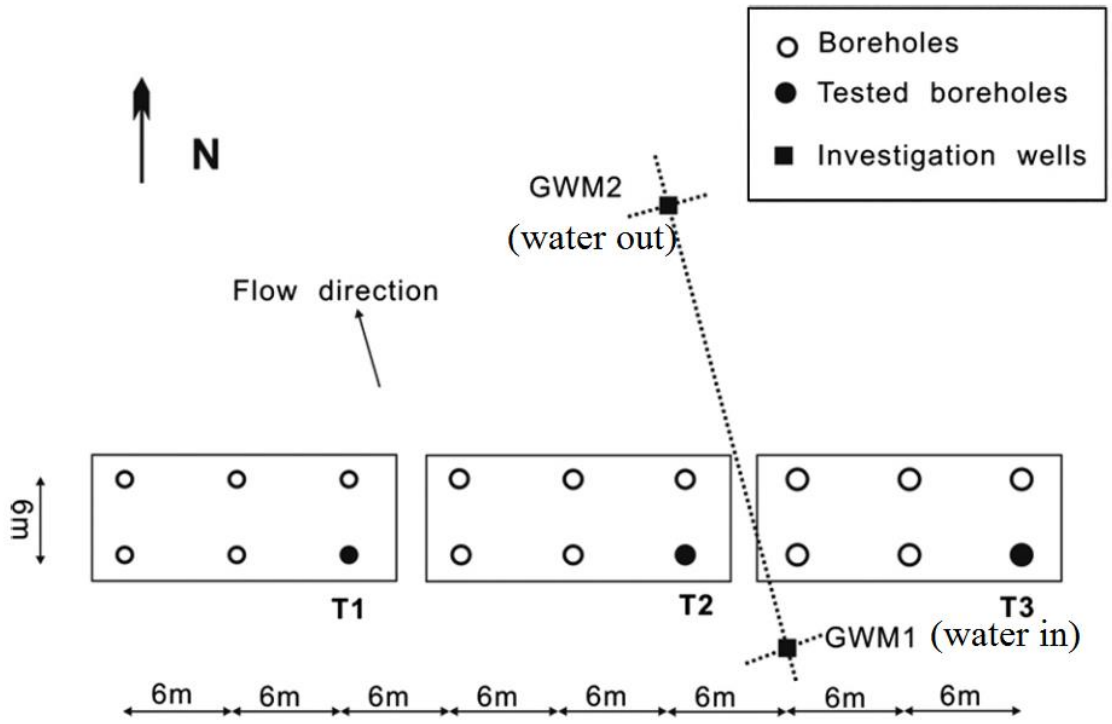

(a)

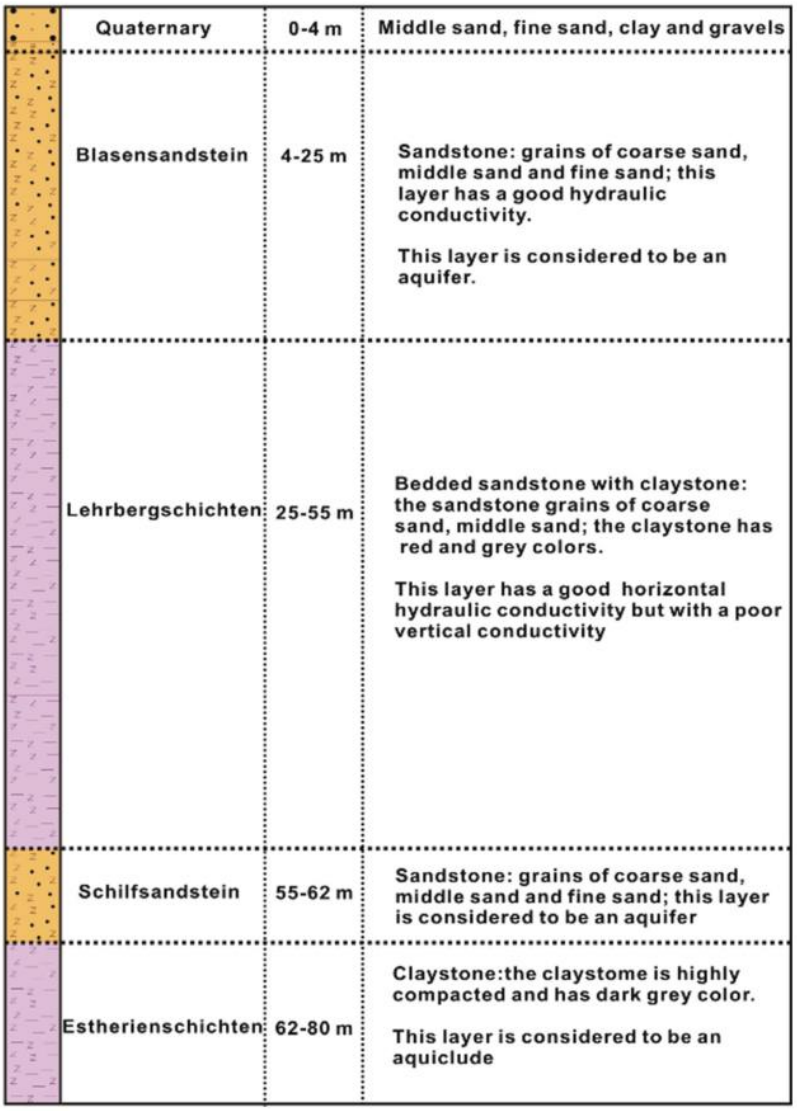

(b)

Figure 2-4 Borehole display for the thermal response tests (a) with Ground layers (b) [48]

Figure 2-4 (b) shows the borehole layout. In the tests, the boreholes are divided into three groups according to different borehole diameters. The first group shown in Figure 2-4 (a), T1 is 121 mm, T2 is 165mm and T3 is 180mm. GWM1 and GWM2 are the two extra wells drilled in the upstream of the borehole field and downstream of the borehole field. From GWM1 and GWM2, the groundwater measurement was carried out. These 18 boreholes and two investigation wells were drilled with 80 m depth. The bullet points listed below give the five different geological layers considered in this research. Within the 80 m underground:

- 0 – 4 m are the middle sand, fine sand gravels (Quaternary).

- 4 – 25 m is the sandstone with good hydraulic conductivity and considered to be an aquifer (Blasensandstein).
- 25 – 55 m are the bedded sandstone with claystone which has good horizontal hydraulic conductivity (Lehtbergschichten).
- 55 – 62 m is sandstone considered to be an aquifer (Schilfsandstein).
- 62 – 80 m is the highly compacted grey claystone layer which is an aquiclude (Estherienschichten).

As stated before, the ground parameters are significant for an accurate measurement. In this research, from GWM1, thermal conductivity and specific thermal capacity were measured and from GWM2, the groundwater was measured.

Besides the ground thermal parameters, the borehole model adopts a numerical method with mesh representing different borehole regions. This numerical model was built in FEFLOW and the heat transfer of borehole was modelled by the fully discretized meshes [50]. The settings of the parameters, numerous of mesh and the matrix in the numerical model took a long time of operating. Depending on the size of the model and the mesh condition, the simulation time increases nonlinearly. The fluid temperature was described as a response to the heat flux per unit length [51]. The heat transfer between the fluid and the borehole wall was represented by the thermal resistance. Through the whole simulation process, to evaluate the heat transfer of boreholes, within the borehole U-shaped pipe, the fluid temperature (in and out) were recorded in time series.

This study brought a detailed temperature profile, heat transfer for different ground layers and the measured thermal parameters. The homogenous ground model and layered subsurface model were compared through the study and the numerical borehole model was validated. From all the simulations and comparisons, the performance of the borehole is very even over the length and the length of the borehole model could be reduced in the future study.

2.3.3 G-function borehole model study

In [52], a full-scale analytical borehole was developed to overcome the complex heat transfer of borehole heat storage in time-space scales. The full-scale model is a composite expression consisting of a composite-medium line-source solution (inner solution), a finite line-source

solution (outer solution), and an infinite line-source solution. As shown in Figure 2-5, different stages of the borehole model are used for different time scales.

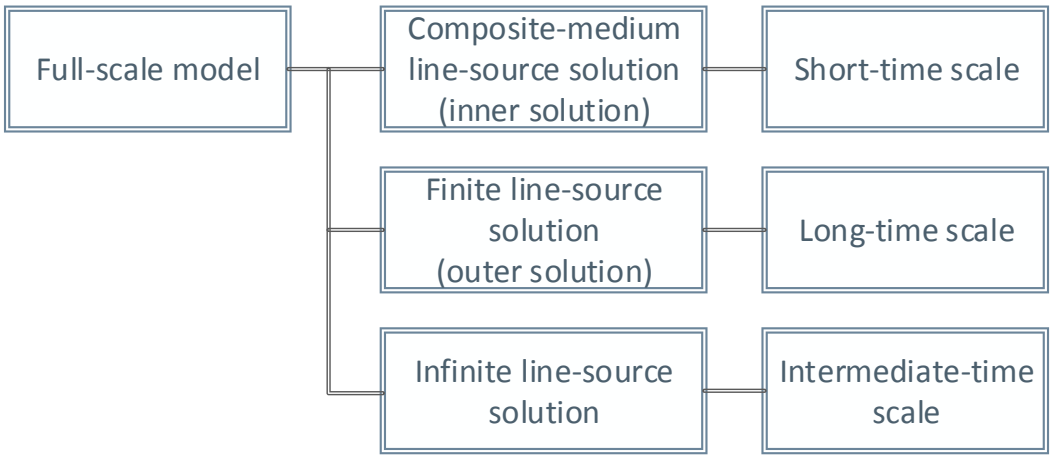

Figure 2-5 Full-scale model structure and usage

In borehole study, the borehole wall temperature study is always the key issue. For the infinite line-source model, the average temperature is expressed as below [52]:

$$G_1(t) = \frac{1}{4\pi k_s}\int_{r_b^2/4a_s t}^{\infty}\frac{\exp(-u)}{u}\,du = \frac{1}{4\pi k_s}E_1\left(\frac{r_b^2}{4a_s t}\right) \quad (2\text{-}1)$$

Where,

- t is time
- k_s is thermal conductivity of soil
- a_s is thermal diffusivity of soil
- u is integral variable
- r_b is the borehole radius

The limitations of the infinite line-source are that the heat transfer ignores the thermal process in the ground and the temperature has no limit of increasing and decreasing. For the short time simulation, the temperature response is considered to be accurate [52].

For the finite line-source, the limitations of the infinite line-source are no longer the issue and are suitable for the long time simulation. The borehole temperature for this model is calculated with the equation below [52]:

$$G(t,z)=\frac{1}{4\pi k_s}\int_0^H\left[\frac{erfc(\frac{\sqrt{r_b^2+(z-z')^2}}{2\sqrt{a_s t}})}{\sqrt{r_b^2+(z-z')^2}}-\frac{erfc(\frac{\sqrt{r_b^2+(z+z')^2}}{2\sqrt{a_s t}})}{\sqrt{r_b^2+(z+z')^2}}\right]dz' \quad (2\text{-}2)$$

Where

- t is time
- k_s is thermal conductivity of soil
- a_s is thermal diffusivity of soil
- z' is the integral variable along coordinates z
- r_b is the borehole radius
- erfc(x) is complementary error function
- H is the borehole length

However, the old G-function cannot present the transient heat transfer process because of the lack of the thermal parameter of the grout (backfilling material) and the ground thermal parameters. The Equation below shows that calculation [52]:

$$G_i(t)=\frac{1}{2\pi k_b}\sum_{m=-\infty}^{\infty}\int_0^{\infty}(1-\exp(-u^2 a_b t))\times\frac{J_{2m}(ur_a)+J_{2m}(ur_b)}{2}\frac{J_{2m}(ur')(\varphi g-\Psi f)}{u(\varphi^2+\Psi^2)}du \quad (2\text{-}3)$$

Where

- a_b and k_b are the thermal diffusivity and conductivity of the backfilling materiel
- r' is the position of the line source
- r_a $r_b$are the radius coordinates of points A and B
- u is the integral variable of the dimension of reciprocal of the length

The calculation is based on the borehole layout below:

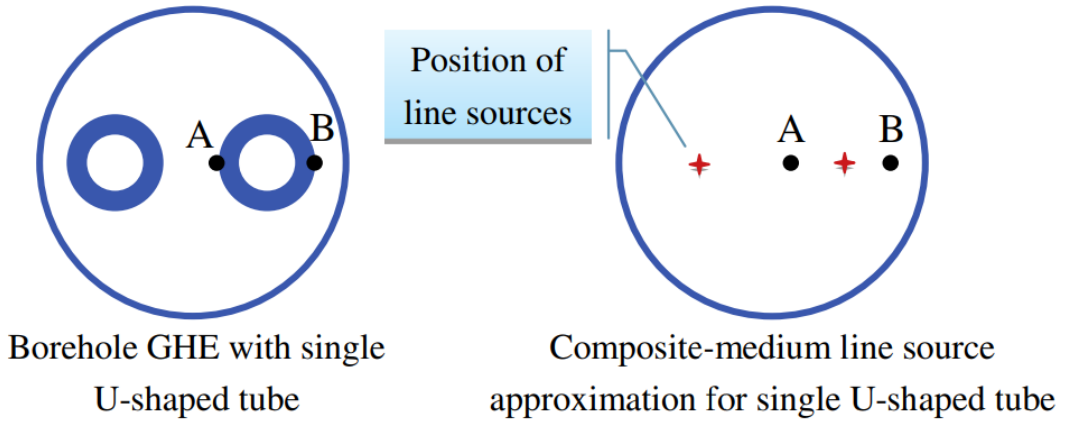

Figure 2-6 Example of borehole wall temperature calculation [52]

For this new model of the borehole, the equation becomes more complicated and it is difficult to solve when the more factors are considered [52].

This research paper introduced the very detailed analytical borehole model. With extra factors considered, such as the length of time and different media [53], a new multi-stage is proposed by Yi Yang. As a result, the time-space scale simulation can be done for the borehole thermal energy storage. The multi-stage model was verified and the difference is very small and can be neglected. When running the simulation, the computation time is reduced compared to the full-scale model.

2.3.4 Moving finite element borehole

In paper [40], authors took the groundwater flow and axial effect into account on the borehole model.

The majority of analytical methods of the borehole heat transfer process were based on the infinite line-source theory in [54]. This model is good at short-term heat response, however, for the long-term test, axial effect is relevant [55] and the temperature response to the heat input/output in the infinite line-source without the groundwater flow effect could not approach the steady state period. With the constant increasing of the heat energy injection or extraction, the temperature increasing or decreasing linearly with the simulation time. In this study, Mikael designed the borehole storage with axial effects considered so that the temperature response

reaches a steady state. More researches have been done on the effect of axial, in [56], a borehole design problem was demonstrated. With the axial effect considered, a more cost-efficient borehole system which reduced 15% of the length of the borehole. Besides the axial effect on the modelling borehole, groundwater flow presents the heat transfer by the moving water. The effect brought by the moving water has been studied in [57-60], and concluded that the temperature distribution within the borehole model is changed.

As a result, Marcotte combined these two effects with the analytical model --- moving finite line model. There are three assumptions made in their new model:

- The homogenous semi-infinite ground has thermal properties independent of the temperature changing.
- The boundary of the ground is set to the fixed temperature as the same as the initial underground temperature.
- The heat flow of this finite line-source is a constant.

The finite line-source model is based on the Green's function [61]. The G-function of the heat transfer process provides the relationship between the heat and the temperature in the borehole model. The model was validated by using a 3D model within a 100 m × 200 m horizontal domain. The simulation was done with 20W/m constant heat input for 20 years.

The thermal parameters are independent of the temperature change. The results show that the temperature responses of the moving finite line-source model and the validation model agreed to each other. Another comparison was made between the traditional finite live-source model and the new model brought up by Marcotte to show the effects of both factors, groundwater flow and axial effects.

The conclusion of this research presents that both factors influence the borehole temperature response to the heat input. The heat loss at the borehole bottom and the surface temperature result in less temperature change in the surrounding area which becomes more evident with longer simulation time. The study also shows that the groundwater velocity in the aquifer and the length of the borehole decides the axial effect (vertical heat losses). As a result, the axial effect can be neglected with high groundwater flow case.

2.3.5 Virtue MATLAB Finite Element numerical simulation

The difference between the analytical model and the numerical model is the temperature distribution domain. In the analytical model, the borehole internal region has been neglected and the heat transfer is between the borehole wall and the surrounding soil. The numerical model solves the temperature across the whole borehole region [62]. In the study [63], Ye Zhang presented a double-borehole model based on the finite line-source through MATLAB PDE toolbox. The heat transfer was divided into inside and outside borehole. Most studies are focusing on the borehole wall temperature response, however, if the borehole is considered as part of the heat pump system, the focus and the difficulty are switched to the outside heat transfer.

After the noble borehole models shown in the following bullet points, most literature is focusing on the single borehole and do not present the borehole region temperature response based on these two models.

- 1948, infinite line-source
- 1987, G-function temperature response

Two research studies have been conducted on the cylindrical coordinate establishment and G-function modification. The whole two-borehole field temperature verification is carried out in MATLAB PDE toolbox as shown in Figure 2-8. Partial Differential Equation toolbox is a numerical finite element method which has humongous number of mesh to solve partial differential equations and the heat map is then developed according to the borehole layout. Figure 2-7 is the borehole layout used in the study and the equivalent diameter model was used:

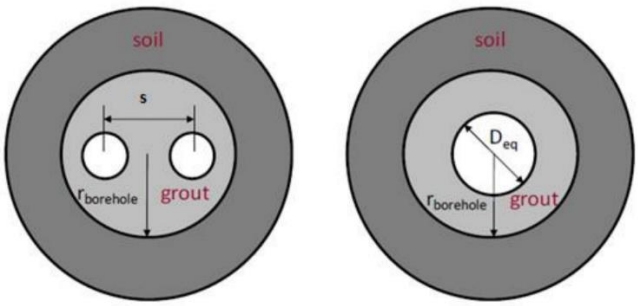

Figure 2-7 Diagram of equivalent diameter [62]

The main steps in creating the borehole are:

- Create solving domain
- Set boundary conditions and equations
- Generate mesh
- Show the temperature map

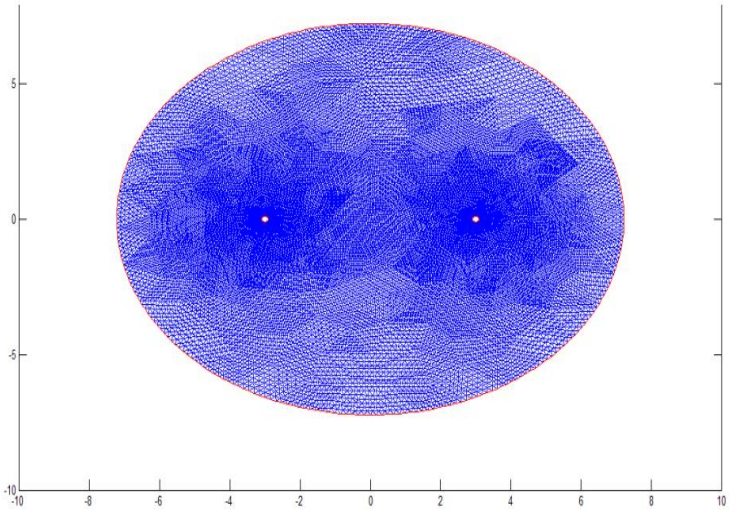

Figure 2-8 Meshing diagram [65]

The initial temperature for certain boundaries and subdomains are set to 15 °C. There are three sets of temperature tests: 1 month, 1 year and 20 years. The study stated that the MATLAB PDE toolbox accurately described the soil temperature changing and the difference between the analytical solution and the PDE toolbox is within 1%.

In research [65], the borehole was built with different media: fluid, backfilling material and the surrounding soil. In this test, the single borehole model was compared with the multi-borehole model. The temperature response was analysed in short-term scale. For the short-term scale, the average temperature across the borehole field in the two models shows little difference. In [66], the model shows the temperature effect of the soil pipe at different radial from the centre and the differences between different soil conditions. The authors in [67] present a study on the efficiency of the borehole coupled GSHP and is carried on different scenarios. The results show the improving efficiency of the system. However, these studies are lack of the thorough research on the long-term (such as 5 or 10 years or lifetime 20 years) borehole behaviour and temperature response for different heat input.

2.4 Research on borehole application

The borehole is used in various aspects such as storing water, providing cooling and heating and in this section the usage as the thermal energy storage in the energy system is reviewed.

Inter-seasonal thermal storage helps to maximize the utilization of solar energy because of the intermittence of the sun radiation [28]. The ground is a very steady heat source through the whole year and the temperature is increasing according to the depth. With a warm surrounding area, the heat loss in the underground thermal storage is relatively small. After the seasonal thermal storage firstly proposed in the 1960s in the states, there has been much research on this topic [30]. Among the commonly used thermal storages such as hot-water thermal energy store, borehole thermal energy store, aquifer thermal energy store, gravel-water thermal energy store, borehole thermal energy storage is preferred for its safety and reliability [68]. Figure 2-9 shows the working process of this system:

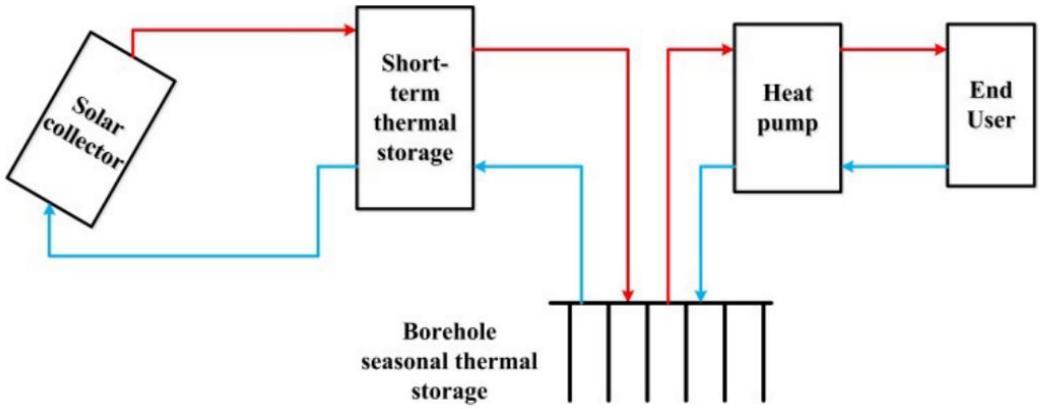

Figure 2-9 A schematic of solar-borehole thermal storage [28]

Surplus solar thermal energy is collected through the solar collector and stored under the ground and during the heating season, the heat pump raises the temperature for the users. With the solar collector installed coupled with borehole thermal storage, the solar fraction is increased, however, the charging time is not flexible due to weather condition and the ability of exchange energy with the electricity network is limited. There is a lot of commercial software to simulate this high dynamic behaviour system including TRNSYS, MINSUN, SOLCHIPS [69, 70]. With the system built, Pahud [71] optimized the system parameters such as storage volume and collector area. Argirious [69] simulated a borehole inter-seasonal storage system for a residential area and indicated the size of the borehole and energy supply

percentage over the total heat demand. Sibbitt et al. [72] found out that with borehole thermal energy storage, the system efficiency increased and the results had been compared with system operating monitoring.

As is shown in Chapter 1, in Europe, 40% of final energy consumption is contributed by the residential buildings [73]. Adhikari [74] presented an energy supply system for different end users including heating, domestic hot water and electricity, in a residential building. In this system, GSHP and vertical ground vertical exchanger are used for the space heating. Compared with the boiler providing the heat demand, the primary consumption is reduced annually dramatically. The CO_2 emission from the space heating is reduced as well. Yujin [43] uses FEFLOW [75] to calculate heat transfer between the borehole and the surrounding ground and the changing pattern of GSHP CoP according to the borehole temperature. From the past years of researching on borehole storage, there are two main focuses based on the analytical and numerical methods:

- Borehole size study
- Borehole thermal performance and validation

Besides the above study, optimization had been done on the short-term heat energy storage system with the influence of energy prices during the 90s [76-79]. A more recent study [80] proposed a hybrid thermal energy storage. The system accumulates solar energy and releases when the heat is needed and the control model uses the weather forecast. The study guarantees a comfortable thermal environment of the room and reduces electricity consumption compared to the traditional electric baseboard heating system.

De Ridder in [81] optimized the control algorithm of managing borehole thermal energy storage Figure 2-10 which helps the system to avoid getting exhausted by intensive usage over long-term operation. In this study, different cases have been set according to the weather conditions in the summer and winter which are classified as hot, mild, normal and cold. This research was the first step to the operation of borehole thermal energy storage and the heat flux various according to the field temperature. During the summer, the cooling system guarantees the field temperature is not too hot for cooling the building and during the winter time the temperature is not too low for heating the building. With the optimized heat flux, the system is very robust in each case.

More current study on the borehole heat exchangers is carried out in 2017 in China and Jin Luo presents three operation conditions for a large scale GSHP system with borehole thermal storage [82]. The study has three key focuses: i) thermos-physical properties are determined ii) heat transfer and accumulation of the borehole is studied iii) energy demand has great influence on the system. In terms of the energy demand on the operation of the system, this paper does a good job, however, the study is lack of research during the charging process and the key temperature used is the fluid temperature which is different from the borehole storage temperature (borehole wall temperature). The current analytical and numerical borehole model are used for modelling the heat transfer mechanism within the borehole, between the group of boreholes and system configuration according to the literatures [89]. In this thesis, the focus will be on the operation of the inter-seasonal borehole thermal storage.

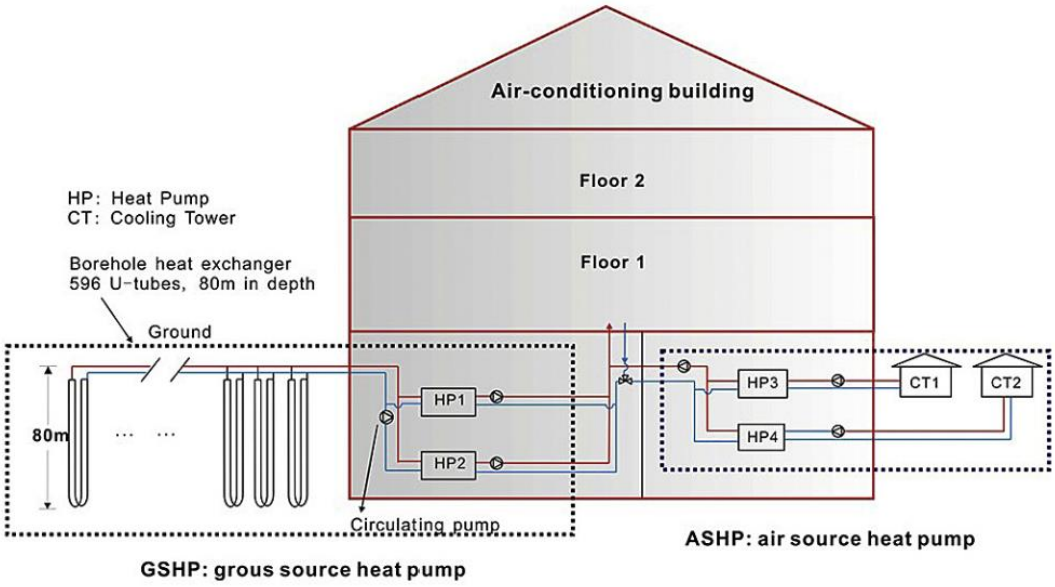

Figure 2-10 Scheme of the storage field and classical installation [82]

2.5 Chapter summary

This chapter provides the general introduction to heat energy storage and the key research on modelling borehole heat energy storage with its application.

Borehole thermal energy storage as a commonly used thermal storage has been studied for decades. Section 2.3 and 2.4 are based on diverse research aspects for modelling the borehole and applications. Each paper studies borehole temperature response from a certain angle, such as axial effect, water flow rate, borehole equivalent diameter, perdition of line source, geometry layers, etc. From different aspects of the research, the borehole modelling is verified.

With the borehole modelling study, more recent research has been focusing on the application of the borehole within the energy supply system. Section 2.3 lists several papers on the application of the borehole thermal storage. Most of the studies emphasize the working process of the system and analyse the performance of the borehole other low carbon technologies such as sizing, efficiency. Optimization on the operation of the borehole based on the given weather conditions has been done and the heat flux output was balanced to meet the demand. However, the borehole temperature behaviour is not thoroughly studied on the system performance. These papers largely inspired the research in this thesis on the modelling of borehole system, temperature behaviour of the borehole over short and long-term and the influence in the system involving other low carbon technologies.

3 Low carbon energy chain benefit quantification

3.1 Introduction

This chapter quantifies the benefit of the active recharge of the borehole array during the summertime on a community level low carbon space heating system including PV, ASHP, GSHP and the borehole. With the active charge, the borehole space heating system requires less electricity compared to the no-active charge scenario and with the increasing operation cycles during the lifetime the difference becomes large. The case study also compares two operation scenarios to the traditional heating method, boilers on CO_2 emission.

3.2 Space heating system introduction

3.2.1 Project introduction

In 2014, Small Business Research Initiative (SBRI) competition was launched by the Department of Environment and Climate Change in October 2014. The innovation designs support the low carbon heat network development and this competition has two phases:

- Phase one investigates the feasibility of the innovative design: i) borehole lump model development ii) initial high level energy chain design iii) borehole energy chain analysis.
- Phase two demonstrates the technology on the existing heat networks

The CHOICES consortium led by Clean Energy Prospector (CEPRO) was developing the new type of energy facility that will buy surplus solar power in summer to run Air Source Heat Pumps, store that heat in a borehole array, then sell the heat into a heat network in winter. This energy chain links two community buildings with a low carbon emission heat network.

This chapter introduces the high-level energy chain for the CHOICES project in phase one followed by the monetary and emission assessment compared with the traditional heating method. Different aspects are involved in this chapter's study, such as temperature condition, solar radiation, and equipment efficiency, etc.

3.2.2 System introduction

The borehole energy chain is based on the energy hub theory. The low carbon space heating system stores the heat generated from ASHP using PV electricity during the summertime and provide high-temperature environment for GSHP during the winter time so that the efficiency of GSHP increases. The high-level energy chain describes the general system layout and the system working process. The whole system diagram involves the input, the hub body and the output. The inputs are the PV electricity, Grid electricity and the gas. The output is to provide the community space heat demand. Figure 3-1 is the proposed project system modelled presented as an energy hub. In this system, the main components are the BH (borehole), ASHP, and GSHP. The Energy Management System is to control each component.

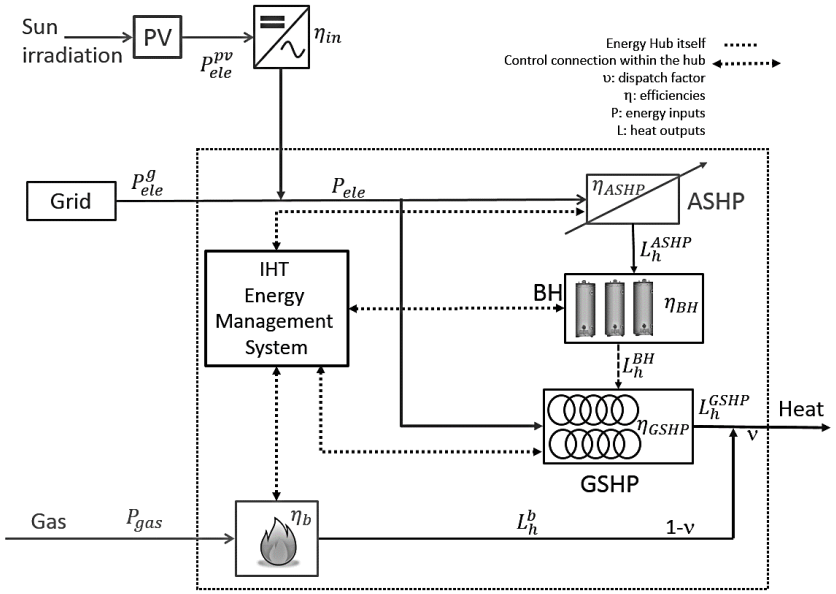

Figure 3-1 CHOICES project system diagram

In order to study the efficiency of the energy chain, the model can be investigated in charging and discharging seasons.

In phase one, the heating system is divided into the charging process and the discharging process. In the charging season, the PV and the grid provide the electricity required by the Air Source Heat Pump. The generated heat energy will be stored in the borehole buried 150m under the ground. Figure 3-2 shows the summer charging hub structure. Figure 3-3 is the single time step calculation flow chart for the charging season. The ASHP has two input parameters to calculate the Coefficient of Performance (CoP) of the ASHP, which in turn determines the

electricity consumption of the ASHP. At t=0, the ambient air temperature and selected ASHP outlet temperature decide the CoP category and inject the heat into the borehole. After each time step, the borehole temperature increases ΔT. If there is no heat injection, the temperature remains the same.

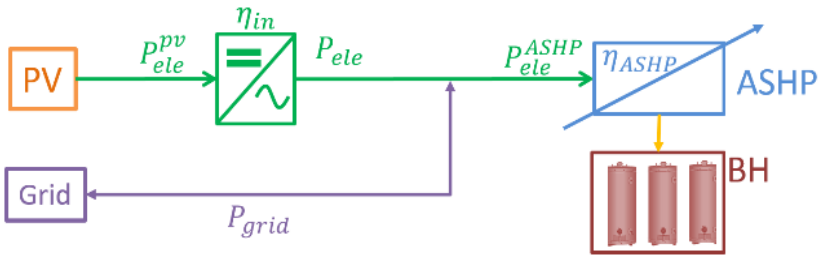

Figure 3-2 CHOICES charging season [1]

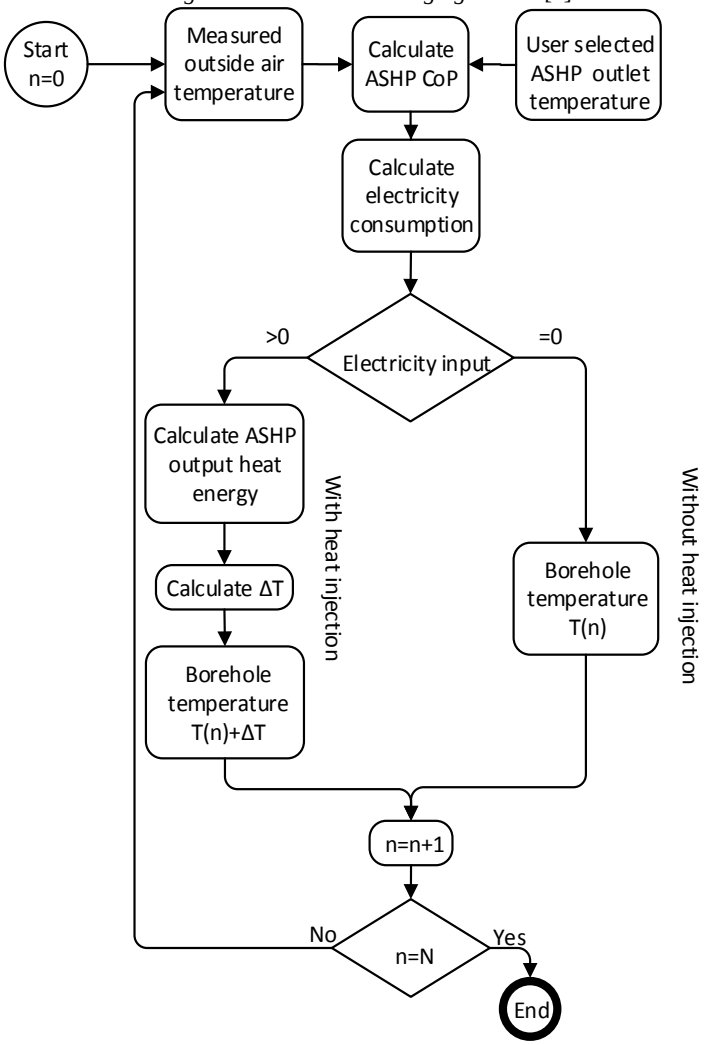

Figure 3-3 Charging system flow chart (n time step number and N total time steps) [1]

In the discharging season shown in Figure 3-4, the GSHP uses electricity from the PV and the grid to provide the electricity needed by the GSHP. During this process, the borehole array

provides a heat source for the GSHP. The higher evaporator inlet temperature makes the GSHP perform better. With higher CoP, under the same heat demand, the electricity consumption will drop. Figure 3-5 is the winter discharging process. From the charging season, the borehole high temperature is the starting evaporator inlet temperature. With the selected output temperature, the GSHP operates under the CoP and calculates the electricity needed from the PV or the grid. During this process, the borehole temperature decreases in each time step.

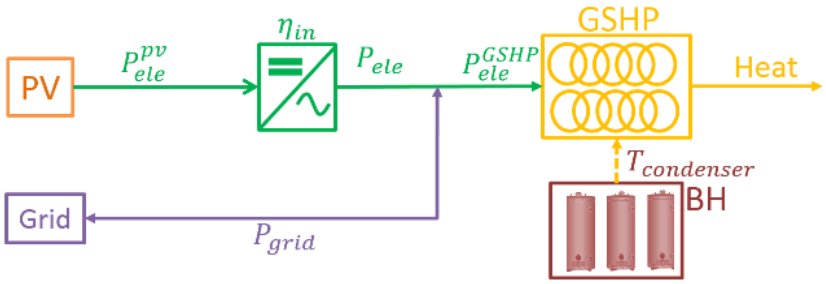

Figure 3-4 CHOICES discharging season [1]

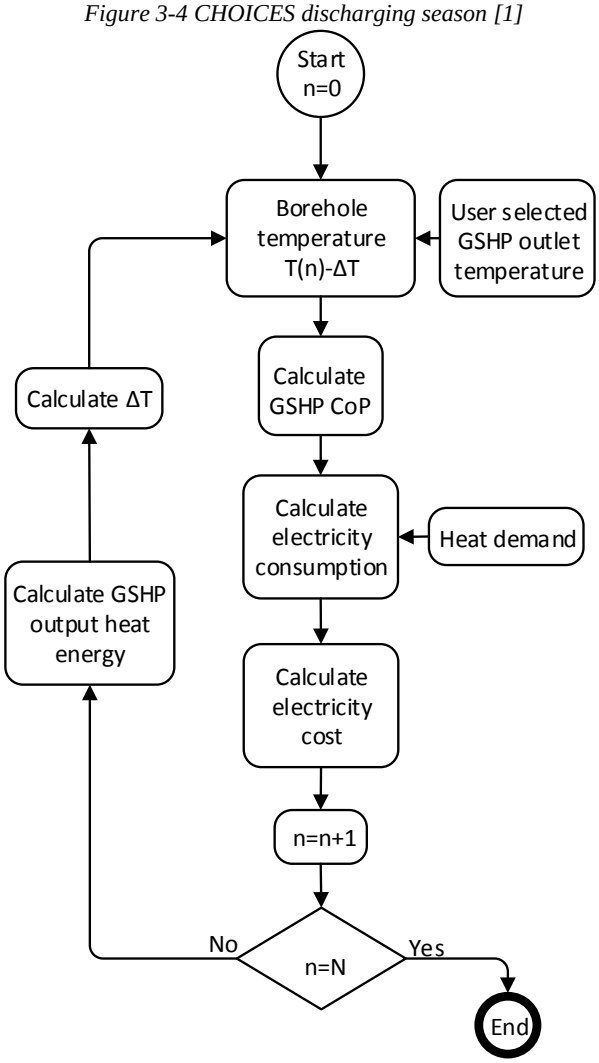

Figure 3-5 Discharging system flow chart (n time step number and N total time steps) [1]

3.3 Case study set up

3.3.1 PV and air temperature data

One of the most important components is the Photovoltaic panels (PV). In the CHOICES project, the community building has PV already installed. The electricity generated from PV provides low carbon electricity for the community. In the CHOICES project, the electricity from PV will be used to drive the heat pumps that charge. This decarbonises the CHOICES energy chain and alleviates grid congestion summer caused by high penetrations of distributed renewables.

The project is located in the Easton Community Centre in Bristol. The PV generation data and sun radiation data are from the "Photovoltaic Geographical Information System" (PVGIS) [83]. The screenshot of the website [83] is shown in the Figure 3-6.

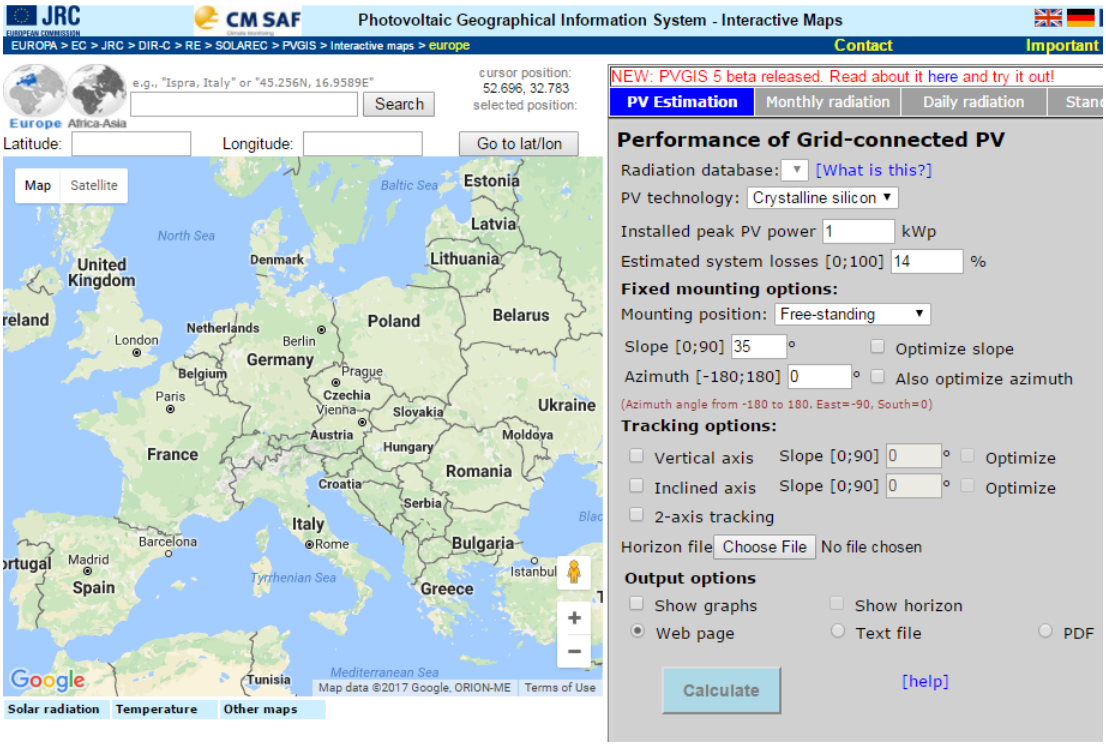

Figure 3-6 PVGIS website information [83]

UK is located in the area which receives 1000 W/m^2 according to the website Figure 3-7.

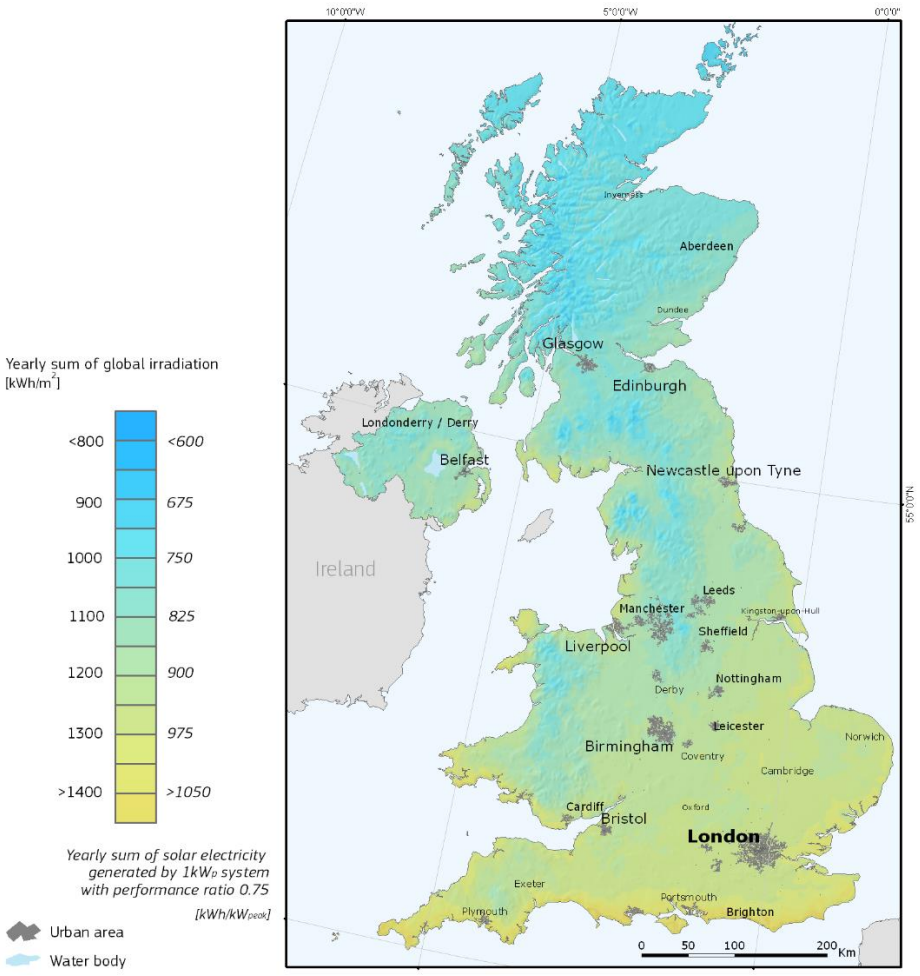

Figure 3-7 Global irradiation and solar electricity potential [83]

This PVGIS app generates the average daily/monthly electricity generation in kWh. The electricity generation is related to the PV generation factor in each month obtained from the PVGIS app.

Current PV installation is 36 kWp which is third-party owned by Bristol Energy Cooperative. Table 3-1 gives the daily electricity generation for the current PV installation. The data will be used in the case study later this chapter.

Table 3-1 Installed PV and electricity generation [83]

Month	Installed PV amount *36 kW*	PV generation amount (kWh)
	PV generation factors	
April	2.17	78.12
May	2.25	81
June	2.32	83.52
July	2.45	88.2
August	1.95	70.2
September	1.74	62.64
October	1.19	42.84
November	0.8	28.8
December	0.5	18
January	0.63	22.68
February	0.96	34.56
March	1.71	61.56

Besides PV electricity generation, the ambient air temperature is another weather aspect to take into account.

As is shown in the overall system diagram, during the summertime, only the ASHP is used to charge the borehole and the efficiency of the ASHP depends on the ambient temperature. Figure 3-8 is the hourly air temperature during the whole year time and the useful temperature must be selected to match the time step for the CHOICES project.

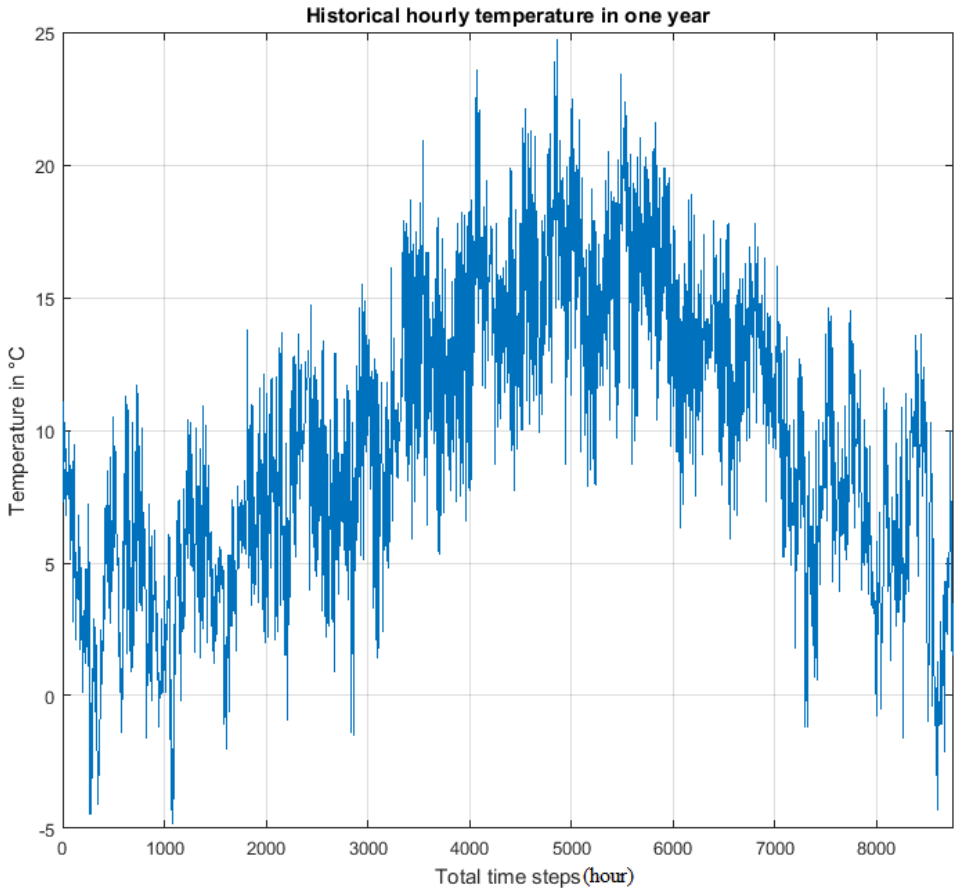

Figure 3-8 Historical hourly ambient air temperature in one year [13]

The temperature data used in the project is the recorded historical hourly temperature data as shown in Figure 3-8. The time step used for the borehole model is 12 hours and as a result, the day is divided into 7:00 to 19:00 (daytime) and 19:00 to 7:00 (night time) according to the community heating demand. In one time step, the temperature is considered to be the mean value during 12 hours. Figure 3-9 shows the charging (summer) time ambient air temperatures according to the summertime steps. The temperature data will be used in the case study for calculating the ASHP CoP during the charging season (summer).

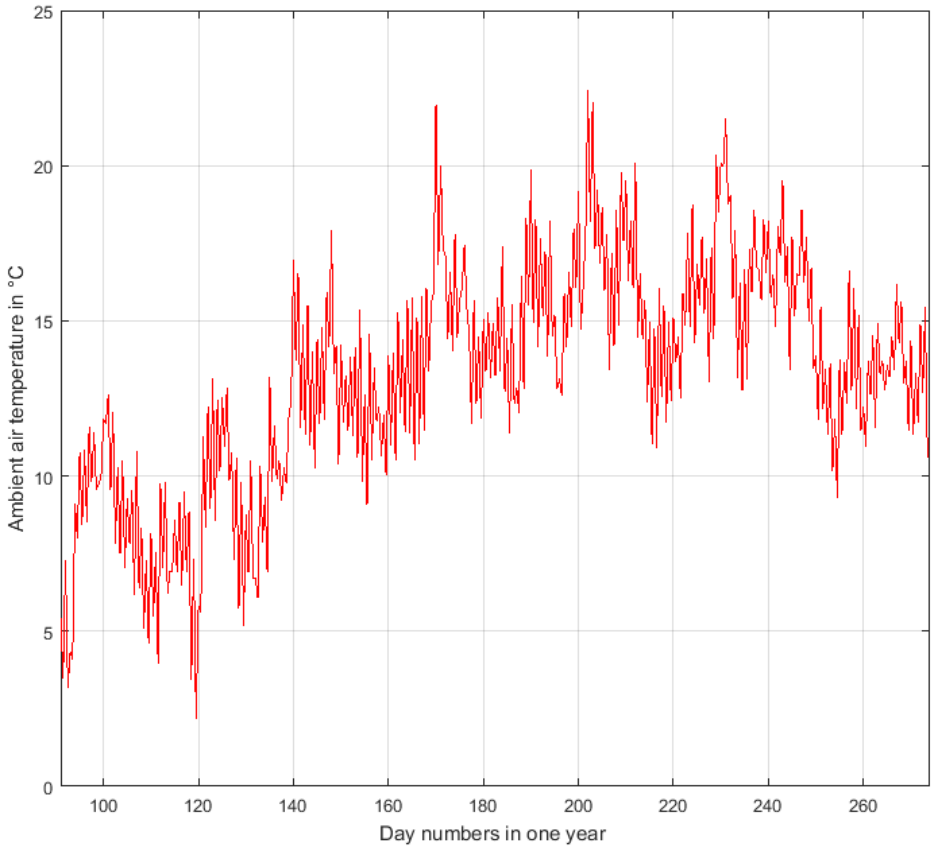

Figure 3-9 Summer ambient air temperatures within a year [13]

3.3.2 Air/Ground source heat pump (ASHP and GSHP)

In CHOICES, the ASHP and GSHP are the major low carbon technologies. The efficiency of the heat pump is called Coefficient of Performance (CoP). [1]

$$H = CoP \cdot P_{electricity} \tag{3-1}$$

Where

- H is the heat output (for ASHP in this thesis, H is the heat energy generated; for GSHP, H is the space heat demand). With higher heat pump inlet temperature, heat pump requires less electricity to generate the same amount of heat energy which results to a higher heat pump CoP and more efficient heat pump performance.
- $P_{electricity}$ electricity needed from the heat pump

The evaluation of the ASHP performance suggested 12% reduction of CO_2 compared to the gas boiler [18]. The operation cost increases 10% according to the application parameters[1] [18] [20]. Compared with the ASHP, GSHP always has a steady heat source. The ground temperature is much higher and more stable than the ambient air temperature in winter. However, the installation is very complicated [1, 19]. Table 3-2 and 3-3 are example heat pump operation temperature category used in the CHOICES project. Each heat pump inlet temperature has a different maximum electricity input which is called the maximum heat pump capacity. The detailed temperature categories of GSHP and ASHP are displayed in the Appendix A.

From the example temperature category, the GSHP and ASHP have the lowest lock-up temperature, and below the lock-up temperature, the heat pump will stop working. On the other hand, the CoP increases when the inlet evaporator or ambient air temperature increases.

Table 3-2 GSHP information [13]

	Evaporator inlet temperature (°C)	**Condenser Water Outlet Temperature (°C)**			
		30			
		Cooling (kW)	**Input (kW)**	**Heating (kW)**	**CoP**
GSHP	**-7**	50.1	16.8	66.2	3.94
	-1	62.8	16.9	79.1	4.68
	4	73.0	17.0	89.5	5.25
	6	78.1	17.1	94.7	5.54
	10	89.1	17.3	105.9	6.12
	11	92.1	17.4	109.0	6.28
	12	95.1	17.4	112	6.44
	15	105.2	17.7	122.5	6.92
	18	112	17.9	129.5	7.23
	21	122	18	139	7.69
	24	132	19	151	8.09

Table 3-3 ASHP information example [13]

	Air temperature (°C)	Condenser Water Outlet Temperature (°C)		
		30		
		Input (kW)	**Heating (kW)**	**CoP**
ASHP	**-20**	11.39	27.36	2.40
	-17	11.54	29.82	2.58
	-15	11.68	31.7	2.71
	-13	11.81	33.51	2.84
	-12	11.88	34.42	2.90
	-10	12.02	36.48	3.03
	-5	12.49	41.89	3.35
	0	12.93	47.92	3.71
	5	13.42	54.33	4.05
	7	13.62	57.07	4.19
	10	13.88	61.17	4.41
	15	14.29	68.02	4.76
	20	14.66	75.01	5.12

There are 6 condenser water outlet temperature categories and 7 condenser water outlet temperature categories for the GSHP and ASHP respectively.

Figure 3-10 and 3-11 show the linear relationship between CoP and inlet temperature for different condenser water outlet temperature categories. In order to simplify the CoP calculation in the following case studies and the operation of the heat pumps in this study is always within the proper inlet temperature range, the CoP value can be modelled with the following linear equation for both heat pumps:

$$CoP = a \cdot T + b \tag{3-2}$$

Where:

- a and b are constants depending on the manual of the heat pump with the required condenser outlet temperature (°C)

– T is the evaporator inlet/air temperature (°C)

Equation (3-3) to (3-15) are the values used in the CHOICES project [13] and are fitted in Figure 3-10 and Figure 3-11. When the condenser outlet temperature goes up, the CoP starts to increase with a lower base value.

- GSHP

  30°C Condenser Water Outlet Temperature

  $$CoP = 0.1362T + 4.8 \quad (3\text{-}3)$$

  35°C Condenser Water Outlet Temperature

  $$CoP = 0.1265T + 4.2 \quad (3\text{-}4)$$

  40°C Condenser Water Outlet Temperature

  $$CoP = 0.1135T + 3.7 \quad (3\text{-}5)$$

  45°C Condenser Water Outlet Temperature

  $$CoP = 0.1002T + 3.3 \quad (3\text{-}6)$$

  50°C Condenser Water Outlet Temperature

  $$CoP = 0.0918T + 2.8 \quad (3\text{-}7)$$

  55°C Condenser Water Outlet Temperature

  $$CoP = 0.0851T + 2.4 \quad (3\text{-}8)$$

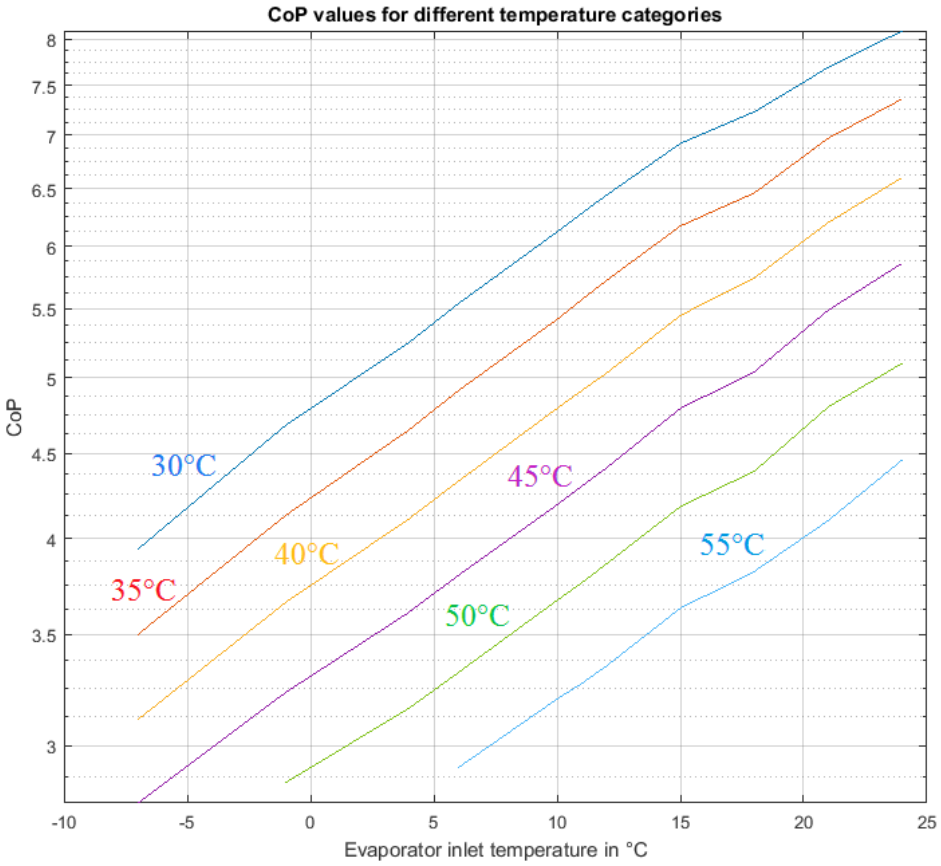

Figure 3-10 GSHP CoP values[13]

- ASHP

30°C Condenser Water Outlet Temperature

$$CoP = 0.068T + 3.7 \quad (3\text{-}9)$$

35°C Condenser Water Outlet Temperature

$$CoP = 0.062T + 3.4 \quad (3\text{-}10)$$

40°C Condenser Water Outlet Temperature

$$CoP = 0.057T + 3.1 \quad (3\text{-}11)$$

45°C Condenser Water Outlet Temperature

$$CoP = 0.051T + 2.8 \quad (3\text{-}12)$$

50°C Condenser Water Outlet Temperature

$$CoP = 0.047T + 2.5 \quad (3\text{-}13)$$

55°C Condenser Water Outlet Temperature

$$CoP = 0.0.042T + 2.3 \quad (3\text{-}14)$$

58°C Condenser Water Outlet Temperature

$$CoP = 0.0.039T + 2.2 \quad (3\text{-}15)$$

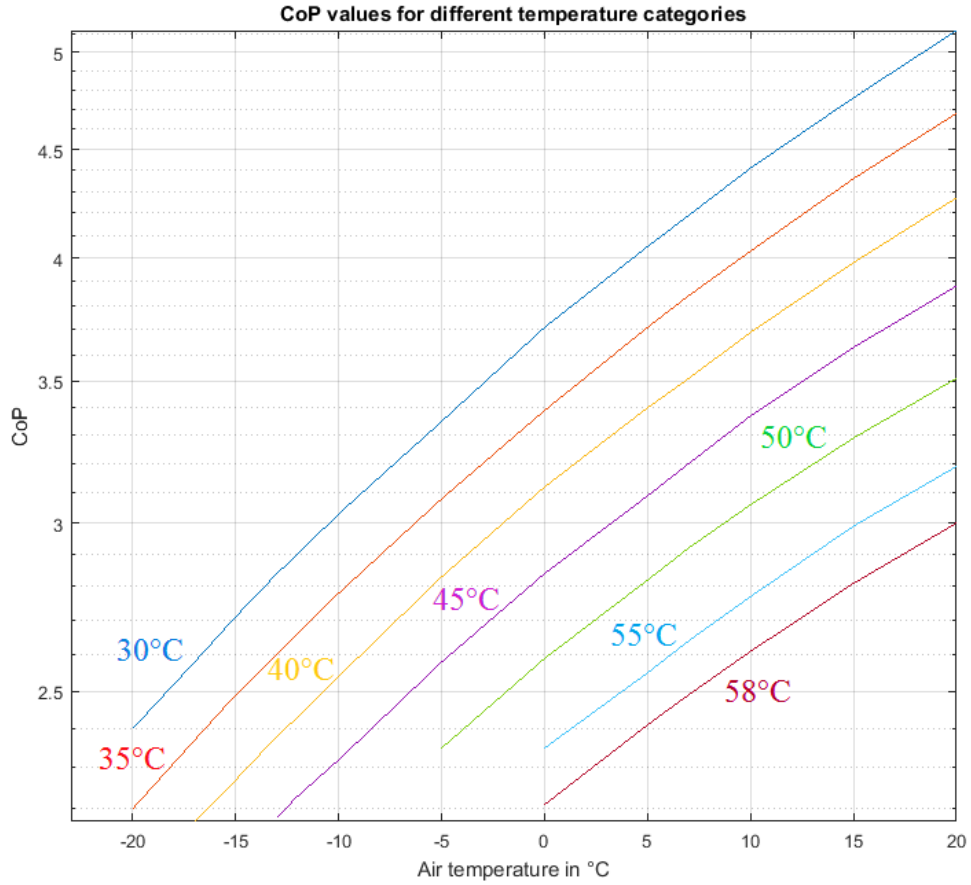

Figure 3-11 ASHP CoP values [13]

3.3.3 Borehole model and related parameters

From the charging and discharging system, the borehole temperature is the key factor affecting the performance of the GSHP in the discharging season. In this case study, the borehole model uses a simplified linear function.

With different heat flux, the temperature increases or decreases [1]:

$$\Delta T = T_{n+1} - T_n = \frac{H_{borehole} \cdot 3600 \cdot 1000}{C_{borehole} \cdot V_{borehole}} \quad (3\text{-}16)$$

Where:

- T_n is the temperature in the nth time step (°C)
- T_{n+1} is the temperature in the (n+1)th time step (°C)
- $H_{borehole}$ is the heat power supplied to(+)/extracted from(-) the borehole within the time step (kWh)
- $C_{borehole}$ is the volumetric heat capacity of the borehole (J/m^3/K)
- $V_{borehole}$ is the borehole array storage volume (m^3)

The CHOICES project has 12 boreholes buried under the ground. The Table 3-4 gives key parameters concerning the borehole array.

Table 3-4 Borehole installation data [13]

Borehole storage – properties	
Number of BH (-)	12
Depth (m)	150
Spacing (m)	6
Storage volume (m3)	50,894
Average ground thermal conductivity (W/m/K)	2.63
Average ground volumetric heat capacity (MJ/m3/K)	2.27

For the high-level energy chain analysis, it is to simplify things by considering the borehole array as a homogenous volume with homogenous heat injection. Using this data, the increased/decreased temperature ΔT changes the GSHP CoP:

$$CoP_{new} = a \cdot (T + \Delta T) + b = a\left(T + \frac{H_{borehole} \cdot 3600 \cdot 1000}{C_{borehole} \cdot 50894}\right) + b \quad (3\text{-}17)$$

In each new time step, the input/output heat energy from the ASHP/GSHP is calculated with the new heat pump CoP.

3.3.4 Heat demand of this community

The heat demand in the heating season in Table 3-5 is the total community heat demand in each heating (winter) season from historical billing data. For the sake of simplicity, heat demand is assumed to be constant during the winter. Therefore in each time step (12 hours) in the heating season, the heat demand is 412kWh calculated with equation

$$\frac{100000+50000}{182*2} = 412\ kWh \quad (3\text{-}18)$$

Table 3-5 Community buildings' heat demand during the winter [13]

Heat load	
Building details	**kWh/PA**
Easton Community centre	100000
Mosque	50000

3.3.5 Energy prices and CO_2 emission data used

Table 3-6 is the energy price for each type used for the later result analysis and comparison.

Table 3-6 Gas and grid electricity price [13]

GAS	**Average Cost £/kWh**	0.05
GRID SUPPLY PRICE WINTER	**Price £/kWh**	0.14

Table 3-7 is the CO_2 emission factors for the components in the study.

Table 3-7 CO2 emission [13]

CO2 Emissions	Gas	Grid Electricity	PV	ASHP	GSHP	Borehole	DC/AC
kg/kWh	0.20421	0.44548	0.07	0.01	0.01	0.01	0.01

3.4 Borehole energy chain case study

In this section, the case studies are dedicated to showing the avoided electricity consumption during the heating season due to different input and CO_2 emissions compared to the conventional gas heating.

3.4.1 Traditional (Existing) community heating network

The incumbent heating for the CHOICES community buildings is from gas boilers used during the winter. The gas boilers have efficiency conservatively estimated to be 0.85. Therefore for a 412 kWh heat demand, gas with a calorific content of 484 kWh will be required in practice.

For the CO_2 emissions, there will be 0.20421 kg CO_2 emission per kWh heat generated [84]. During the heating season, the total CO_2 emission will be about 30,631 kg CO_2 emission per heating season. The detailed excel document of boiler operation is in Appendix B.

3.4.2 Borehole operation with active charging during the summer

In this case, the installation of PV is 36 kW. The electricity generated from the PV is used for the operating heat pumps in both charging and discharging season. However, during the winter time, the grid and PV will work together to support the GSHP electricity consumption.

During the summertime, the ASHP injects heat to the borehole and the condenser water category is 30 °C so that Equation (3-9) is used. According to the ambient air temperature Figure 3-9, the ASHP CoP during the summer is shown in Figure 3-12.

With the electricity generated from the PV, the heat from the ASHP can be calculated using Equation (3-1). With the heat injection the borehole temperature increases.

In Figure 3-13, the blue line is the heat output from ASHP as well as the borehole heat input. The heat energy values during the charging time are calculated from the temperature profile in Figure 3-9. The red line is the borehole temperature change due to the heat input. From this figure, with the constant heat input, the borehole temperature keeps increasing.

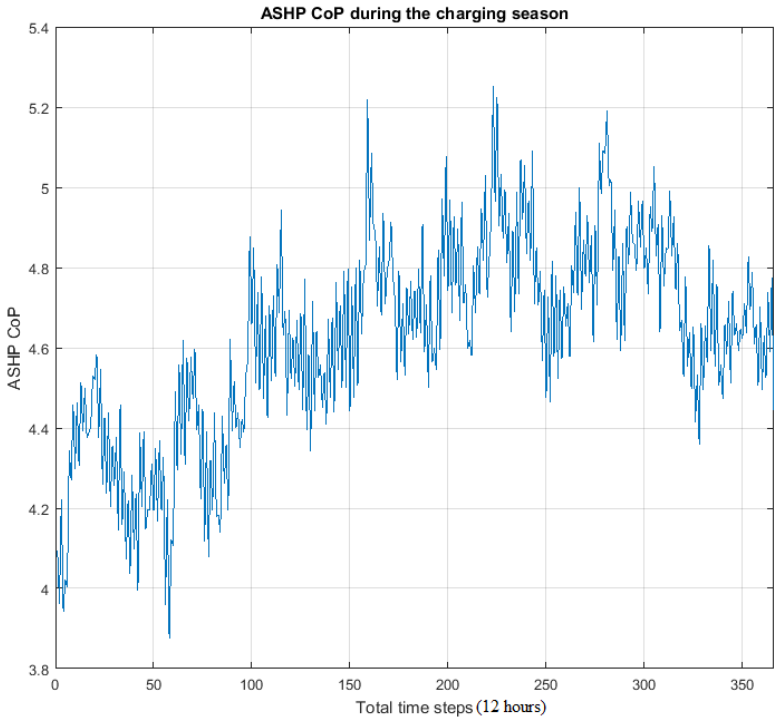

Figure 3-12 ASHP CoP during the charging season

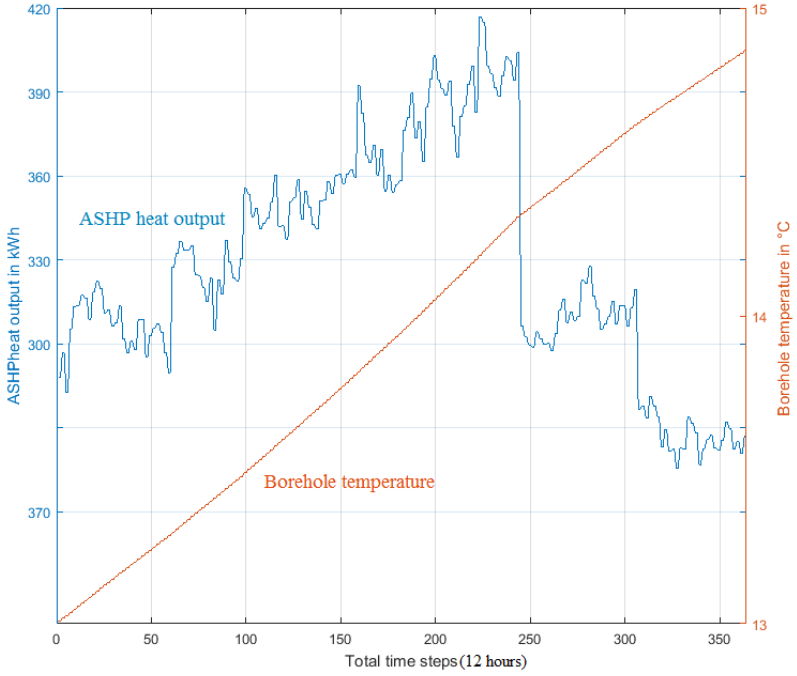

Figure 3-13 ASHP heat output and borehole temperature profile in charging season

The borehole in this chapter is a lumped model including the whole storage area as a result, the model is considered that there is no heat transfer outside the whole borehole storage volume. Because, as an inter-seasonal heat storage, the discharging season closely follows the charging season, so that the borehole temperature at the end of the charging season is the starting temperature in the borehole discharging season. The heat demand is for community buildings and for this high level energy chain analysis, it is assumed to have a constant heat demand at the same level. In the discharging season, with the constant heat extraction from the borehole, the temperature decreases as shown in Figure 3-14. In each time step, the temperature decreases according to Equation (3-16).

As stated early in this chapter, the borehole provides the evaporator inlet temperature for GSHP so that the CoP of GSHP is related to the borehole temperature. In this CHOICES project, the GSHP condenser water outlet temperature is set to 45 °C. According to the GSHP operation information, Equation (3-6) is used under 45°C category. The value of CoP in each time step decides the electricity consumption of the GSHP. Figure 3-15 shows the GSHP CoP values and electricity consumption during the discharging season. With constant heat withdraw from the borehole, due to the dropping temperature, GSHP electricity consumption is increasing along with the decreasing CoP value.

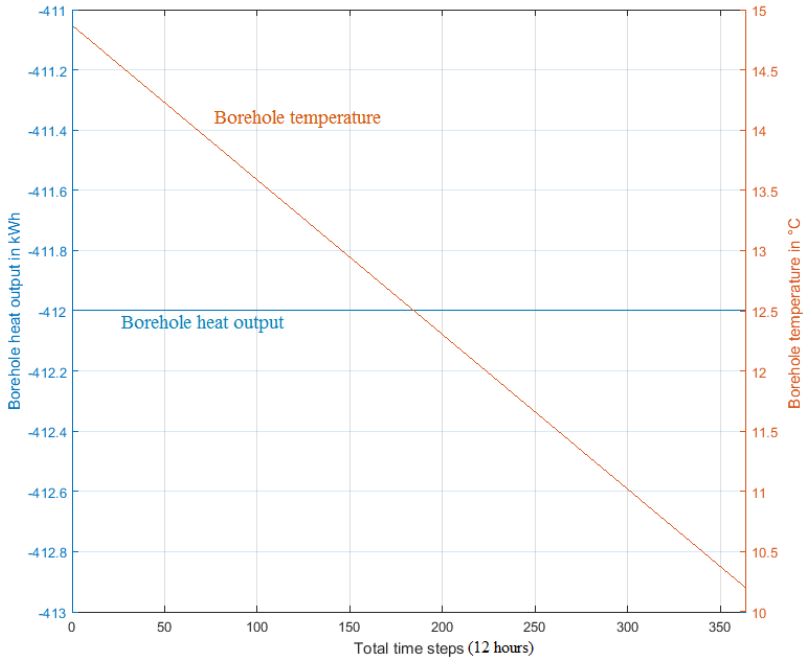

Figure 3-14 Borehole heat extraction and temperature profile in discharging season

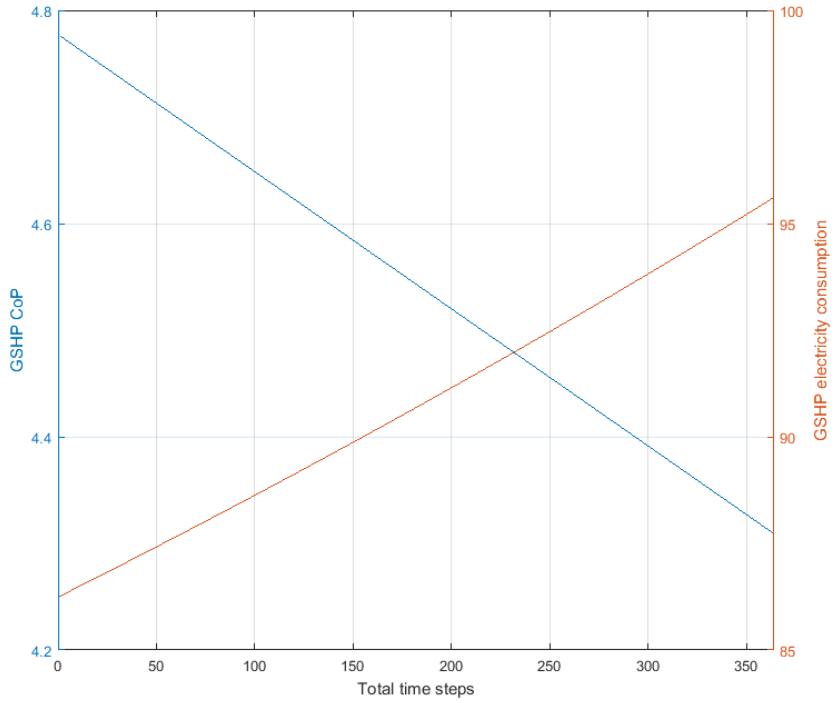

Figure 3-15 GSHP temperature and CoP profiles

3.4.3 Borehole operation without active charging

In this scenario, the borehole is not charged during the summer and the electricity generated by the PV and the grid electricity provide the GSHP electricity consumption. The borehole starting temperature is the same as the ground temperature which is 13°C.

Under the same discharging season heat demand, the borehole temperature is shown in Figure 3-16. In this scenario, the borehole temperature reaches the lockout the temperature of the GSHP within a few discharging seasons, thus making a strong case for active recharging.

The decreasing borehole temperature leads to a decreasing GSHP CoP in Figure 3-17. With the heat extraction from the borehole during each time step, the temperature is decreasing. From the heat pump information in this chapter, with the decreasing evaporate inlet temperature, the CoP of GSHP is decreasing accordingly and the electricity consumption during the discharging season increases due to the dropping GSHP performance as is shown in Figure 3-17.

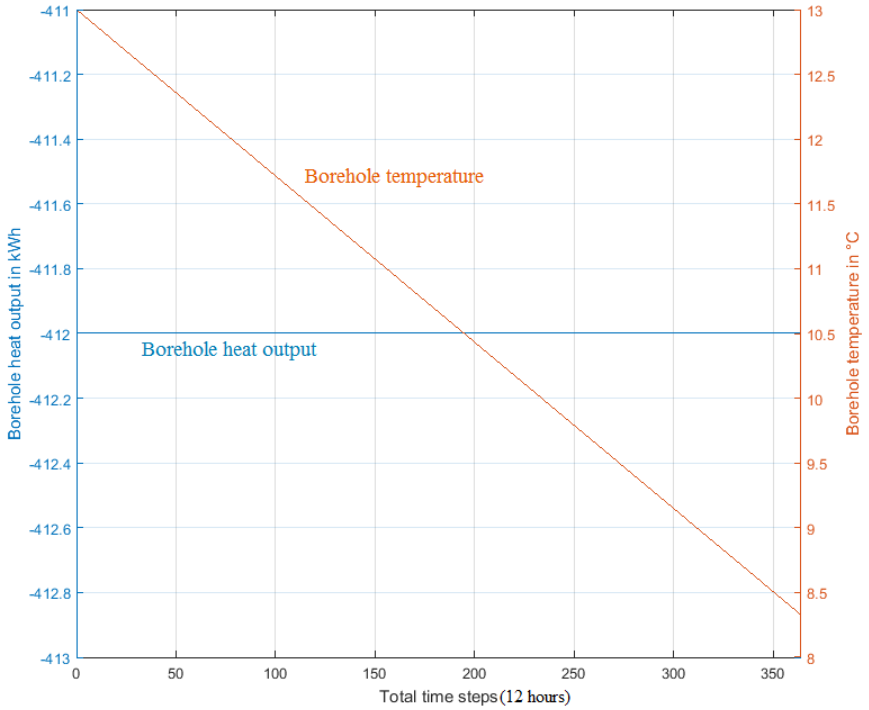

Figure 3-16 Borehole heat extraction and temperature profile in discharging season

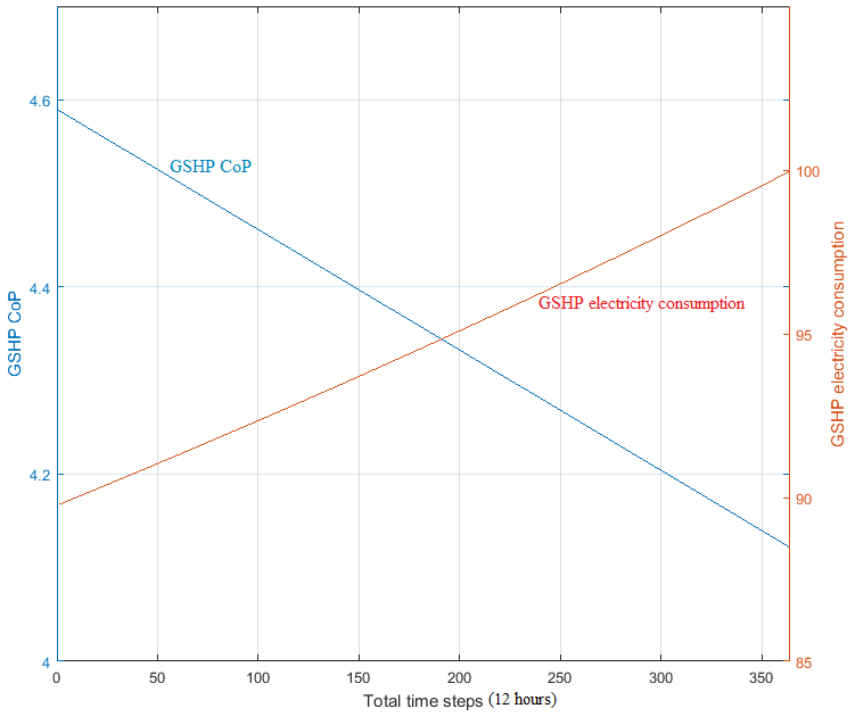

Figure 3-17 GSHP temperature and CoP profiles

3.5 Case study comparison and analysis

In the borehole system, the GSHP supplies the same amount of space heat demand as the gas heat network for the community buildings. The cost of operating the borehole system during the discharging season depends on the amount of grid electricity consumed by the GSHP excluding maintenance fees.

The comparison between different cases in this chapter is based on the same total space heating demand, according to the CHOICES project and community information, the installed conventional gas boiler uses £8,823.5 of gas to supply the community space heat demand. For the proposed borehole space heating system, electricity is used to provide the space heating the electricity mainly comes from free PV electricity and the grid electricity. In the two borehole system cases, the grid electricity costs during the winter time are £4,382.4 in the non-charged case and £4,269.6 in the charged case. The electricity and gas price can be found in Table 3-6.

During one discharging season, the CO_2 emission is shown in Table 3-8.

Table 3-8 CO_2 emissions in three systems in discharging season

CO_2 emission in one discharging season	**kg**
Boiler	30631.5
Charged case	16863.1
Non-charged case	17222.2

The borehole system generally reduces over 40% CO_2 emission in one discharging season. The boiler operation table is in Appendix B.

By comparing the two base case studies, the electricity consumption with summer charging is less than the case without the summer charging as is shown in Figure 3-18. Because the borehole model used in this chapter is a lump model with its storage area and it is assumed that there is no extra heat transfer outside the storage volume, when the heat is extracted from the borehole the temperature decreases linearly, as a result, the CoP of the GSHP is decreasing according to the borehole temperature. For the same heat energy proving to the community centre at each time step, GSHP consumes more electricity. The total electricity consumption difference is 806 kWh in one discharging season.

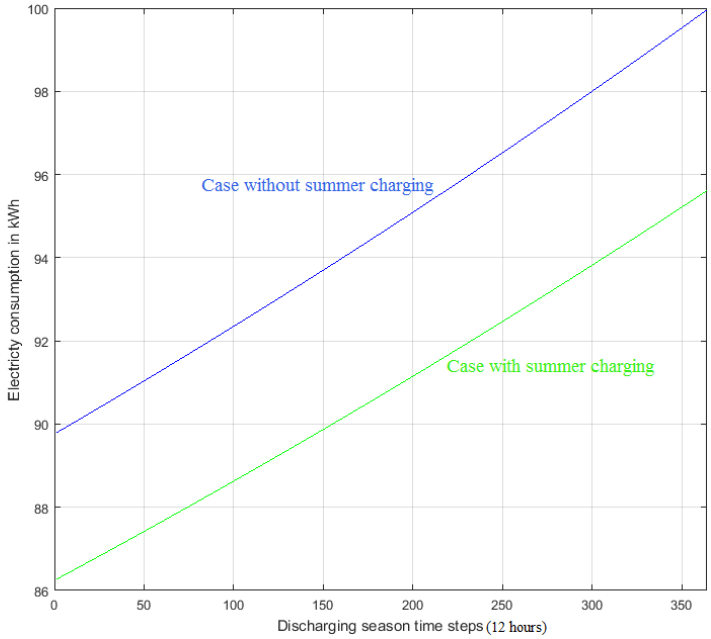

Figure 3-18 Electricity consumptions in two cases with summer charging and without summer charging

Within the GSHP electricity consumption during the discharging season, both installed PV and the grid contribute to GSHP electricity usage. The installed PV during the discharging season has the same total electricity generation 3,164.58kWh, which is not enough to operate the GSHP to supply the community space heating. The grid provides 2.6% more electricity in the non-charged case than the charged case.

In the long-term study for both cases, such as 5 years, the borehole temperature changes as shown in Figure 3-19. In each discharging season, the temperature difference is increasing. In the case with summer charging, the summer charging process helps to lift up the borehole starting temperature at the beginning of each discharging season. From the temperature figure, both cases have a decreasing temperature trend and it is possible that GSHP would face the lockup the temperature and stop working eventually due to the lack of active charging. With enough charging during the summer, this situation can be avoided.

In Figure 3-20, the yellow line is the 5 years discharging season grid electricity consumptions in the non-charged case and the red line is for the charged case. From the first year of the operation, the electricity consumption is increasing fast from 30,000 kWh to 55,000 kWh (yellow line) and with active charging each year, the electricity consumption increases slowly. The stem numbers show the percentage of extra grid electricity needed in the non-charged case compared with the charged case and the percentage is increasing from 0.5% to 4.5% which

indicates that without the active charge the efficiency of this space heating system is decreasing each year during the heating season.

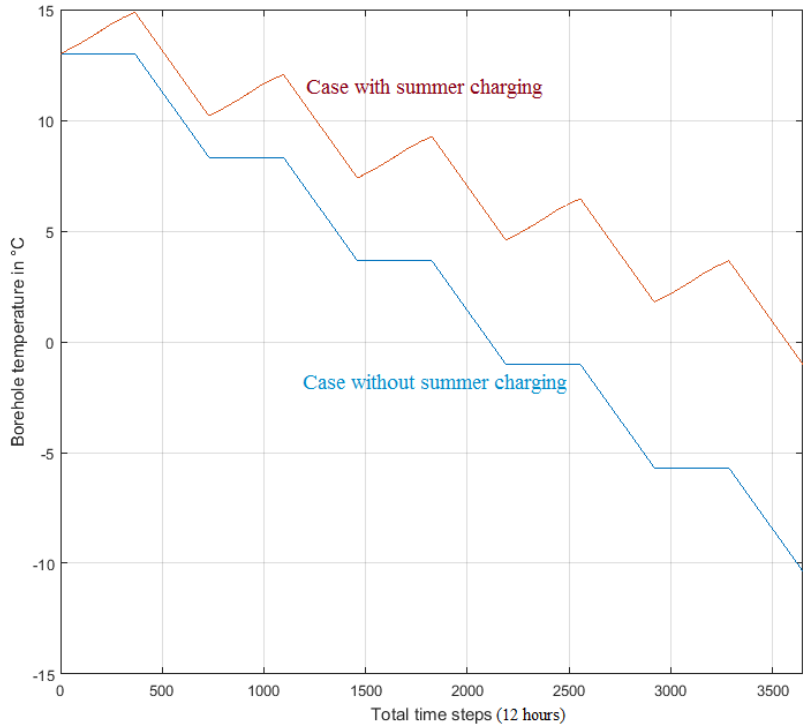

Figure 3-19 Borehole temperatures in 5 years

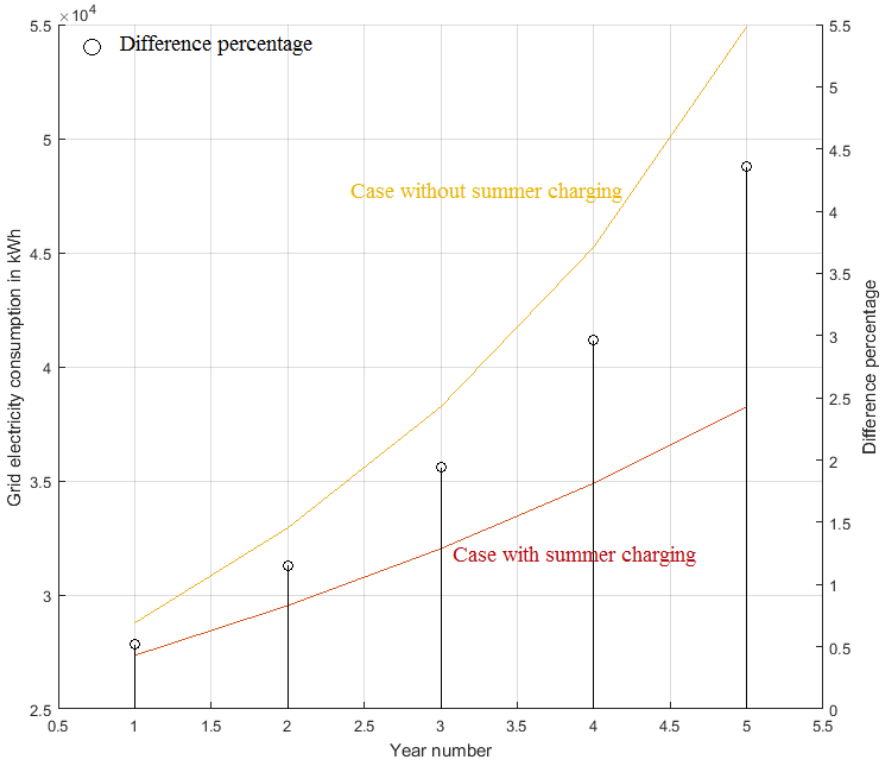

Figure 3-20 Discharging season grid electricity consumption comparison

3.6 Chapter summary

This chapter describes the high-level energy chain analysis conducted for the phase 1 feasibility study for the CHOICES project, an innovative decarbonised heat network project using borehole inter-seasonal heat transfer. The high-level energy chain is introduced followed by different charging case studies. This high-level energy chain study gives a brief introduction of the borehole heat energy storage and its long-term benefit and advantages compared to the traditional gas heating.

The borehole model used in Chapter 3 is a simplified linear function, using a homogeneous thermal mass with uniform heat injection. The linear function does not consider the distributed nature of the various heat storage media, their different properties and the heat transfer between the boreholes and the surrounding soil and bedrock. The simplified model suggests that the system quickly reaches the GSHP lock up the temperature even with moderate summer recharging. This suggests heavy summer recharging is required just to make the scheme viable as a primary source of heating.

The conclusion from this chapter is the requirement for an accurate borehole array model that accounts for detailed heat transfer between different media. Therefore in Chapter 4, the borehole system will be built in the MATLAB environment to facilitate detailed short-term and long-term operational case studies.

4 Borehole field modelling

4.1 Introduction

In this section, a Finite Element model of the community level borehole storage is introduced. The basic borehole information is from the practical project CHOICES funded by DECC (now BEIS) under the SBRI heat networks stream. From the phase one, the borehole model is based on the linear function which does not take the surrounding environment into account. In Chapter 4, the accurate borehole model responds to an input/output heat with the temperature changing. The temperature dictates the performance of the heat pump. In this section, the modelling environment is introduced, followed by a detailed modelling of the borehole arrays based on the actual CHOICES project borehole layout. The borehole behaviour due to the heat flux injection/extraction over a certain time period is presented and discussed in the later sections.

4.2 PDE Toolbox

The borehole layout and the ground parameters from the CHOICES project are used as the borehole field modelling basic settings. For the modelling of the borehole, the borehole real geometry. The modelling of the borehole array is achieved using the Partial Differential Equation (PDE) toolbox in the MATLAB environment. The PDE Toolbox allows the user to model the geometric layout and generates the borehole heat map by solving the partial differential equations associated with transient heat transfer through conduction. The Finite Element solves Partial Differential Equations in different dimensions (2D and 3D) and time. As a result, the borehole model under this condition can thoroughly and accurately present the temperature behaviour and the heat transfer between different media and boreholes. There are 4 PDE solvers are elliptic, parabolic, hyperbolic, and eigenvalue problems. The PDE can solve problems across diffusion, heat transfer, structural mechanics, electrostatics, magnetostatics, conductive Media DC, and AC power electromagnetics, as well as custom, coupled systems of PDEs.

For setting up the PDE problem, there are several steps:

- Choose the appropriate area.

Different problems will have the different Boundary/PDE specification settings.

- Create the geometry for the problem.

  In creating the geometry of the problem, the operators are '+', '-', and '*' are the set union operator, the difference operator and the intersection operator, among which '-' has higher precedence. Using these three operators, boundaries, edges and subdomains can be created between the circle object, polygon object, rectangle object and ellipse object.

- Set boundary/edge/subdomain conditions and PDE coefficients in the geometry.

  After the boundaries, edges, and subdomains are defined, the appropriate boundary condition (Neumann and Dirchlet) and the PDE specification (Elliptic, Parabolic, Hyperbolic and Eigenmodes) with its unique value.

  In the PDE tool there are two types of boundary condition:

  Neumann: $$n * k * grad(T) + q * T = g \quad (4\text{-}1)$$

  Dirchlet: $$h * T = r \quad (4\text{-}2)$$

  g: Heat flux.

  q: Heat transfer coefficient.

  h: Weight.

  r: Temperature.

  Four types of PDE specification as mentioned before, and for the heat transfer of this borehole model, Parabolic is used:

  Parabolic: $$rho * c * T' - div\big(k * grad(T)\big) = \mathrm{Q} + \mathrm{h} * (T_{ext} - \mathrm{T}) \quad (4\text{-}3)$$

  k: Coefficient of heat conduction.

  Q: Heat source.

  h: Convective heat transfer coefficient.

  T_{ext}: External temperature.

  u: Solution of temperature.

  c, a, f, and d are coefficients. Each of the coefficient is given an expression in the triangle centres of mass which includes x- and y- coordinates, sd the subdomain number, ux and uy the derivatives of the solution and t the time.

  The Fourier's law:

$$q_x = -k\frac{dT}{dx} \quad (4\text{-}4)$$

States that the heat flux is equal to the thermal conductivity through multiplied by the temperature gradient. Borehole model is a function of transient temperature change due to the heat flux which has thermal resistance and thermal capacitance. The heat storage ability is a transient problem so that the differential equation will be used. Equation (4-3) the parabolic performs the temperature calculation.

- Generate mesh.

  The initial mesh generates fewer triangles to fill the subdomains, then the mesh is refined or jiggled, the model tends to give more accurate results, however, the model takes a longer time to solve and display the result.

- Initial conditions.

  Initial condition gives the result status at $t_{(0)}$ time, length of the time interval and total simulation time.

The PDE toolbox working environment is easy to operate:

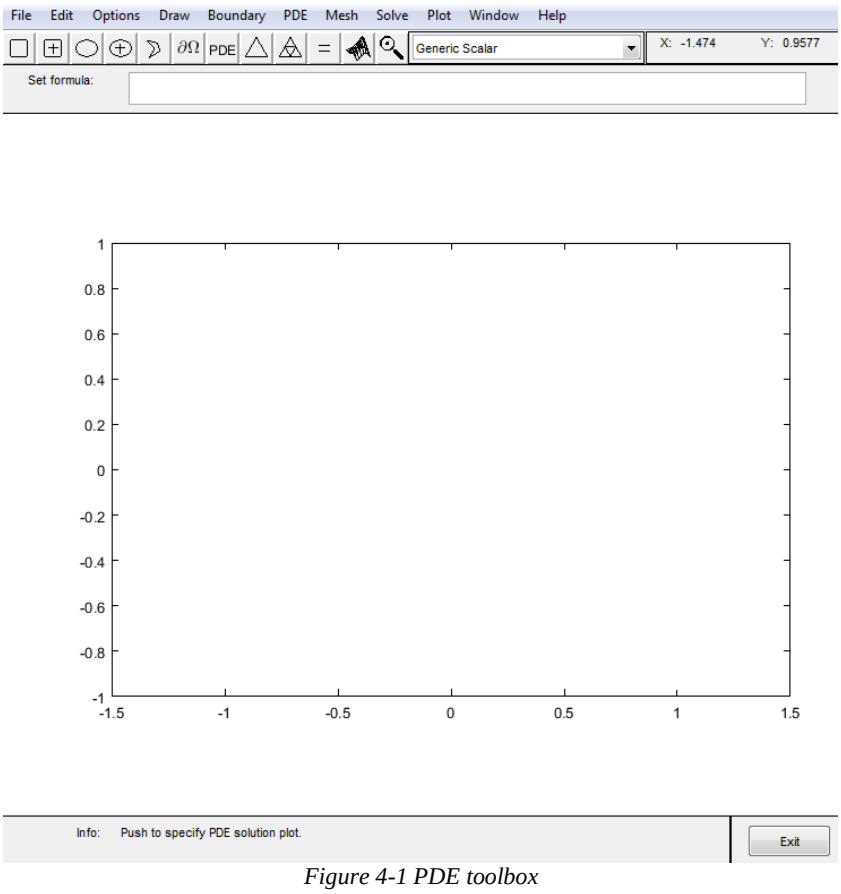

Figure 4-1 PDE toolbox

The square, circle and random shape buttons are used for drawing boundaries and dividing subdomains. The menu bar provides visual displays and results in exportation. The set formula can be manually typed in to define the subdomains.

Solving the PDEs programmatically through command-line function is an alternative to the PDE app when there are other functions involved, such as nonstandard boundary conditions, different variables in the system, variable constraints, etc.

By using the command-line functions, the geometry, boundary condition, boundary, mesh data, and coefficients will be a different matrix and other data types according to the mesh coordinates. The export facility mentioned before helps to provide correct syntax of different data structures.

4.3 Borehole model and parameters

4.3.1 Borehole model layout

The CHOICES project was carried on in the community park in Bristol as is shown in the Figure 4-2 below:

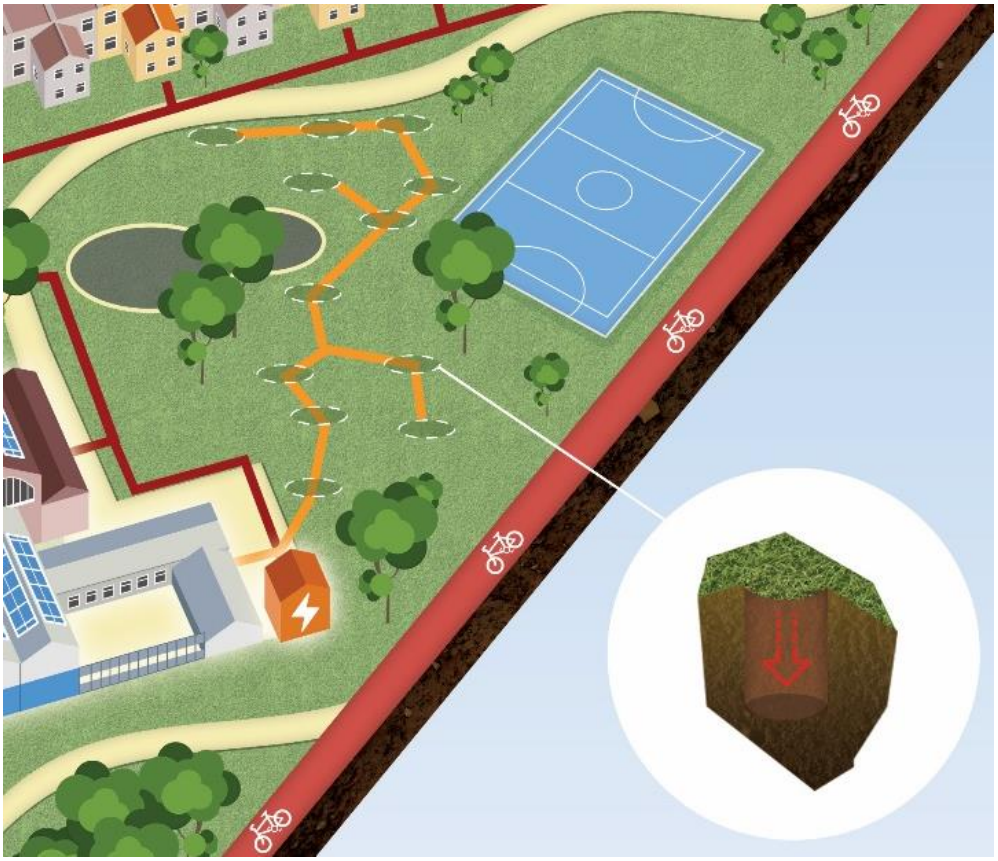

Figure 4-2 Proposed CHOICES project borehole arrays layout in the park

In the borehole arrays layout picture, the dashed line circles represent the 12 boreholes used to provide community building space heating. The geometry location will be used in the model in Figure 4-3.

Each borehole has its own x- and y- coordinates according to the CHOICES project, (-24.3, -3.4), (-11.4, -8.1), (3.5, 5.2), (-17.1, 4.1), (-6.6, 3.8), (-6.6, 11.8), (7.5, 1.7), (16.7, 1.7), (23.9, 10.5), (23.9, 19.3), (26.5, 1.7), (33.4, 7.9), as shown in Figure 4-3:

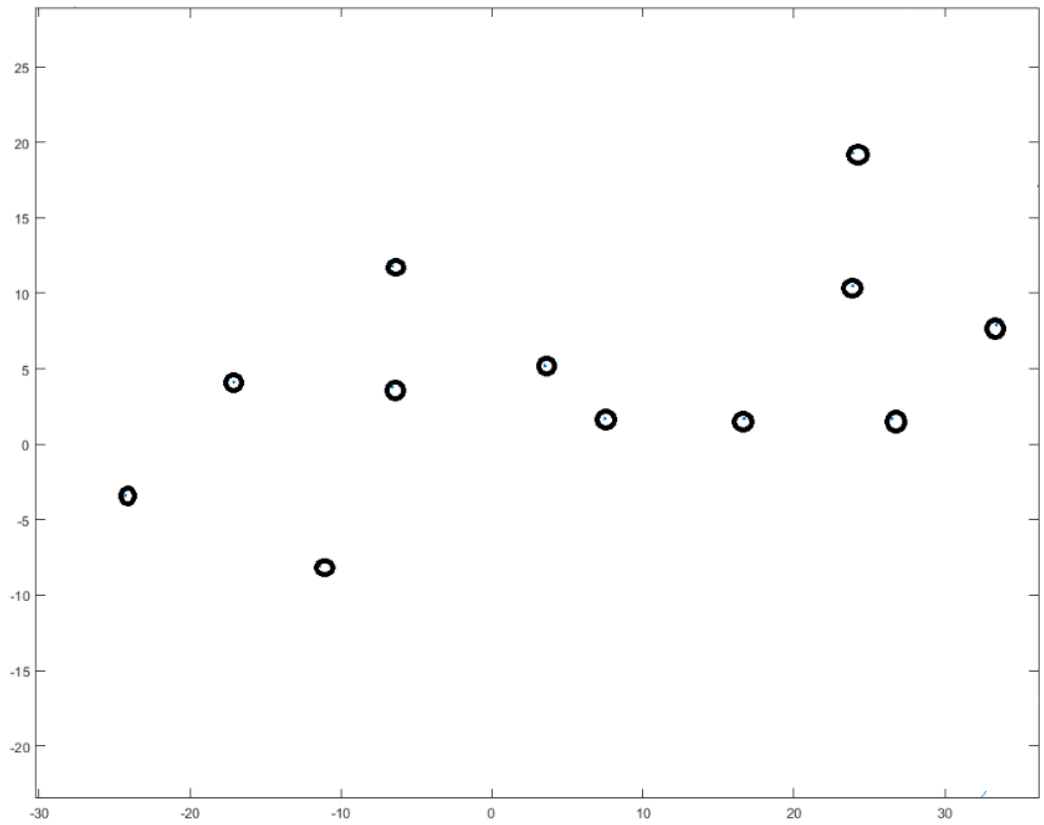

Figure 4-3 Borehole coordinates

The dark circles are the borehole locations. The borehole connection has two types:

- In parallel
- In series

In this project and model, the parallel connection is used. For each borehole, the heat flux is considered as $1/12^{th}$ of the total heat injection and extraction.

For each borehole, there are a U shaped tube, grout, and the surrounding soil. The cross-sections look like Figure 4-4.

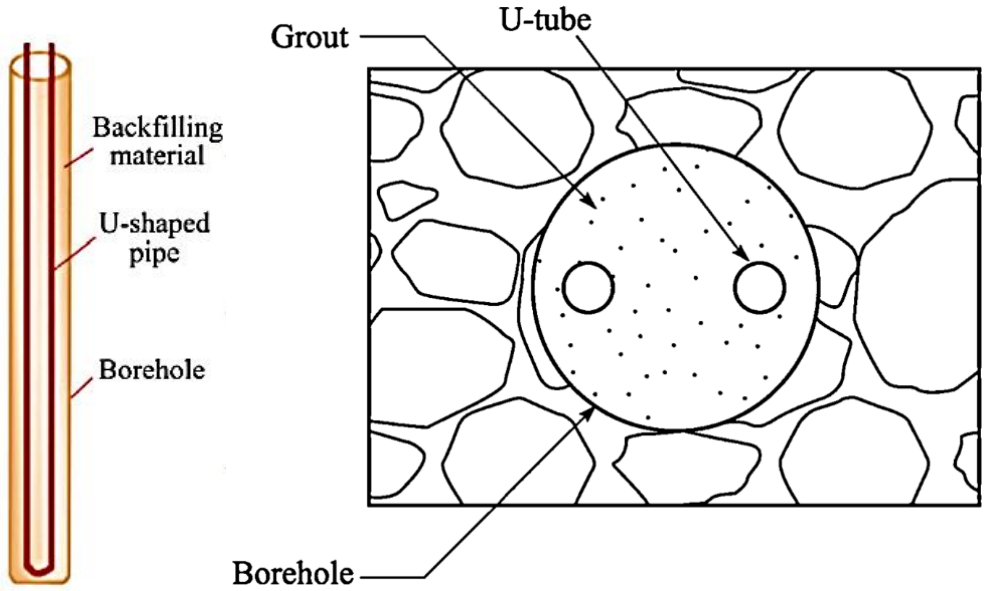

Figure 4-4 Borehole vertical and horizontal cross-sections [34, 52]

In the CHOICES project, the borehole diameters of the borehole and U-tube are 15cm and 3.26cm. Due to the small size of the borehole U-tube, the fluid circulating regions for one borehole can be simplified to a single circle region. However, the diameter of the U-tube becomes the radius (r) of this new single circle region. As a result, the horizontal cross-section in the FE model is as below:

For each borehole, the volume in the U-tube is related to the cross-section area and the depth of the borehole (d). In CHOICES project, l equals to 150 m. As a result, the volume of a single borehole is:

$$V = \pi r^2 * d = 0.5\, m^3 \tag{4-5}$$

According to the real size of the Owen Community Park, this 12-borehole system is built within a 40 radius circle in MATLAB as shown in Figure 4-6. The MATLAB code is in Appendix C.

As is shown in Figure 4-4, the borehole is a 3-D model, however, in this chapter, the depth dimension is assumed to be uniform so that the 2-D model was built to study the borehole temperature behaviour due to the heat flow. As the borehole cross-section is considered as unstructured grid, the triangular mesh is used. In this borehole layout map, there are approximately 1,275,659 triangles generated and the final heat map will be the temperature result formed by these 1,275,659 triangles. For all the nodes (vertex), there is one simultaneous

equation and the unknown is the temperature. The edges connect the adjacent vertices. The mesh in each region represents different material and the material heat transfer parameters are set in the model. The temperature is measured at each node and the desired nodes are the ones

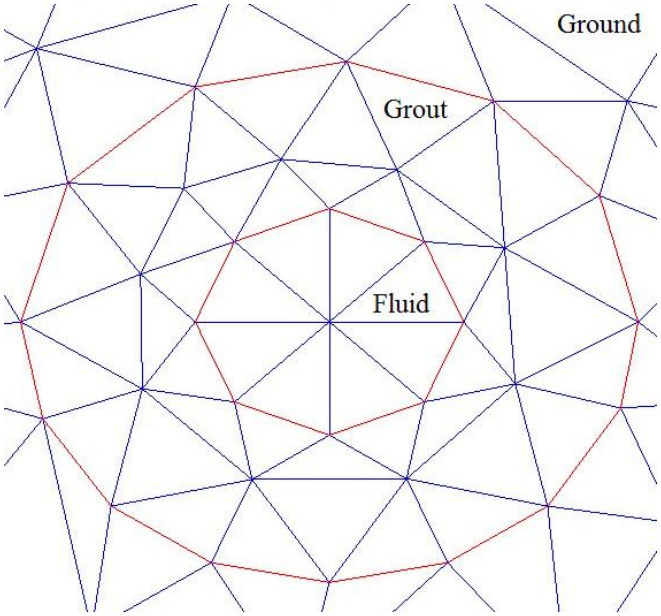

Figure 4-5 Single borehole in the FE model

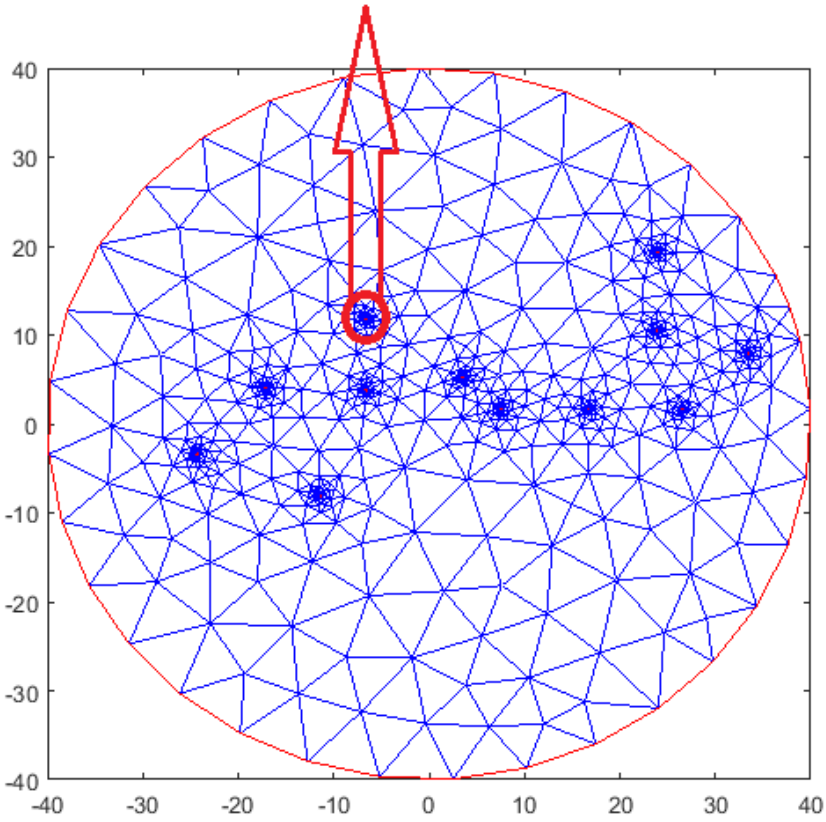

Figure 4-6 12-borehole system layout in MATLAB FE model

at the borehole walls. As a result, in the later study, the borehole wall points will be selected from the temperature excel file generated by running the model.

4.3.2 Borehole geometry parameters

The soil temperature varies in location and from month to month. It is a function of solar radiation, rain, air temperature, type of soil and depth underground. However, the ground temperature below certain depth is very steady. The temperature of the soil is approximately 8-10 °C 15 m below the surface of the earth which is close to the annual mean air temperature, and the temperature increases by, on average, 2.6°C per 100 m. Hence, during the winter time, the ground temperature is higher than the air temperature [85]. In this CHOICES project, the ground temperature used is 12.67°C.

As mentioned in the last subsection, borehole U-tube has two layers which are the circulating fluid and the grout (backfilling material), which are surrounded by the ground. Different locations have various ground density, heat capacity and thermal conductivity which will affect the heat transfer between each material. The table below shows the unique parameters for each material in the CHOICES project:

Table 4-1 Borehole parameters [13]

	Ground	**Fluid**	**Grout**
Density (kg/m^3)	2770	1052	1550
Heat capacity (J/(kg.K))	883	3795	1000
Thermal conductivity (W/(m.K))	2.89	0.5	2.1

4.4 Borehole behaviour study

The input heat flux will vary with time and the borehole model may be used to discern the temperature variation. In the PDE toolbox, the unit of heat flux is in W/m^3. In this section, the characteristics of the borehole temperature due to the changing heat flux are presented.

Heat flux is the rate of heat energy flow through a surface per unit time. The unit of heat flux is in W/m^2. However, under the MATLAB PDE toolbox, the heat flux is measured in W/m^3 for transient heat transfer problem. From Chapter 3, the heat flux input is related to the air

source heat pump which is affected by electricity generated by the roof-mounted photovoltaic and the ambient air temperature. As a result, the heat flux varies between 0 to 800 W/m^3.

The borehole heat energy storage discharges during the winter time so that one year can be seen as split between charging and discharging seasons. In this section, for the simulation, the time interval was set to 24 hours. There will be 180 total simulation steps in each season within the charging season, it is assumed that, the heat flux injection and extraction are constant processes during the charging and discharging seasons respectively. The simulation has 5 cases, no charging, maximum charging capacity, discharging only, short-term and lifetime simulation.

4.4.1 Borehole wall temperature selection

The PDE toolbox exported the temperature of all nodes of the borehole model which are 1438 points. All the temperature nodes in the model are used to calculate the temperature changing across the borehole model step after step and all the heat transfer process is happening between each node so that the single node's temperature profile includes all the influence coming from the surrounding area. As is shown in Figure 4-6, the majority of the nodes are located outside of the borehole wall and for the later study, the only borehole wall temperature is assumed to be the fluid temperature. During the charging process, the fluid temperature is much higher than the borehole wall temperature. However, the fluid the temperature settles down quickly between the fluid and the borehole wall and the fluid uses the energy stored in the borehole wall during the discharging season, it is assumed that the fluid and the borehole wall have the same temperature so that the borehole wall temperature nodes are selected for the study.

In section 4.3.1, Figure 4-5 clearly shows the single borehole structure. By the end of charging/discharging season, the central node represents the fluid which is the highest/lowest 12 points and the borehole wall is defined as the inner surface of the grout part which are the second highest/ lowest 8 points for each borehole. From the massive mesh points temperature excel file generated by running the borehole code, point 332 to 343 are the 12 fluid points and point 63 to 110 and 173 to 220 are the borehole wall points. Figure 4-7 and 4-8 are the detailed point to point temperature at the final time step in charging and discharging seasons. The borehole wall and fluid temperature points are marked in the following figures and in the latter study, the average borehole wall temperature and fluid temperature are automatically selected.

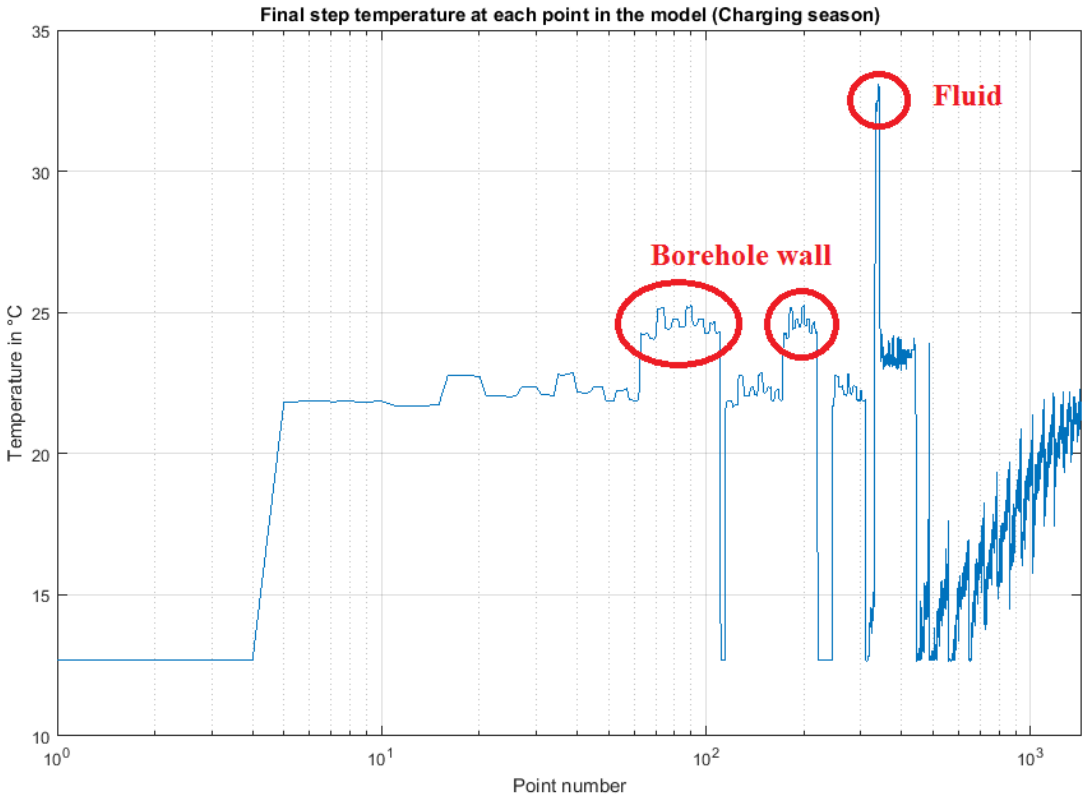

Figure 4-7 Charging season point temperature

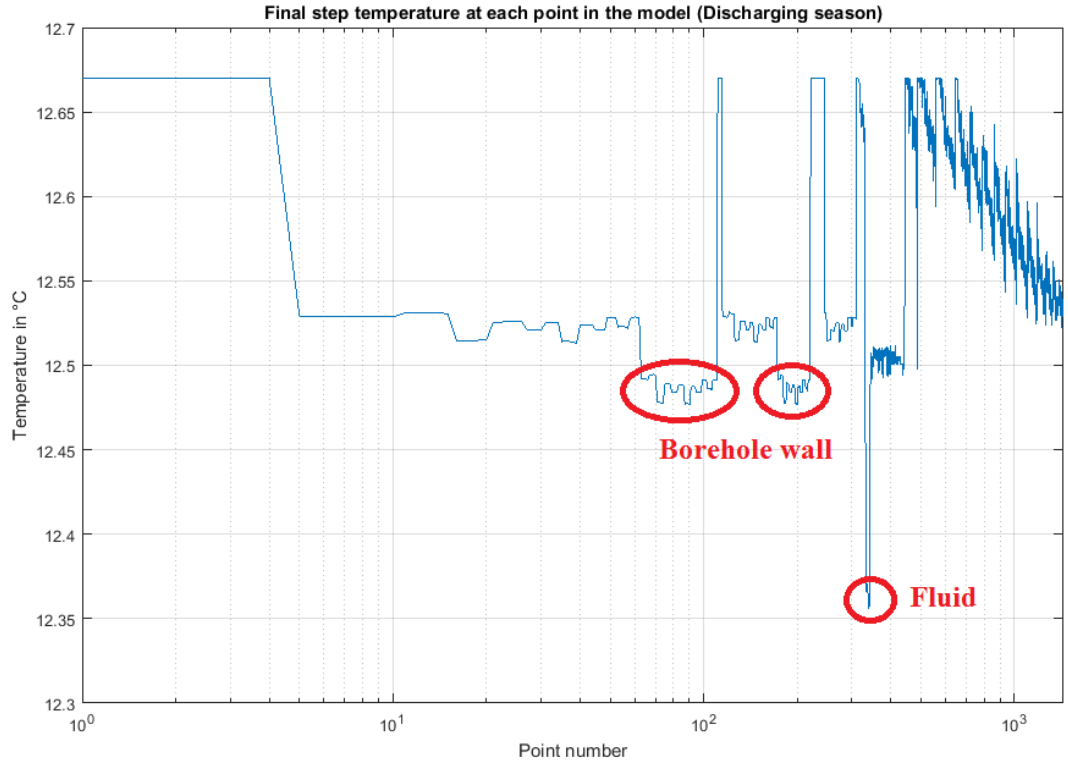

Figure 4-8 Discharging season point temperature

These two figures share the same characteristics. By crossing check the number and temperature of each point, the fluid and borehole wall temperature points are defined as the red circle marks.

The fluid temperature is very straightforward because there are only 12 points. For the Borehole wall temperature, the mean value of the 96 points is measured due to the reason that the 12 boreholes are connected in parallel. In the latter study, only the borehole wall temperature is selected from each temperature file to determine the performance of GSHP.

4.4.2 No heat flux input/initial study

With no heat flux input or the initial point, the borehole fluid and grout (backfilling) temperatures remain the same as the initial ground temperature, 12.67°C.

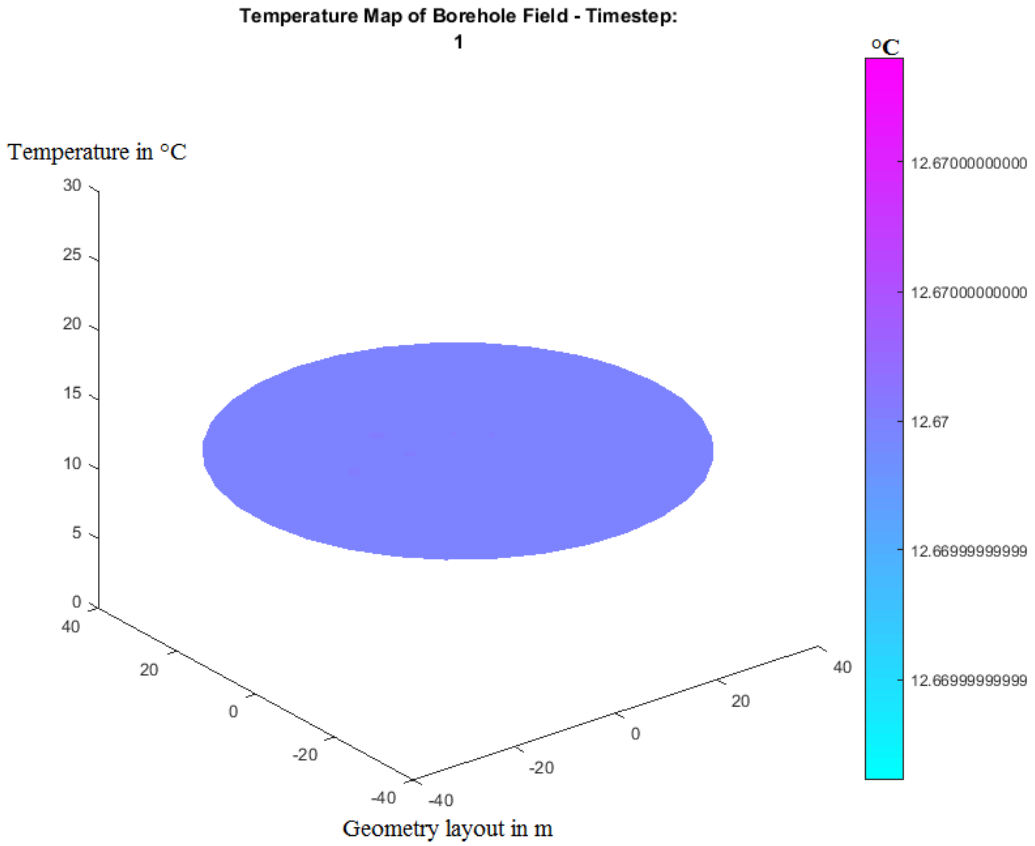

Figure 4-9 0 W/m^3 heat flux input/ initial Heatmap

4.4.3 Maximum heat flux charging season study

Considering that in practice, the borehole heat input in the charging season depends on the air source heat pump. Therefore in this case study, different maximum input heat flux will be studied to show the borehole temperature reaction to different maximum charging.

For the current community heating system, the air source heat pump provides 800 W/m^3 maximum heat flux at any given time. For a larger heating system, the maximum available heat flux could be larger. During the case comparisons, two heat flux values are used during the charging seasons: 800 W/m^3 and 1600 W/m^3.

Figure 4-10, 4-11 and 4-12are the borehole heat maps and temperature comparison between different maximum charging cases. It is obvious that higher heat flux input leads to a higher final temperature. With lower heat flux input in Figure 4-10, the maximum temperature is lower than the higher heat flux input in Figure 4-11. In both figures, the temperature is higher around the centre of each borehole especial the fluid and the far field almost remains the initial temperature.

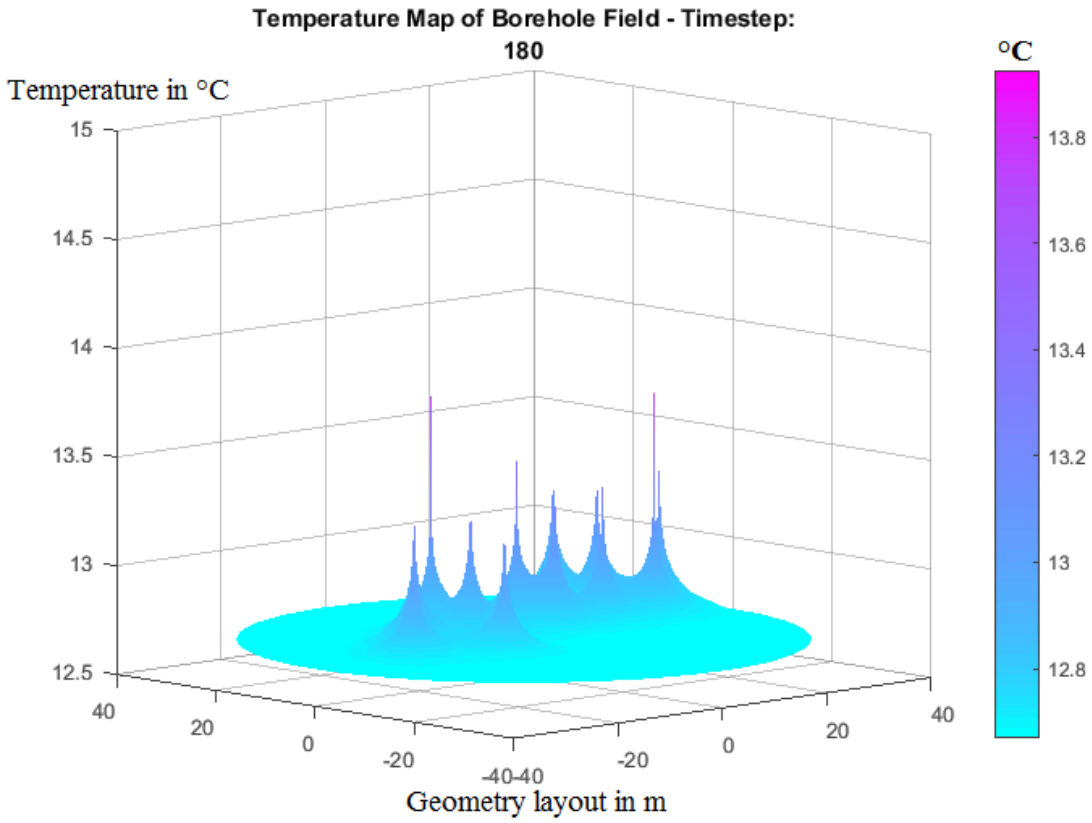

Figure 4-10 Maximum charging heat map (800W/m^3)

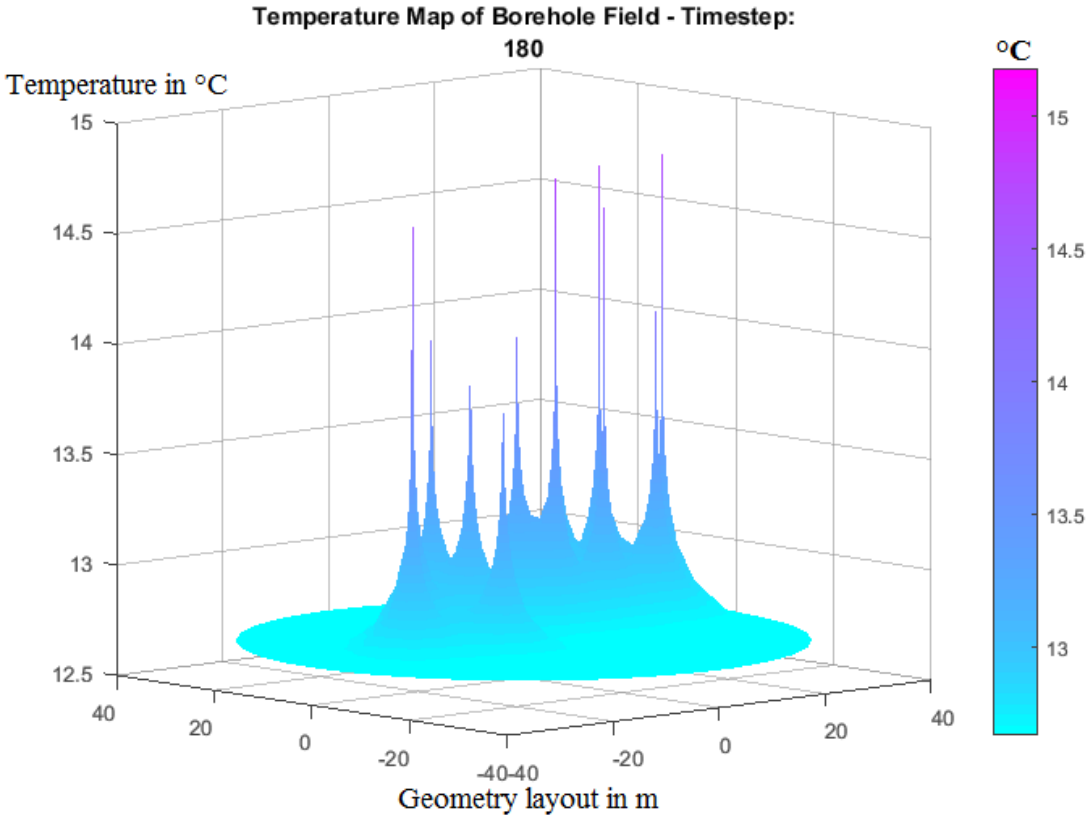

Figure 4-11 Maximum charging heat map (1600W/m^3)

Comparing these two temperature profiles, the discharging (end of charging season) start temperature is very different in Figure 4-12. With higher heat flux input, the borehole temperature is 1 °C higher than the low heat flux input. The temperature influence on this borehole model will be shown in the later study.

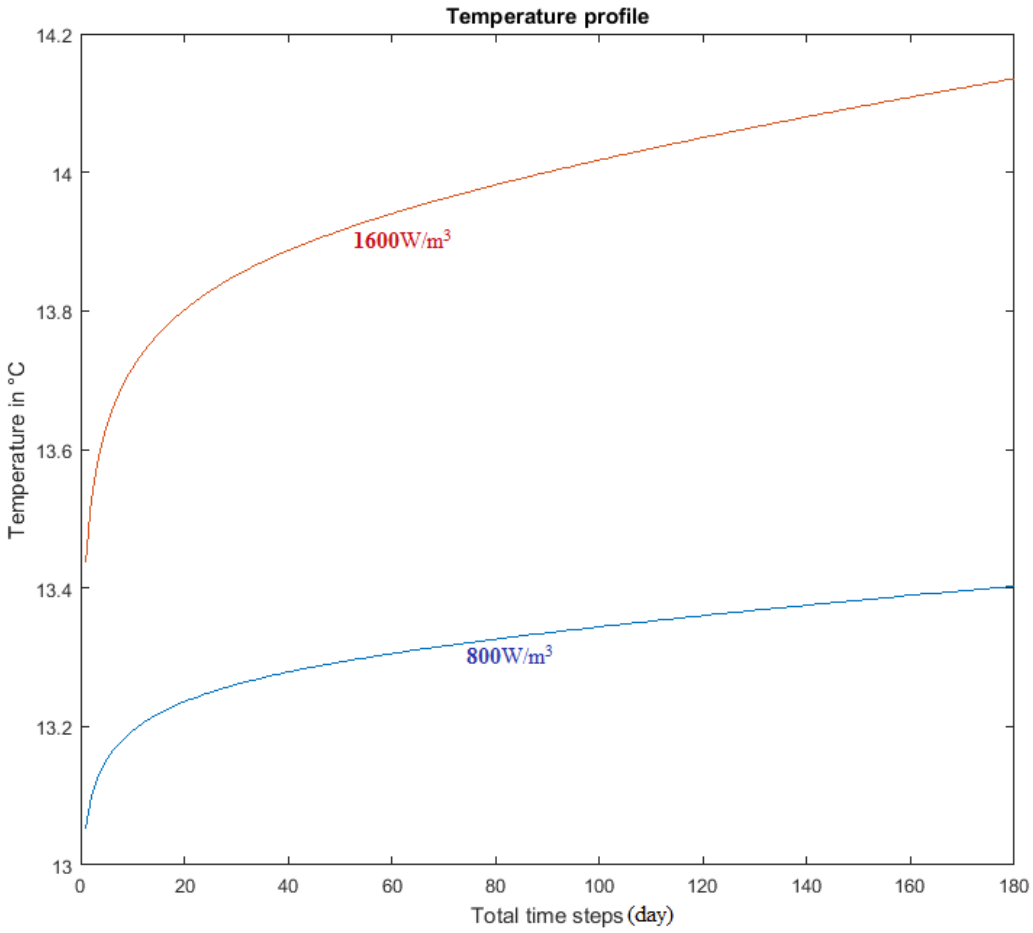

Figure 4-12 Charging season borehole wall temperature profile comparison between 800W/m^3 and 1600W/m^3

4.4.4 Borehole discharging season study

In this case, the borehole is discharged without charging season. This discharging heat flux is assumed to be the same during the whole discharging season which is -418 W/m^3. From the phase one study, in the discharging season, the heat demand is very steady from the history data as is for community buildings which can be seen as a constant heat demand. As a result, the heat demand is the mean value alone the heating season.

In Figure 4-13, the blue spikes represent the final temperature of the borehole after the discharging season. The surrounding soil and bedrock are the heat source during the discharging process and the heat transfer between the ground and these 12 boreholes provides the heat demand over these 180-time steps in discharging season. The borehole forms a heat

pit due to no heat source. The temperature of the surrounding soil and bedrock decreases constantly over the heating season. Because of the natural heat replenishment from the surrounding soil and bedrock, it prevents the borehole from dropping to very low temperature as the fluid, and thus the heat pump is going below its minimum operating temperature. (However over successive discharging seasons without active replenishment this may not be the case). With the constant discharging, the borehole wall temperature decreases fast in the beginning and slowly reaches a saturated temperature as is shown in Figure 4-14.

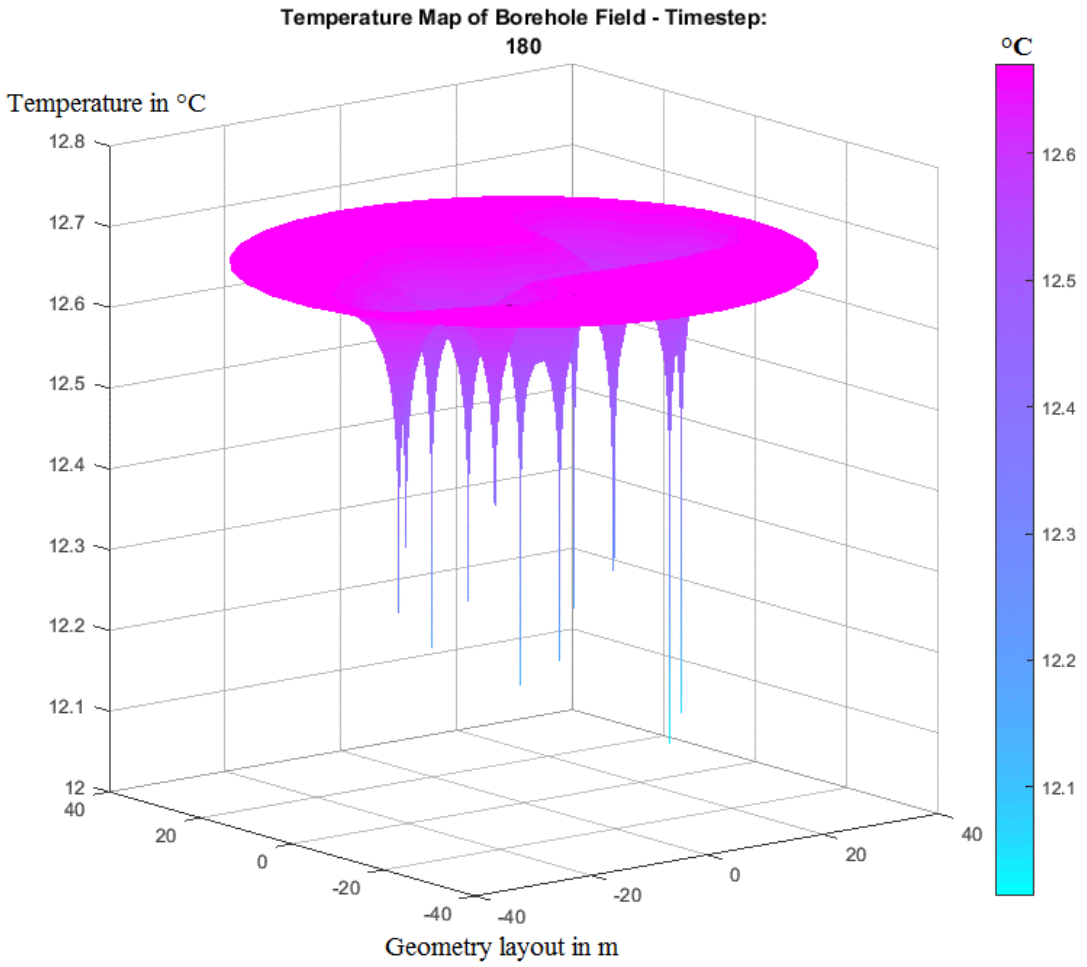

Figure 4-13 Discharging season heat map

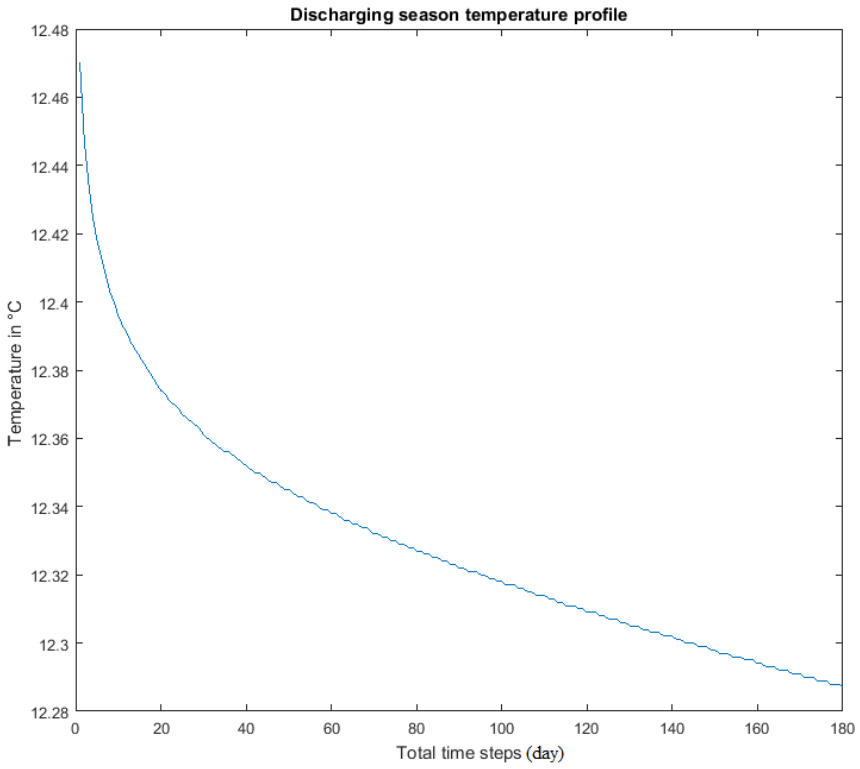

Figure 4-14 Discharging season borehole wall temperature profile

4.4.5 Short-term simulation study (one year single charging/discharging cycle)

In this case study, the one year short-term simulation is carried out. In the short-term study, charging and discharging seasons are combined. There are two cases to compare with. In Chapter 4.4.3, the higher and lower input heat flux are used again with the same output heat flux, 800 and 1600 W/m^3. This study is to show the borehole reaction to different input and the influence over the discharging season.

For the different charging scenarios in such short time simulation, the heat maps are Figure 4-15 and 4-16. In Figure 4-15, the charging heat flux is two times lower than that in Figure 4-16. As a result, the borehole wall temperature and the surrounding soil temperature in Figure 4-15 are between 12.68 °C and 12.75 °C and in Figure 4-16, the temperature range is around 12.7°C and 12.8°C.

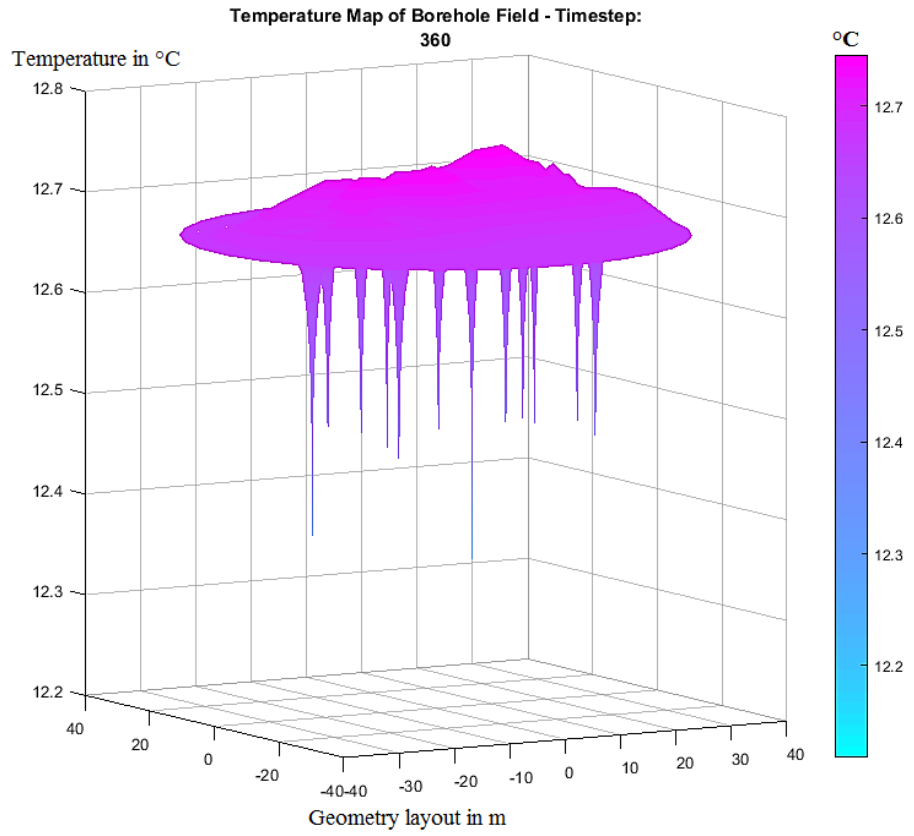

Figure 4-15 Short-term heat map (800W/m³ in charging season)

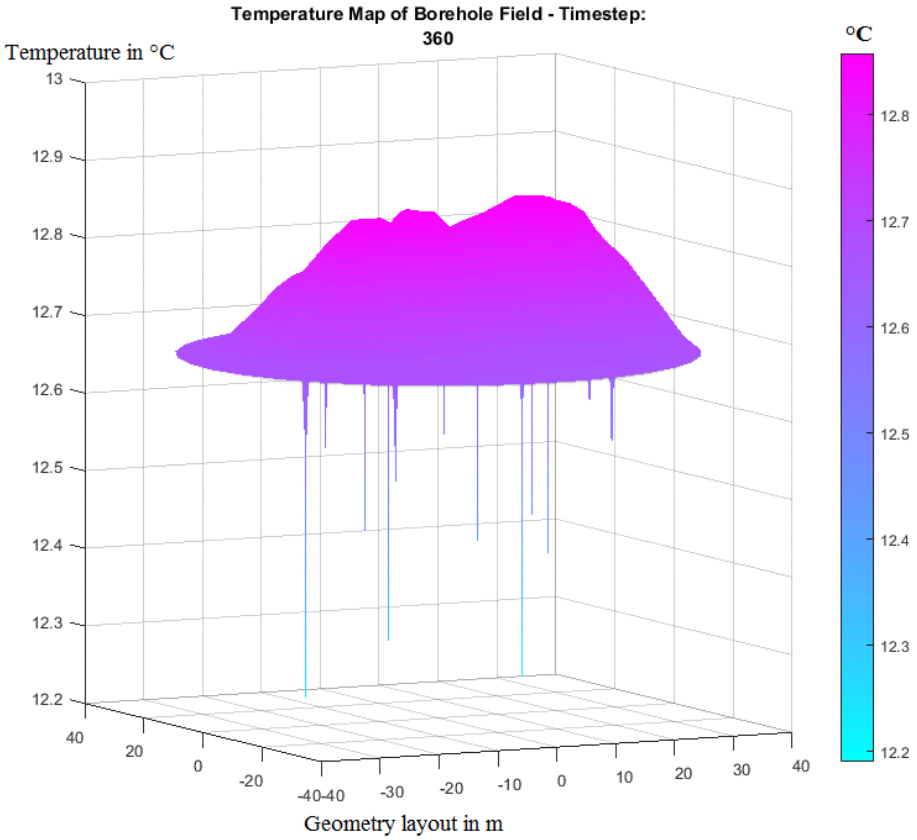

Figure 4-16 Short-term heat map (1600W/m³ in charging season)

Figure 4-17 shows the borehole wall temperature changing in charging and discharging seasons. Between charging and discharging seasons, the temperature drop is dramatic which shows that the heat transfer between the borehole and the ground is very fast due to the huge temperature difference. With higher heat flux input during the charging season, the temperature drops from 14.1 °C to 12.8 °C and with lower heat flux during the charging season, the temperature drops from 13.2 °C to 12.6°C.

However, the higher heat flux input raises up the base temperature level so that with higher maximum charging amount, the final borehole temperature at the end of charging season is slightly higher by 1°C and the borehole surrounding area results in a higher temperature at the same time. From the earlier sections, the borehole temperature accumulates slowly in the ground and reaches a saturated level according the material parameters, adding the constant heat loss of the system, the temperature difference between these two cases is not huge under 800W/m^3 and 1600W/m^3 cases. In the next case, the long-term simulation will be carried out and heat map results will be compared with short-term simulation.

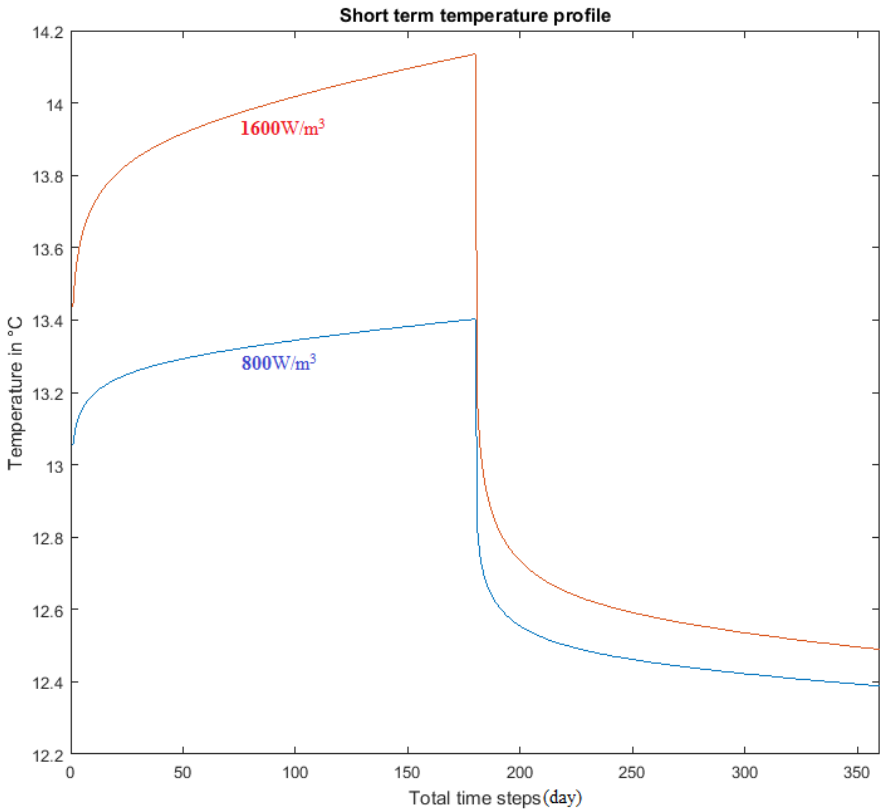

Figure 4-17 Short-term borehole wall temperature comparison between 800W/m^3 and 1600W/m^3

4.4.6 Lifetime simulation study

Combining the charging and discharging seasons together, the operation of the borehole over its designed lifetime, taken here to be 20 years, have been simulated. The comparison is carried out between charging the borehole and without charging the borehole. Figure 4-18 is the two charging cases simulation with the maximum heat flux 800 W/m^3 and 1600 W/m^3 during the charging season and the heating extraction during the discharging season is the same.

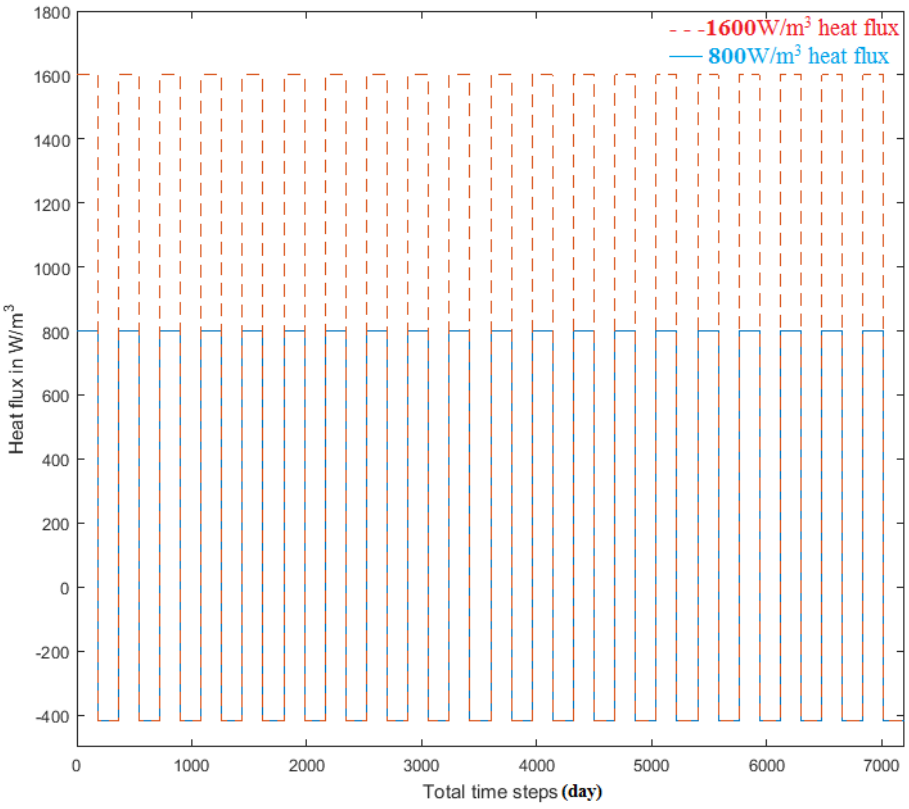

Figure 4-18 Lifetime heat flux with charging

Figure 4-19 is the opposite situation with zero heat flux charging during the charging season over the whole life operation time. However, the heat extraction during the heating season is the same as in Figure 4-18.

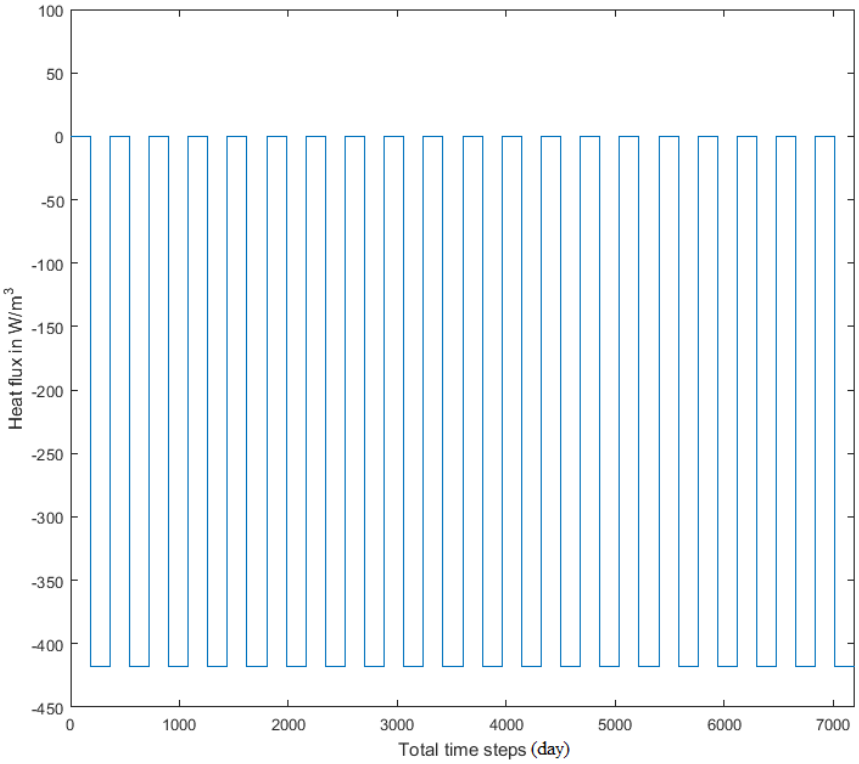

Figure 4-19 Lifetime heat flux without charging

With the continuous charging and discharging process, Figure 4-20, 4-21 and 4-22 shows the final temperature state of the borehole by the end of the lifetime simulation.

From the previous study on the charging and discharging seasons, the heat is accumulated in the borehole and the surrounding soil and bedrock in Figure 4-20 and 4-21. Because the borehole gets supercharged during each charging season, the excessive heat builds up under the ground and lifts up the ground temperature to 13 and plus degrees forming a hot spot.

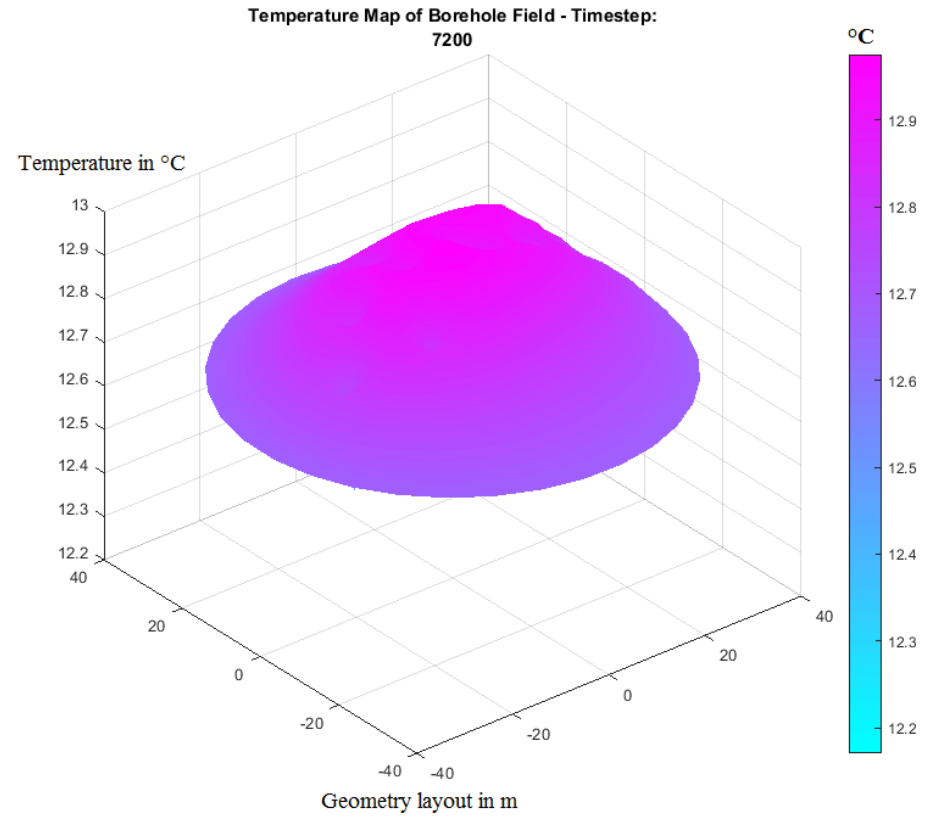

Figure 4-20 Lifetime heat map with maximum 800W/m^3 heat flux charging. For the borehole discharging season, the heat flux is assumed to be a constant value per time step which is -418 W/m^3 heat flux discharging

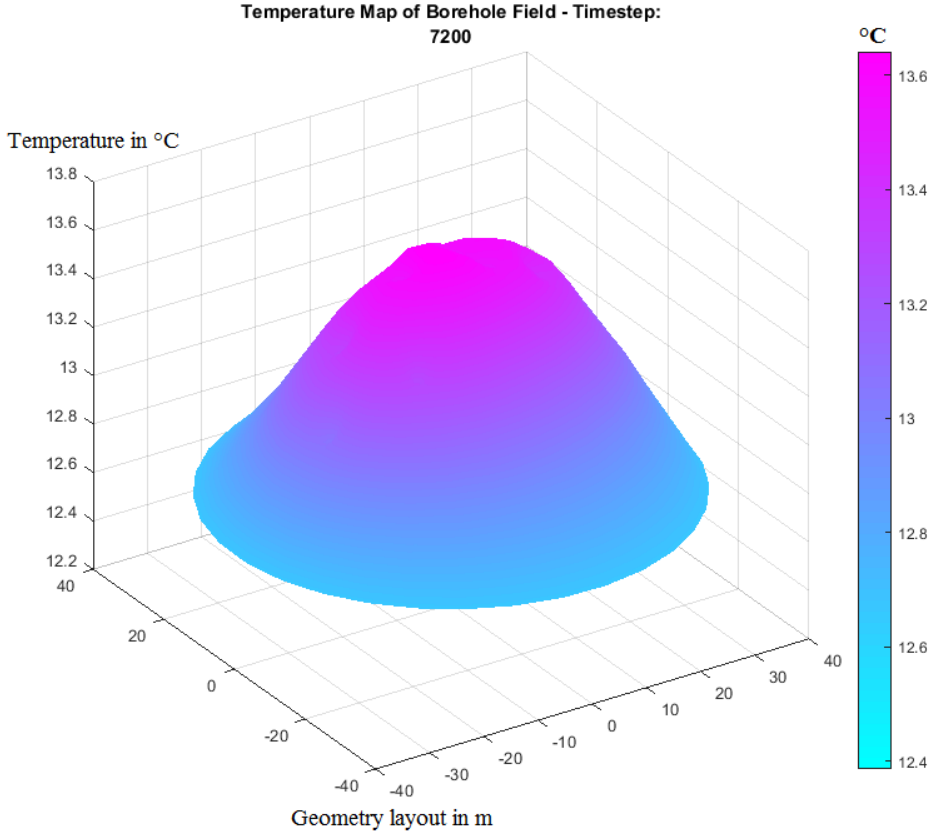

Figure 4-21 Lifetime heat map with maximum 1600W/m^3 heat flux charging For the borehole discharging season, the heat flux is assumed to be a constant value per time step which is -418 W/m^3 heat flux discharging

On the other hand, in the case with no charging, the borehole takes advantage of the natural ground heat with the cold spots in resulting "temperature pit" moderated by surrounding heat. In this scenario, the ground heat transfer prevents the system from reaching a low temperature.

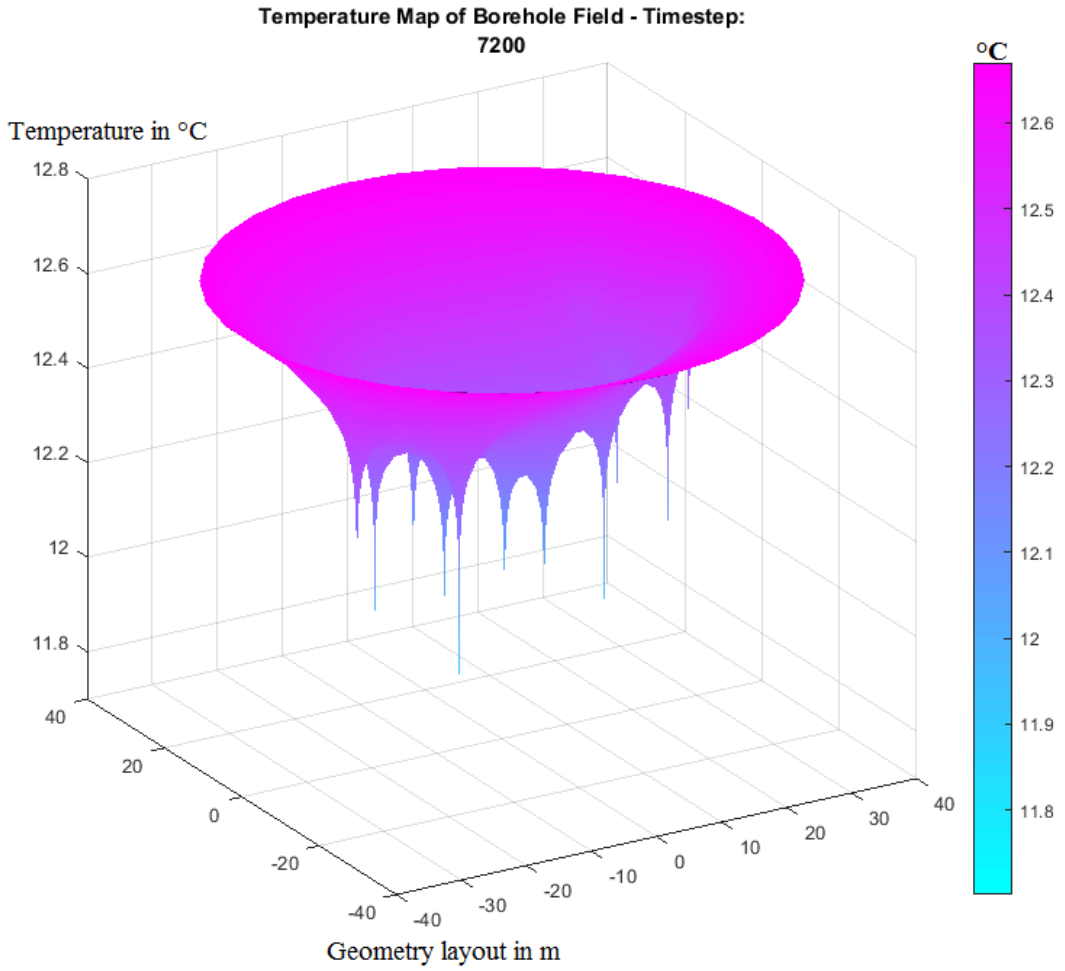

Figure 4-22 Lifetime heat map with 0W/m^3 heat flux charging. For the borehole discharging season, the heat flux is assumed to be a constant value per time step which is -418 W/m^3 heat flux discharging

The temperature profile shows in Figure 4-23 is the gradual temperature change over the 20 years. The red/blue lines are with maximum heat flux charging scenario and the yellow line is without the charging in each charging season.

The yellow line has a very unique temperature changing pattern. As stated before, the soil and bedrock provide the heat demand so that the temperature change between the charging and discharging seasons are very small. However, for the red/blue lines, the high-temperature fluid

makes the heat transfer between the borehole and the surrounding area fast. The base temperature is lifted up and helps to preserve the heat within the lifetime.

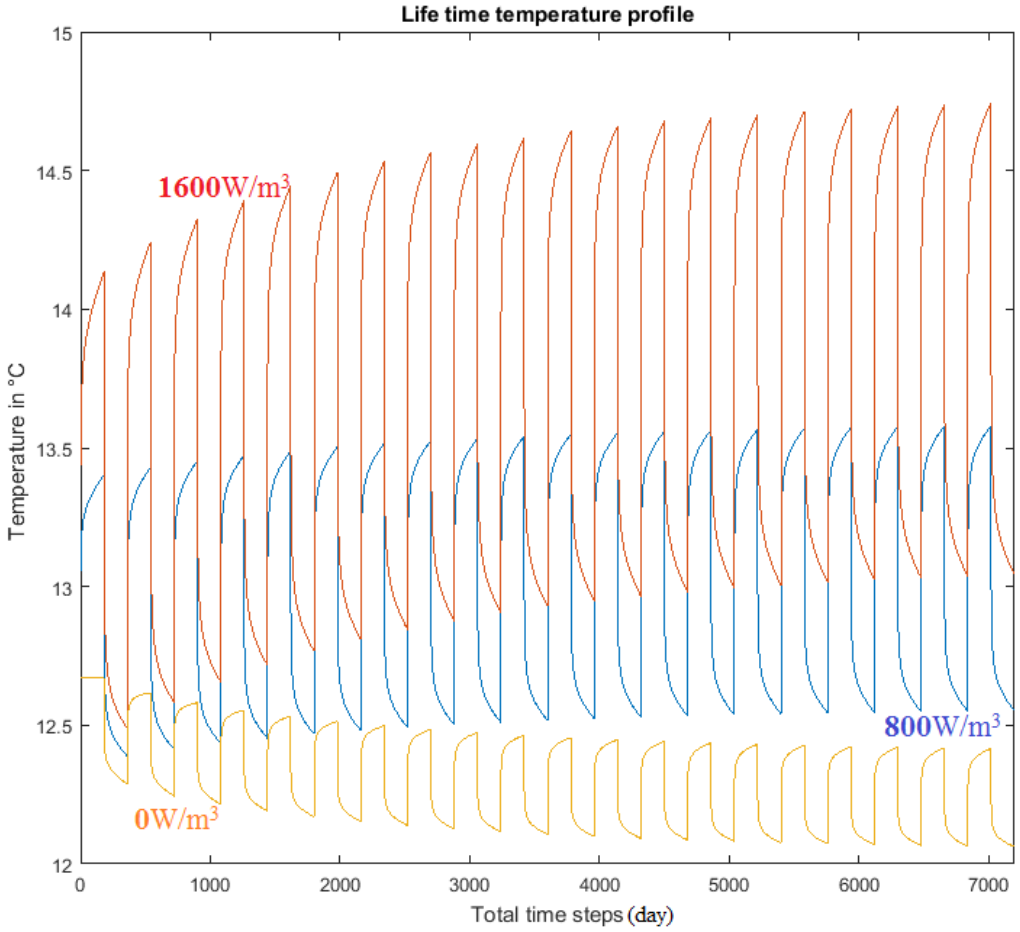

Figure 4-23 Lifetime borehole wall temperature profile

4.4.7 CoP response to borehole temperature during the discharging season

In this section, thorough studies on the borehole temperature reaction to different heat flux over various time periods are carried out.

From the single and short-term charging and discharging seasons, the borehole heat storage always approaches a saturated temperature after continuous heat injection or extraction. With a higher base temperature and higher charging heat flux, the borehole tends to have higher storage temperature as is shown in which helps obtain a higher GSHP CoP when the space heating is needed. In Figure 4-24, the red line is the CoP in the discharging period under higher

charging heat flux and the blue line is under the low heat flux charging and the value difference is around 0.3-0.6. The CoP tends to approach a saturated value as the temperature changing pattern.

From the lifetime simulation, the conclusion is that sufficient charging is definitely beneficial each winter for GSHP's performance. In Figure 4-25, the CoP is very different between the maximum charging and zero charging. With borehole reactive charge during the charging season, the average CoP value is increasing over the years as is shown the red and blue lines, however, without reactive charging, the CoP value is decreasing in each heating season as the yellow lines.

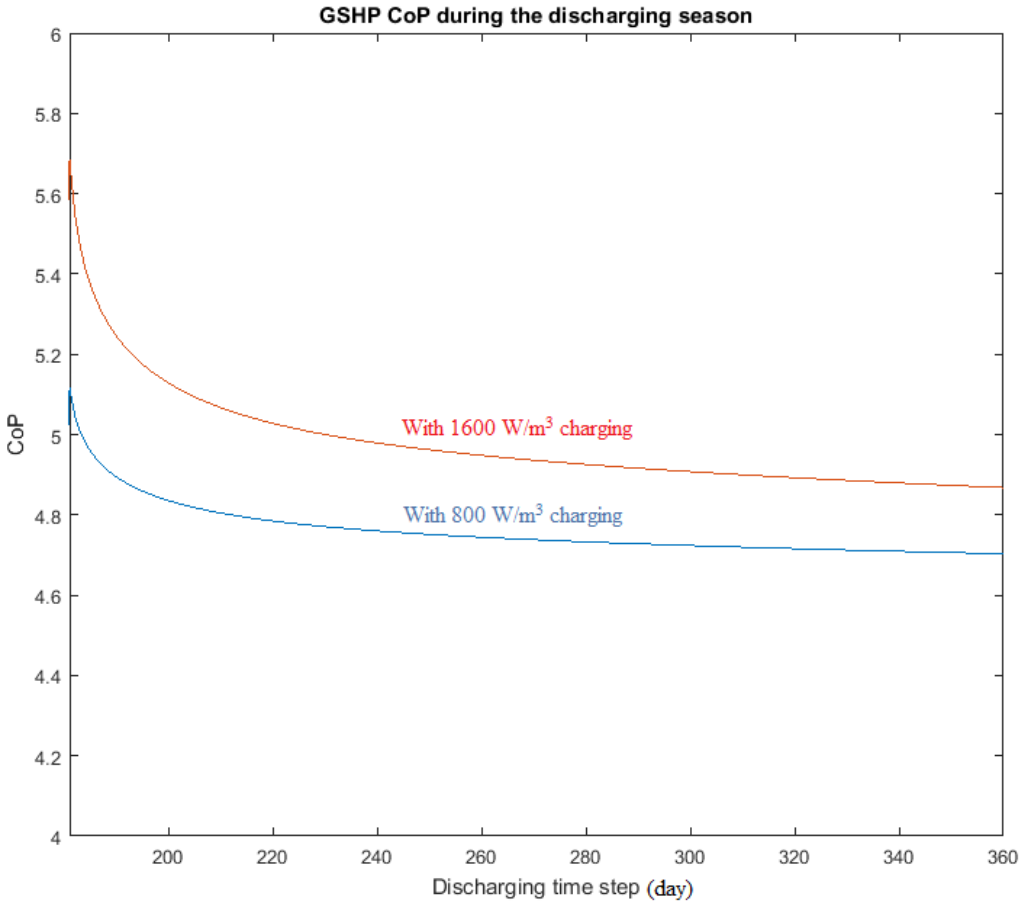

Figure 4-24 Short-term discharging season

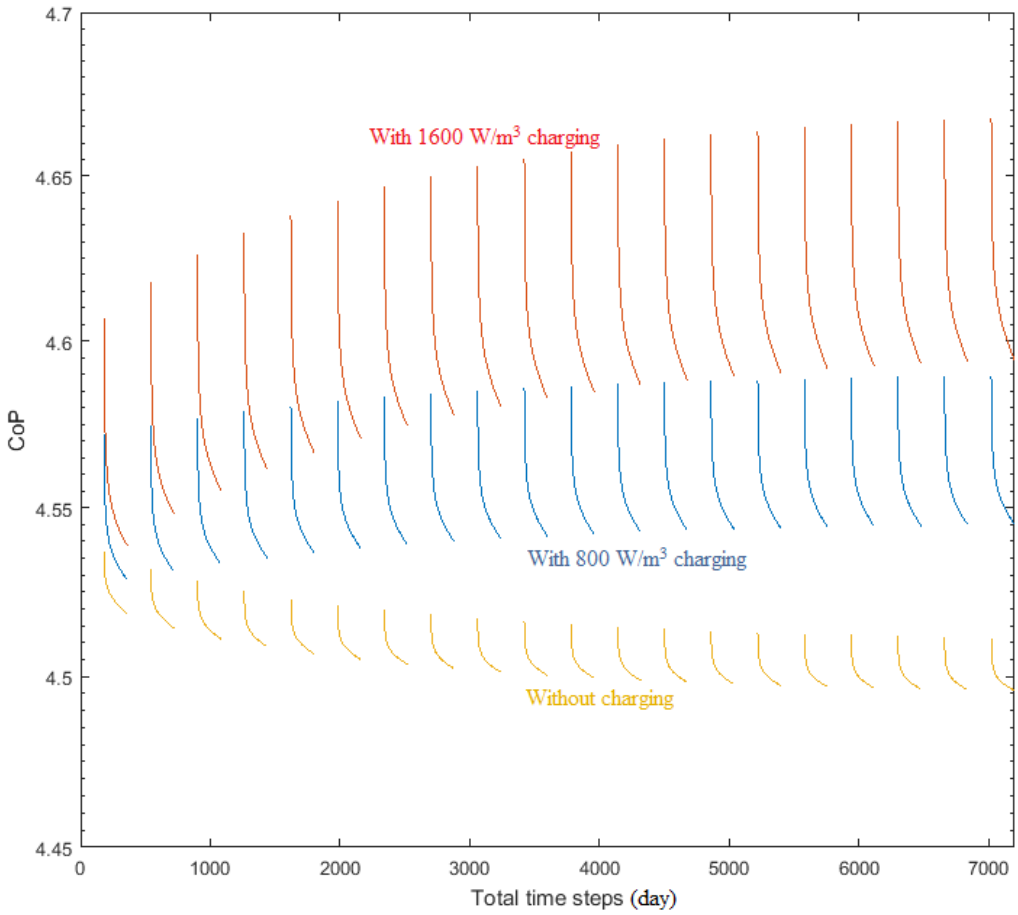

Figure 4-25 20 years of discharging seasons

4.5 Chapter summary

This chapter is focusing on investigating the borehole behaviour under the two extreme charging strategies, maximum and zero charging. From the temperature profile, it is clear to see the temperature response to the heat flux input and output and the useful temperature points are selected as the borehole temperature for further usage. By comparing different scenarios, with borehole active charging, the temperature is increasing and during the discharging period, the average heat pump efficiency is increasing.

However, in practice, the proposed space heating system uses the borehole coupled with heat pumps and the charging heat flux may be limited by the natural condition or facility functioning. As a result, in the future chapters, the model will be studied with different constraints on an operational level.

5 Borehole charging optimization

In this chapter, the optimization is carried on the proposed space heating system. With an accurate borehole model which can simulate the correct heat transfer between the borehole and the surrounding ground and the borehole wall temperature behaviour, finding an efficient method of operating this system is the next important stage.

The borehole inter-seasonal heat storage in this system provides a warm environment to the GSHP which helps to increase the performance of GSHP. From the Chapter 3, high-level energy chain, with the active charge of the borehole during the summer time using PV electricity supplying ASHP, the system is very effective in terms of reducing CO_2 emission and GSHP electricity consumption. However, the heat stored underground involves heat transfer between different media constantly, as a result, heat loss and temperature of the borehole will affect the system efficiency under different charging strategies.

The following section presents an optimized charging strategy for operating this system within one charging/discharging cycle. With the same GSHP performance during the heating season, a more efficient charging method is introduced.

This chapter contains the journal paper which is under review in Access and the figures, tables, and equations are numbered independently. The structure of this chapter is based on the alternative thesis format.

5.1 Optimization of borehole energy storage charging strategy within a low carbon space heat system

This declaration concerns the article entitled:			
Optimization of borehole energy storage charging strategy within a low carbon space heat system			
Publication status: Published			
Publication details (reference)	W.Wei, C. Gu, D. Huo, S. Le Blond, and X. Yan, W. Wei, C. Gu, D. Huo, S. LeBlond, and X. Yan, "Optimal Borehole Energy Storage Charging Strategy in a Low Carbon Space Heat System," *IEEE Access,* pp. 1-1, 2018.		
Candidate's contribution to the paper	The lead author proposed the idea of the paper, she designed the methodology and predominantly executed the coding to derive the experimental results. Other authors helped the candidate with the design of case studies, the format of the paper, and improvement of academic writing. The percentage of the candidate did compare with the whole work is indicated as follows: Formulation of ideas: 100% Design of methodology: 90% (10% of the work is from the discussion with other co-authors) Experimental work: 90% (system parameters and PV/load information are from the project and other reliable sources in the references)		
Statement from candidate	This paper reports on original research I conducted during the period of my Higher Degree by Research candidature. This paper is published.		
Signed	Wei Wei	Date	21/11/2018

Published as: Wei, W, Gu, C, Huo, D, Le Blond, S & Yan, X 2018, 'Optimal Borehole Energy Storage Charging Strategy in a Low Carbon Space Heat System', IEEE Access, vol. 6, 8550636, pp. 76176-76186 and available online via: https://doi.org/10.1109/ACCESS.2018.2883798

Optimal Borehole Energy Storage Charging Strategy in a Low Carbon Space Heat System

Wei Wei[1], Chenghong Gu[1], Da Huo[1], Simon LeBlond[1,2], and Xiaohe Yan[1]

[1]Dept. of Electronic and Electrical Eng., University of Bath, Bath, BA2 7AY, UK

[2]Swanbarton, Wiltshire, SN16 0NX, UK

ABSTRACT Domestic heating is the major demand of energy systems, which can bring significant uncertainties to system operation and shrink the security margin. From this aspect, the borehole system as a interseasonal heating storage can effectively utilize renewable energy to provide heating to ease the adverse impact from domestic heating. This paper proposes an optimal charging strategy for borehole thermal storage by harvesting energy from PV generation in a low carbon space heating system. The system optimizes the heat injection generated by Air Source Heat Pump in the charging seasons to charge the borehole, which provides high inlet temperature for Ground Source Heat Pump to meet space heating demand in discharging seasons. The borehole is modelled by Partial Differential Equations (PDEs), solved by the Finite Element method at both 2D and 3D for volume simulation. The Pattern Search Optimization is used to resolve the model. The case study illustrates that with the optimal charging strategies, less heat flux injection can help the borehole to reach a higher temperature so that the heating system is more efficient compared to boilers. This work can benefit communities with seasonable borehole storage to provide clean but low-cost heating and also maximize PV penetration.

INDEX TERMS Inter-seasonal borehole thermal energy storage (BTES), Air source heat pump (ASHP), Ground source heat pump (GSHP), Optimal charging strategy, Photovoltaic (PV).

I. INTRODUCTION

The massive utilization of fossil energy has resulted in air pollution and global warming [1, 2]. In order to reduce the damage, renewable energy and other environmentally friendly technologies have been widely introduced worldwide. According to the Department of Environment and Climate Change (UK), around 30% of energy consumption is in the domestic sector, responsible for 38% of greenhouse gas emissions [3]. Further, within domestic energy consumption, there are mainly four major energy appliances: Cooking (3%); Lighting and appliances (18%); Water (18%); and Space heating (61%) [4]. It is clear that space heating is the largest energy demand and thus it is important to decarbonize the space heating system by using low-carbon technologies. However, it is very challenging to reduce the energy consumption in space heating [4, 5], as it fairly complicated affected by the behaviours of occupants, the heating systems, house types, and other societal factors [6]. Many efforts have been dedicated to increasing the efficiency of heating energy, such as cavity wall insulation, but they do not always effectively save energy [7].

Heat pumps are more convenient to operate and have better opportunities to reduce carbon emissions by providing efficient heating [8]. In heat pumps, electricity drives a refrigerant cycle to move heat from a low-temperature source to a high-temperature sink. Electric heat pumps are forecasted to be able to reduce CO_2 emissions by more than 90% by 2050 [9]. It is assessed that the air source heat pump (ASHP) could reduce 12% CO_2 emission compared to gas boilers, but the operation cost might increase by 10% decided by operation parameters [8]. Compared to ASHP, ground source heat pump (GSHP) always has a steady heat source, as the ground temperature is much higher and more stable than the ambient air temperature. However, the installation of GSHP is very complicated.

The borehole thermal energy storage (BTES) is a ground-based heat storage with longer asset lifetime compared to other energy storage. In BTES, there are four components – borehole, backfilling material (grout), U-shaped tube and the fluid, which will be explained in the later section. The borehole array is buried deep underground, requiring less maintenance and minimal heat replenishment. The flowing fluid in the borehole pipe is water with mono-ethylene glycol and the glycol prevents the fluid freezing until the temperature reaches -15 °C so that it is suitable for operating along with heat pumps. BTES allows the heating system to store heat and use it later more efficiently. The charged borehole has less heat loss to the surrounding mass because of the steady temperature and good insulating properties of the ground.

The modelling of borehole field response can be realized in several ways. In the early studies of borehole heat energy storage, the analysis of the heat transfer of borehole is challenging due to the transient heat transfer between the media and surrounding geometry [10]. Some studies have been dedicated to this topic mainly by using analytical approaches [11-16] and numerical methods [17-20]. The main difference between the two methods is in the treatment of temperature distribution. In analytical models, the borehole internal region is neglected and the heat transfer is mainly between the borehole wall and surrounding soil. By

contrast, numerical models solve the temperature across the whole borehole region [21]. From the past years of studies on borehole storage, there are three main objectives based on the analytical and numerical methods, determining borehole size, quantifying borehole thermal performance, and validating the borehole model.

There are several papers investigating Finite Element numerical simulation for borehole study, such as [22, 23]. Authors verify the borehole model and simulate the long-time heat transfer process with constant heat inputs. In [22], the authors explain the difference between the middle point temperature and the borehole wall temperature. In [23], the authors compare the single borehole and group borehole area temperatures. A more thorough research on borehole operation was carried out in [24]. In [24], the authors consider heating and cooling under different weather conditions with temperature as a constraint, but borehole arrays geometry layout is ignored. To summarize, the current work on borehole modelling lacks thorough focus on the long-term borehole wall temperature behaviour response under different heat injections and extractions. The borehole modelling involves borehole geography layout and optimizing the borehole storage process within a whole heating system. However, most borehole modelling is conducted in an isolated manner, without integrating it into a local heating system and exploring the charging.

This paper proposes a novel local heating system by combining photovoltaic (PV), heat pumps and seasonal borehole heating storage. This work is a part of a practical borehole heating project demonstrated in Bristol UK [8]. The system allows PV energy to charge the borehole with high-temperature fluid via ASHP, providing high evaporate inlet temperature for heat pumps during the discharging season. This paper mainly focuses on the borehole wall temperature and the efficiency of heat pumps during the charging season. Numerical borehole modelling is developed to generate accurate temperature profiles. According to the geography layout, a group of boreholes are displayed in a certain area using Partial Differential Equations (PDEs). The Finite Element method is used to solve the PDEs in different dimensions, 2D for cross section simulation and 3D for volume simulation. The Pattern Search Optimization is used for the charging to enable better heat pump performance. With the optimal operation, borehole heat storage and heat pumps can cooperate efficiently to store heat for discharging the season.

The main contribution of the paper is: i) it designs a more efficient method to charge the borehole via using renewable energy to reduce total energy demand and CO_2 emissions; ii) it studies the impact of temperature and borehole geometry on charging efficiency; iii) it develops an optimization model to provide heat pumps with a high-temperature environment; iv) it extensively compares different indexes to measure the effectiveness of three charging strategies.

The remainder of the paper is organized as follows: Section II, an overview of the heating system is presented. Section III, a borehole model is built to provide the temperature data and the heat pump model is built to study the efficiency. In Section IV, the optimization method is introduced followed by Section V with system input and the case study with results comparison. In Section VI, conclusions are drawn.

II. OVERVIEW OF THE LOW CARBON HEATING SYSTEM

Combined with heat pumps, the inter-seasonal borehole heat storage can be efficiently operated to gain maximum benefits. The main components of this low carbon heating systems include a) PV panels providing electricity to heat pumps, b) heat pumps generating heat flux, and c) borehole storing heat energy. Figs. 1 and 2 illustrate the system working mechanism in charging and discharging seasons.

In the summer charging season, the temperature is high and thus there is no space heating demand. Fig. 1 is the process of borehole active charging during the summer time. The PV installed along the borehole generates electricity to support the Air Source Heat Pump (ASHP), which produces heat without incurring extra costs of electricity consumption. The generated heat will be stored in the borehole to increase the base temperature of the ground.

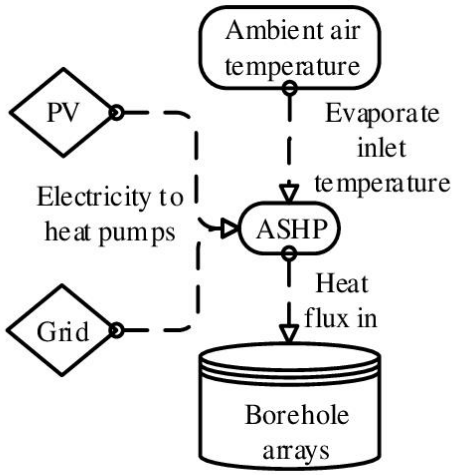

FIGURE. 1 The charging process of the heating system (in summer)

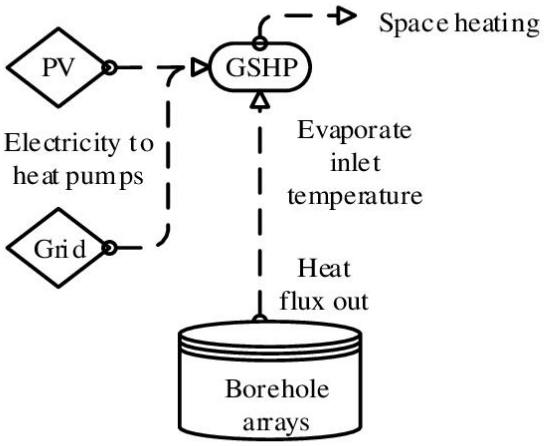

FIGURE. 2 The charging process of the heating system (in winter)

In the winter discharging season as shown in Fig. 2, it is too cold to operate ASHP due to low ambient air temperature but the GSHP with relatively steady heat source can supply the heat demand. The hot water stored in the borehole during the summer is the heat source, providing GSHP with a higher input temperature. With higher inlet temperature, GSHP has batter performance to provide space heating. Because of the low PV generation during the winter, the grid electricity will provide the extra demanded electricity for the GSHP.

III. SYSTEM MODELLING

A. BOREHOLE MODELLING

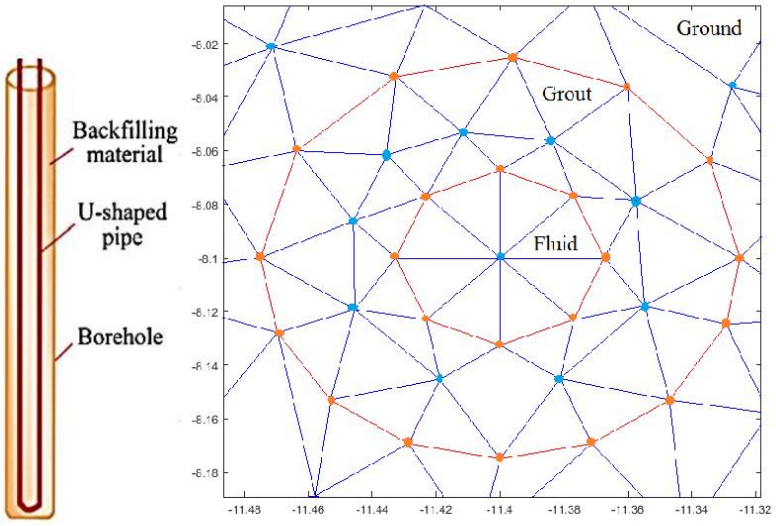

(a) The single borehole [1] (b) Cross-section view of a single borehole

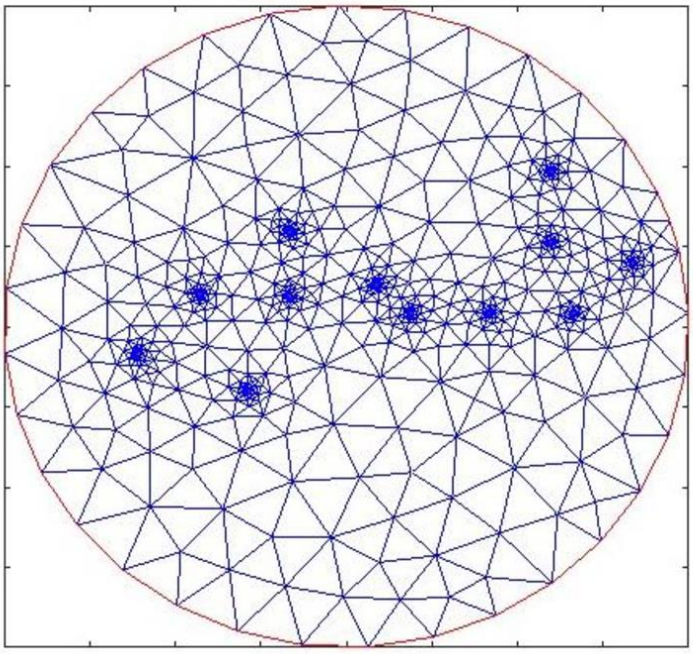

(c) 12-borehole geometry layout of the system

FIGURE. 3 The layout and geometry of boreholes

This paper uses the Finite Element model, which can accurately reflect borehole temperature map, to calculate heat transfer in the whole area. For a single borehole in Fig. 3 (a), the U-shaped pipe can be simplified to a single cylinder pipe [10] and the cross-section view is in Fig. 3(b). The fluid area represents the combined area of the U-shaped tube placed in the middle of the borehole. According to the different heat flux along the simulated time, the temperature of all nodes is exported as a matrix and the nodes representing the borehole wall will be selected for further calculation. The grout in Fig. 3(b) represents the backfilling material in Fig. 3(a). Fig. 3(c) is the total 12-borehole layout. In the model, the edges are set as Neumann boundary with heat flux/temperature information and the subsections are set as the Dirichlet boundary.

The temperature used in the system is the borehole wall temperature instead of fluid temperature. The pipe carries high-temperature fluid varying dramatically and the heat energy settles in the borehole wall and its surrounding area. When the borehole needs to discharge, the heat already settles in the borehole and the fluid extracts heat from the borehole wall and surrounding area. Fig. 4 details the system flowchart of calculating the borehole temperature across the whole storage area starting with modelling set up and the initial conditions of the borehole material and surrounding ground. With all the input information, borehole model calculates the temperature step by step. The flowchart Fig. 4 can be realized with the following two fundamental steps:

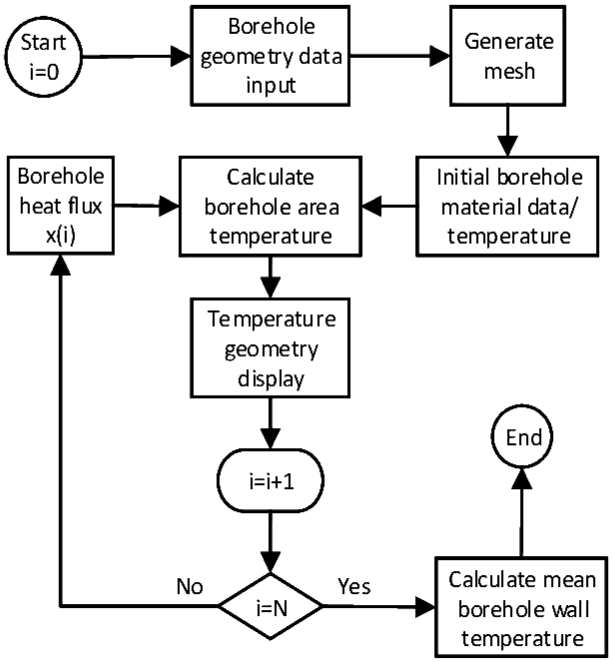

FIGURE. 4 The flowchart for borehole temperature modelling

1) GEOMETRY AND COEFFICIENTS SETTING

Boundaries, edges and subdomains can be created by circle, polygon, rectangle and ellipse objectives, which separate the regions of different materials as shown in Fig. 3. Once the boundaries, edges, and subdomains are defined, the boundary conditions and PDE specifications are set.

The boundary conditions used in this borehole model are:

Neumann:

$$n \times k \times grad(U) + q \times U = g \tag{1}$$

Dirichlet:

$$h \times U = r \tag{2}$$

Where, k is the coefficient of heat conduction, g is the heat flux, q is the heat transfer coefficient, n, h and r are the function of space, and U is the temperature solution.

In PDE for the heat transfer, the Parabolic equation is used.

Parabolic:

$$d\frac{\partial U}{\partial t} - \nabla \cdot (c\nabla U) + aU = f \tag{3}$$

Where, U is the temperature solution in the form of matrix. Temperature solution U is a matrix of **N** -by-**T**, **N** is the temperature calculation of each node in the mesh in PDE and **T** is the number of time steps. a, c, d, f are the scalar PDE coefficients. The coefficients define each node in the mesh during the heat transfer process.

2) GENERATING MESH

Fig. 3 (b) is one of the parallel-connected 12 boreholes in this system. The mesh represents the materials used in the borehole as shown in Fig. 3 (a). The number of triangles affects the simulation time and each node in the mesh represents the temperature point, where all points form the temperature solution matrix.

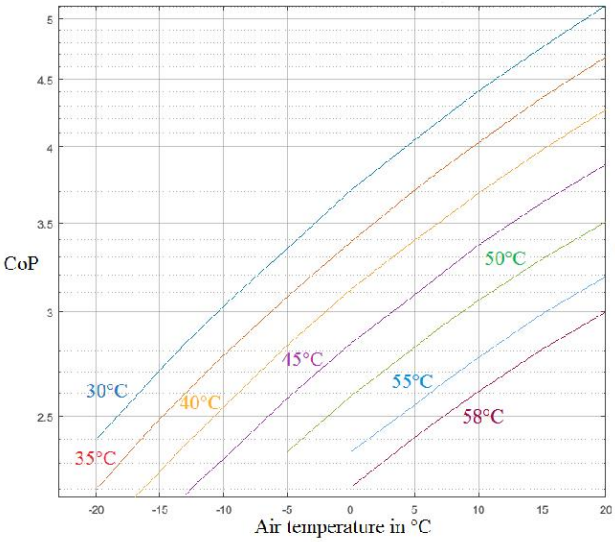

FIGURE. 5 ASHP CoP in different outlet temperature categories

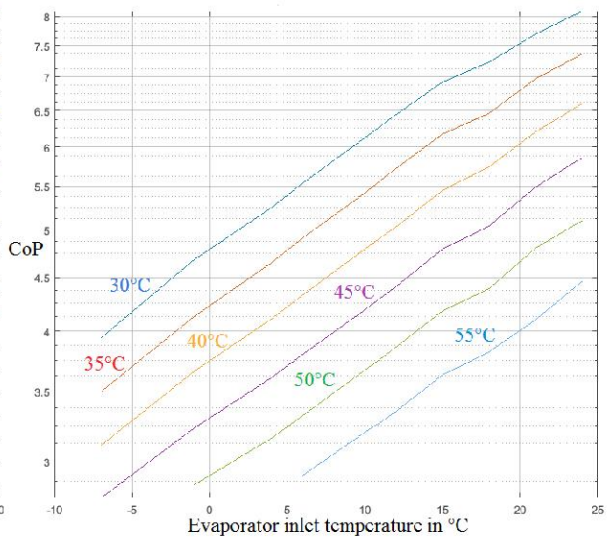

FIGURE. 6 GSHP CoP in different outlet temperature categories

TABLE I

ASHP/GSHP CoP PARAMETERS

Condenser outlet temperature		30°C	35°C	40°C	45°C	50°C	55°C	58°C
ASHP	A	0.068	0.062	0.057	0.051	0.047	0.042	0.039
	B	3.7	3.4	3.1	2.8	2.5	2.3	2.2
GSHP	A	0.136	0.126	0.113	0.100	0.091	0.085	---
	B	4.8	4.2	3.7	3.3	2.8	2.4	---

B. HEAT PUMP MODEL

The ASHP and GSHP are the major low carbon technologies for meeting daily heating demand in this proposed space heating system. The heap pumps data is from the demonstration project in Bristol. From Figs. 5 and 6, for the temperature of each heat pump outlet condenser labelled beside each line within a certain temperature range, the Coefficient of Performance (CoP) can be assumed to be a linear function of the heat pump inlet temperature. The condenser outlet temperature is treated as the heat pump output temperature. With the selected heat pump output temperature, the CoP of the heat pump depends on the heat pump inlet temperature. In general, higher condenser outlet temperature results in lower CoP category, shown in both figures. Within each condenser outlet temperature category, the CoP increases when the evaporate inlet temperature rises higher.

In this paper, the heat pump inlet temperature is within the linear range so that the CoP value is fitted by

$$CoP_t = A \times T + B \tag{4}$$

Where, A and B are constants which depend on the heat pump condenser outlet temperature shown in TABLE I. In this paper, the condenser outlet temperature of ASHP and GSHP are chosen at 30 °C and 45 °C respectively [8]. With the chosen parameters A and B, the heat pump CoP value can be calculated. t is the chosen outlet temperature, and T is the heat pump evaporator inlet temperature (°C).

With increasing evaporator inlet temperature, the CoP value increases as well. However, with higher condenser outlet temperature, CoP is generally lower. Table I provides the parameters used in this paper to calculate the heat pump CoP [8]. Equation (5) models the heat output from the heat pump in terms of its electricity consumption:

$$H = CoP_t \times P \tag{5}$$

Where, H is heat output and P is input electricity for the heat pump.

IV. SYSTEM OPTIMIZATION

Based on the system diagram in Figs. 1 and 2, heat pumps convert electricity into heat in both charging and discharging seasons. An optimization model is designed to obtain the lowest system electricity consumption over the whole charging time so that the system uses minimum energy during the charging season to supply the heat demand in the discharging season.

The optimization is carried out by using Pattern Search. The objective function (6) is to find the minimum total heat flux provided by the ASHP during the charging season which is also the minimum electricity consumption from the ASHP. The constraint in (7b) is the upper and lower boundaries of the variable x which is the heat flux value in W/m^3. The heat injected into the borehole is from ASHP and the electricity required by operating ASHP is related to its CoP, decided by the inlet evaporate temperature (ambient air temperature) and outlet condenser temperature. According to the ASHP data, the average maximum ASHP heat flux output is around 4541 W/m^3. In the MATLAB PDE tool, for the transient analysis, the heat flux unit is the heat produced per unit volume per time. In the discharging season, x equals the heat demand. During the discharging season, the GSHP is assumed to consume a fixed total amount of electricity ($E_{GSHP\ fixed}$) to cover the space heating demand. The $E_{GSHP\ fixed}$ is obtained from one of the base cases explained in the case study.

$$\text{Obj} = \min \sum_{i=1}^{26} x_{(i)} \tag{6}$$

$$0 = E_{GSHP\ fixed} - \sum_{n=27}^{52} E_{GSHP(n)} \tag{7a}$$

$$\begin{cases} 0 \le x_{(i)} \le 4541, \ i = (1:26) \\ x_{(n)} = heating\ load, \ n = (27:52) \end{cases} \quad (7b)$$

Where, $E_{GSHP(n)}$ is GSHP electricity consumption at step n.

$$x_{(i)} = \frac{1000 \times H_{ASHP(i)}}{24 \times 7 \times N_{borehole} \times V_{borehole}}$$

$$= \frac{1000 \times E_{ASHP(i)} \times (A \cdot T_{air(i)} + B)}{24 \times 7 \times N_{borehole} \times V_{borehole}} \quad (8)$$

Where, $H_{ASHP(i)}$ is ASHP heat generation at time step i in kWh, and $T_{air(i)}$ is the ambient air temperature at time step i. $E_{ASHP(i)}$ is ASHP electricity consumption in kWh provided by PV or the grid. $N_{borehole}$ is the number of the borehole in the system. $V_{borehole}$ is the volume of every single borehole in Fig. 6(a). GSHP operates under the same concept, but the inlet evaporating temperature is the borehole wall temperature. During the discharging season, the borehole wall temperature can be calculated in the Finite Element borehole model and the GSHP electricity consumption is from (9):

$$E_{GSHP(n)} = \frac{H_{GSHP(n)}}{CoP_{GSHP(n)}} = \frac{x_{(n)}}{A \cdot u_{(n)} + B} \quad (9)$$

Where, $u_{(n)}$ is the selected borehole wall temperature matrix (1 -by-T) from the temperature solution matrix u. The borehole wall temperature value is the average value of all borehole wall temperature points. $H_{GSHP(i)}$ is GSHP heat output, which is the heat demand in the system.

V. CASE STUDY

A. SYSTEM INPUT

The size of the borehole is as follows: i) 12 x 150 m under the ground; ii) U-Pipe diameter x thickness (mm) 40 x 3.7; iii) the material data is in TABLE II.

TABLE II

BOREHOLE MATERIAL PARAMETERS

	Ground	Fluid	Grout
Density (kg/m^3)	2770	1052	1550
Heat capacity (j/(kg.K))	829	3795	1000
Thermal conductivity (W/(m.K))	2.61	0.5	2.1

Due to the enormous mesh size of the borehole, simulation is very time-consuming. As a result, the mesh of the borehole is not refined and the time step is set at one week, which means the borehole is constantly injecting heat during each step. The charging season only involving PV electricity would have more heat loss when the borehole is not charging making the reality worse. The GSHP provides the space heating so that the condenser outlet temperature is set at 45°C in Table I.

One of the most important components in the heating system is the PV panels. The electricity generated from the PV provides low-carbon electricity to the borehole system. The PV weekly generation data and sun radiation data are from the "Photovoltaic Geographical Information System" (PVGIS) [25]. The PV electricity generation used is in the blue line in Fig. 7(a). It is assumed that the surplus PV electricity is exported to the grid with a flat Feed-In-Tariff (FIT) rate of £0.12/kWh. During the summertime, PV generates more electricity compared to the winter time. Grid electricity will be used when the PV electricity output cannot meet the electricity demand of the heat pumps. The heat load and the grid electricity price are from the historical data in [4, 26]. The purple line in Fig 7(a) is the space heat demand which is provided by the GSHP only during discharging season (from week 27 to week 52). The heat demand varies from week to week. Fig. 7(b) shows the weekly electricity price from the historical data [26]. In this system, the maximum available heat output of ASHP is 4,541 W/m^3 and the heat pump information is from [8].

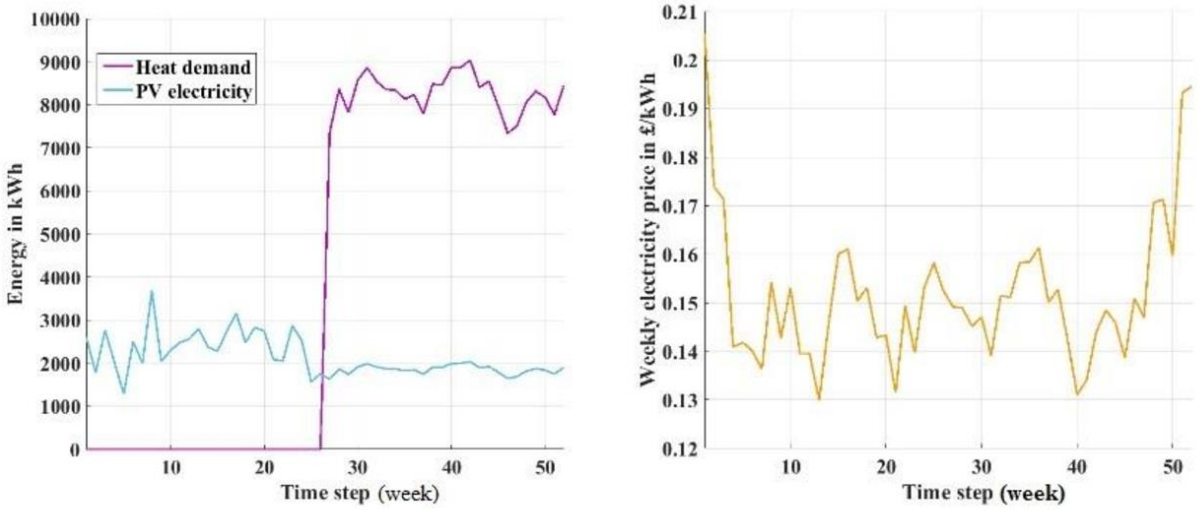

(a) Heat demand and PV electricity generation during the simulation time window [25,26]

(b) Weekly grid electricity price during the simulation time window[26]

FIGURE. 7 Weekly PV generation, heat demand and electricity price

B. CASE SETUP

The system is based on a practical project which provides space heating to a community building and some houses. The case study is designed to study the benefits of different operation of the proposed system between no active charging, with active charging, and with optimized active charging. The impact of heat accumulating in the borehole storage is illustrated. Due to the enormous mesh of the borehole model which

dramatically affects the optimization time, one week is set as the time step for the simulation. Three cases are here to validate and demonstrate the proposed models: Case 1- without active charging in charging season; Case 2- with active charging according to PV generation; and Case 3- with optimized charging strategy.

1) CASE 1 WITHOUT ACTIVE CHARGING IN CHARGING SEASON

This is the base case, where the borehole is installed to provide the space heating all through the discharging season (heating season) from September to March. In the charging season from April to August, there is no active charging to the borehole, which means the borehole only extracts heat during the discharging season by using the surrounding ground (bedrock) as a heat source. The borehole starting temperature is the same as that of the ground 12.67°C.

In Fig. 8, the solid line represents the heat flux injection/exportation in each time step. The dotted line is the borehole wall temperature responding to the heat flux. Without active charging during the charging season, the borehole temperature remains the same as the ground temperature. When the discharging season ends, the borehole temperature drops from ground temperature to 11.3 °C.

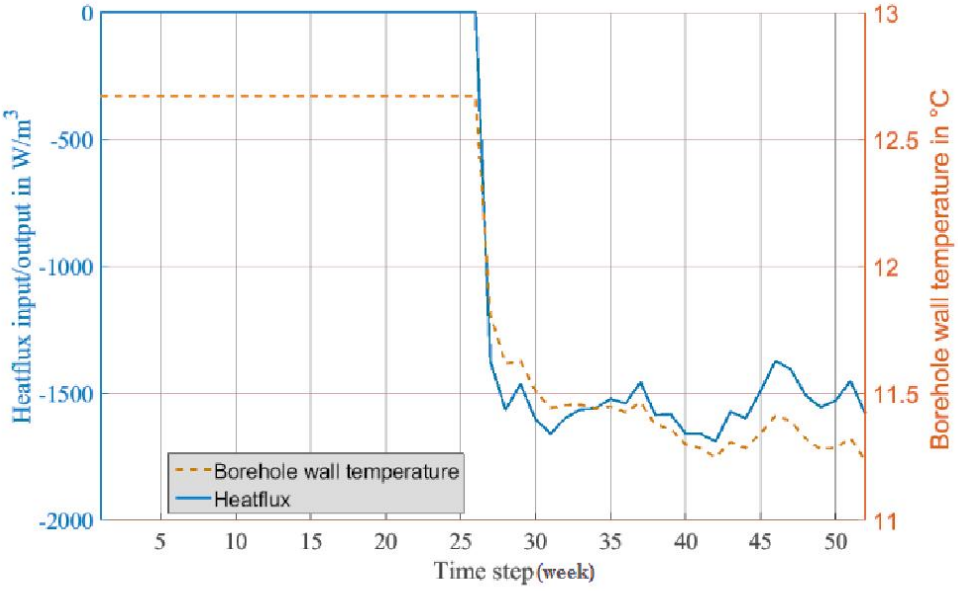

FIGURE. 8 Case 1 borehole wall temperature response to heat flux

2) CASE 2 WITH ACTIVE CHARGING ACCORDING TO PV GENERATION

In this case, the PV is used to provide the electricity needed by the ASHP during the charging season and the surplus PV electricity is exported to the grid. In Fig. 9, during the charging season, the borehole wall temperature in the dotted line changes according to the amount of heat flux injection. Because of the limited PV output, the heat flux from ASHP is only around 2,000W/m^3 during the charging season. With larger heat

flux, the temperature increases fast and with lower heat flux, the temperature could decrease due to the heat dissipation to the surrounding ground. Overall, the borehole wall temperature still increases due to heat input. When the discharging season starts, the borehole temperature drops from 14°C to 11.7°C. During the charging season, the total heat flux injection from ASHP supported by the installed PV is 49,886W/m^3.

3) CASE 3 OPTIMIZED CHARGING STRATEGY

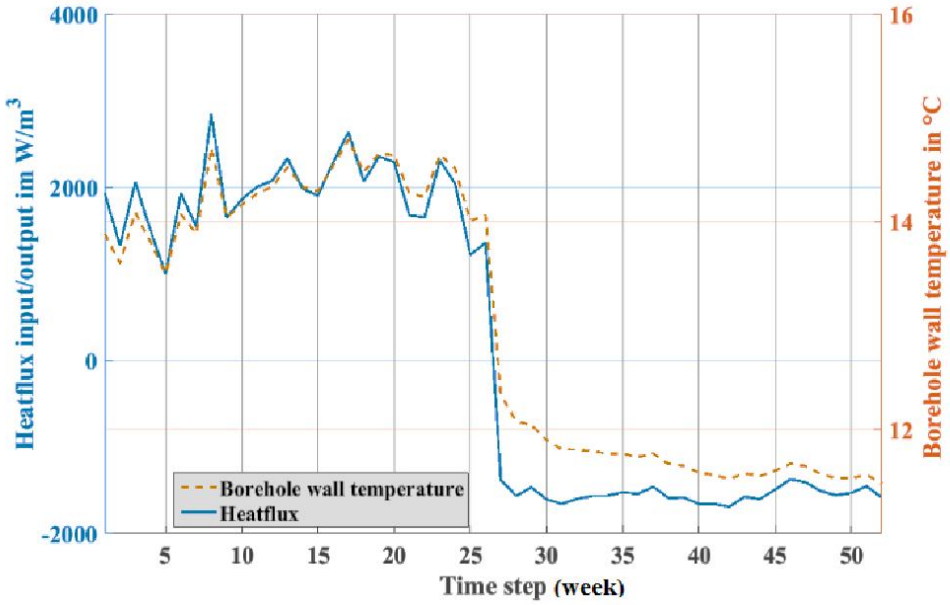

FIGURE. 9 Case 2 borehole wall temperature response to heat flux

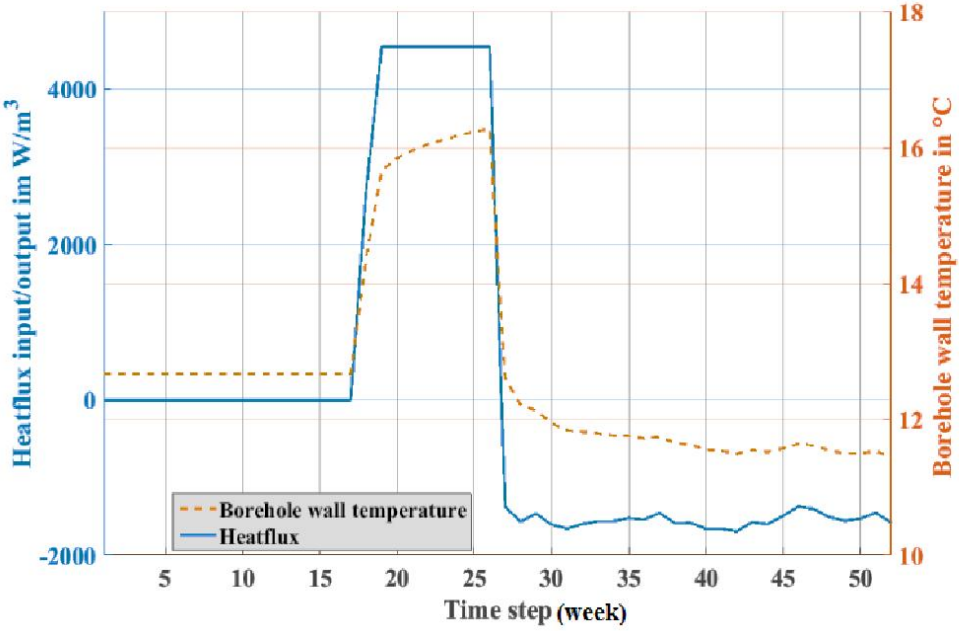

FIGURE. 10 Case 3 borehole wall temperature response to heat flux

In the borehole inter-seasonal storage system, most heat loss appears during the charging season, so that it is significant to optimize the borehole charging. Cases 2 and 3 both require to charge the borehole during the charging season and Case 3 is carried out based on the data obtained from Case 2. By using the optimization method proposed in section IV, with the same total GSHP electricity consumption during the discharging season as in Case 2, the optimized heat flux injection is shown in Fig. 10 by the solid line. As shown, the ASHP starts charging the borehole arrays in the later time steps with the maximum available heat flux (4541W/m^3) output from the ASHP and before time step 16, ASHP is not operated.

To summarize, in these 3 cases, the heat demand during the discharging season is the same. The optimized charging strategy indicates that concentrated charging method leads to more efficient system performance than dispersed charging method as in Case 2. The solid line is the heat flux input which reaches the maximum level in the later stage of the charging season. With the maximum heat flux input, the borehole wall temperature (dotted line in Fig. 10) increases fast to a higher temperature level around 16°C, which provides the GSHP with an even higher temperature environment at the beginning of the discharging season.

C. RESULTS AND ANALYSIS

This section extensively compares the results of different charging strategies in terms of heat pump performances; total system operation cost and CO_2 emission compared to the traditional boiler.

1) HEAT FLUX WITH BOREHOLE TEMPERATURE

The charging strategies of cases 2 and 3 are compared in Fig. 11(a). In both cases, the borehole is charged during the charging season. Case 2 charges the borehole whenever there is free electricity provided by the installed PV (blue dotted line). Case 3 is the optimized charging strategy, i.e .a more concentrated charging (green solid line). In both cases, GSHP consumes the same amount of electricity. However, during the charging season in Case 3, the total heat flux injection from ASHP is 39,028W/m^3, which is much lower than 49,886W/m^3 in Case 2.

In Case 2, with a limited amount of PV generation, ASHP provides lower heat flux between 1000 - 3000 W/m^3 in each time step. It is difficult to for the heat to cumulate and the heat loss is much higher in the whole charging season. In Case 3, the heat loss only occurs when the borehole starts charging. During the discharging season, the borehole temperature changes in a similar pattern as shown in Fig. 11(b) by the solid and dotted lines. Because of the active charging in the charging season, both cases 2 and 3 provide GSHP higher temperature environment than base Case 1 in discharging season.

From Fig. 11(b), the temperature changes dramatically when charging or discharging starts. The reason for this dramatic change is that the U-shaped pipe carries high-temperature fluid, which is much higher than the ground temperature. When the temperature difference is big, the heat transfer is faster. When the heat settles down in the surrounding ground, due to the heat transfer parameters of different media, the temperature slowly reaches a steady state. As a result, the heat transfer happens faster in the beginning.

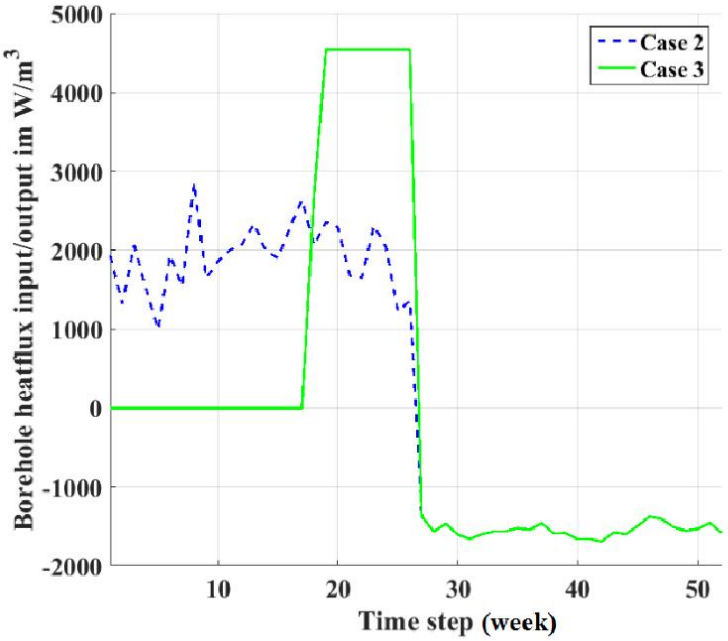

(a) Borehole charging strategy comparison between Case 2 and 3 (heat flux injection/extraction)

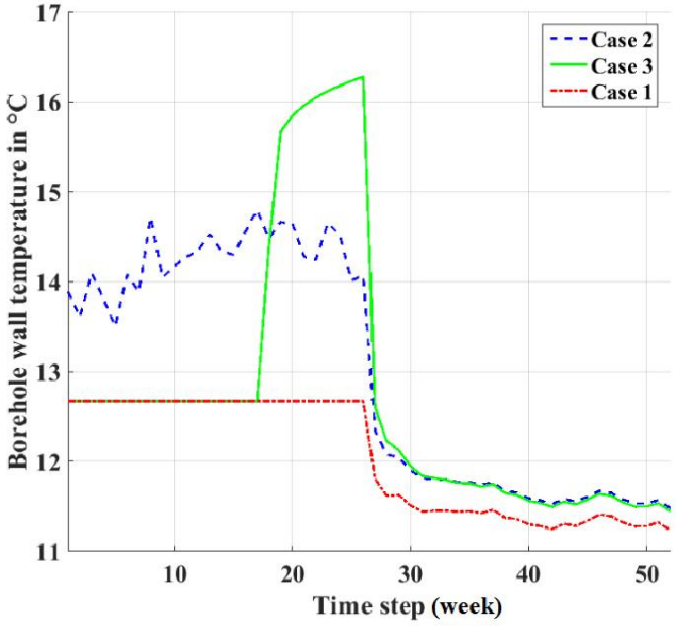

(b) Borehole wall temperatures changing pattern in Case 1, 2, and 3)

FIGURE. 11 Charging strategy and borehole wall temperature

2) GSHP PERFORMANCE AND ELECTRICITY CONSUMPTION

Because of the active charging, cases 2 and 3 have higher borehole wall temperature Fig. 11(b), which affects the performance of GSHP in each time step during the discharging season. During the discharging season, the heat flux is extracted from the borehole and the borehole temperature is dropping constantly so that the CoP value is dropping during heating season Fig. 12(a). GSHP CoP values (between 4.56 to 4.44) in Cases 2 and 3 are shown in Fig. 12(a) compared to that in Case 1 (between 4.47 to 4.41) and in general, Case

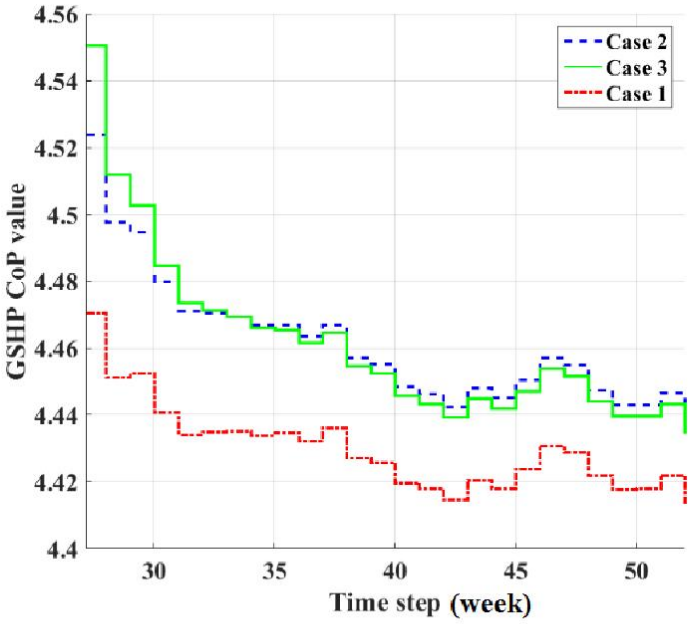

(a) Case 1, 2, and 3 GSHP CoP values comparison during the discharging season

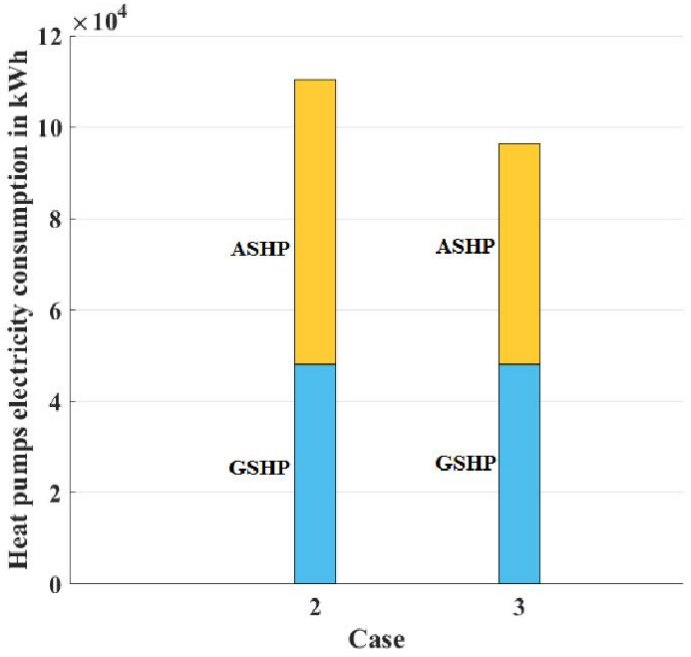

(b) Case 2 and 3 ASHP and GSHP electricity consumption comparison

FIGURE. 12 GSHP CoP comparison and ASHP electricity consumption comparison

2 and 3 have higher GSHP CoP value. As shown in the figure, Case 2 and Case 3 have slight difference GSHP CoP values due to the different charging strategies during the charging season, but the total electricity consumptions of GSHP in the discharging season are the same, which will be discussed later. Between the cases with active charging (Case 2 and 3) and with no-active charging (Case 1), the average borehole wall temperature and GSHP CoP values during the discharging season are around 0.31°C and 0.04 higher respectively according to the Fig.11(b) and 12(a).

Table III shows different GSHP electricity consumption in each case. In Case 1 and Case2 or 3, GSHP uses 48,448.52 kWh and 48,107.69 kWh electricity during the discharging season respectively. The electricity consumption is reduced by 340.88 kWh in Case 2 and 3 compared to Case 1.

TABLE III
DISCHARGING SEASON TOTAL ELECTRICITY CONSUMPTION

kWh	Case 1	Case 2 and 3
GSHP electricity consumption	48,448.52	48,107.64

3) ASHP PERFORMANCE AND ELECTRICITY CONSUMPTION

ASHP electricity consumption varies according to the charging strategies. Case 2 and Case 3 both charge the borehole during the charging season and the only difference is that in Case 3, the optimized charging strategy is applied.

In Fig. 12(b), the bottom part of the bars is the total GSHP electricity consumption during the discharging season in Case 2 and Case 3. The top parts of the bars are the electricity consumption of ASHP during the charging season. By adopting the optimized charging method, ASHP consumes 48,317kWh electricity in Case 3 which is 13,911kWh less than that in Case 2. The system uses less energy input to create the same heat output during the discharging season. As a result of the efficient electricity usage and effective borehole charging during the charging season, the electricity consumed by heat pumps (ASHP+GSHP) in the whole year is reduced by 12.61%.

4) TOTAL SYSTEM ELECTRICITY COST

This low carbon space heating system involves both PV and grid electricity and thus PV Feed-In-Tariff (FIT) and grid electricity price need to be considered in calculating costs. During the operation period, the import of electricity from the grid is needed when PV output is not sufficient to meet heat pump demand. Thus, the operation cost considered is due to buying electricity cost from the grid to meet heat pump minus the FIT earned by PV to export electricity to the the grid. Maintenance cost is neglected as it is relatively low and this study is not performed under lifetime simulation.

$$C_{system} = (E_{HP} - E_{PV}) \times P_{grid} - FIT \times E_{exporting} \quad (10)$$

Where, C_{system} is system operation cost (£), E_{PV} is PV electricity for heat pump usage (kWh), E_{HP} is total electricity consumption of heat pump (kWh), $P_{grid\ electricty}$ is grid electricity price (£/kWh), E_{export} is PV output exported to the grid (kWh), and FIT is the unit benefit for PV to export extra electricity to the grid (£/kWh).

In Case 2, instead of exporting PV electricity to the grid, ASHP uses all the electricity generated by PV to charge the borehole. However, the injected heat flux is restrained by the PV generation so that the ASHP could not reach the maximum output heat flux the whole charging season.

In Case 3, the optimal charging strategy allows the PV to export electricity to the grid when the system decides not to charge the borehole during the charging season. The ASHP is supported by both the PV and grid to reach the maximum heat flux when it needs the system to charge. With the exported PV output, the total electricity cost actually decreases. The system costs in all three cases are shown in Fig. 13. The heating system in Cases 1 and 2 cost £2,572 and £2,524 respectively during the whole simulation time. In Case 3, the total cost is £2,014, decreasing by 21.69% and 20.19% compared to Cases 1 and 2.

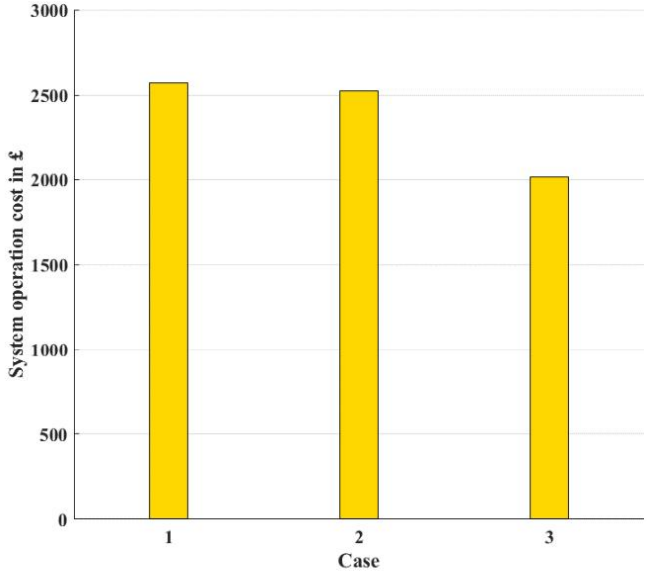

FIGURE. 13 Total system operation cost based on heat pumps electricity consumption

5) CO_2 EMISSION

By comparing these 3 cases with the conventional heating system such as a boiler, the proposed borehole heating system CO_2 emission is reduced during the discharging season. Gas boiler CO_2 emission data is obtained from the British Gas website [27]. The total space heat demand is 214,591.77kWh. For the same

amount of heat supplied by the boiler, 39,484.89 kg CO_2 is generated. By using the results from Table III and Fig. 5(a) of PV electricity generation, the CO_2 emission from the grid and PV during the discharging season is listed in Table IV. During the discharging season, Cases 1, 2 and 3 generate around 11,000 kg CO_2, reducing by around 70% compared to the case with pure boilers.

TABLE IV
CO_2 EMISSION IN DISCHARGING SEASON (kg)

CO_2 emission	Case 1	Case 2 and 3	Boiler
Grid plus PV	11,693.12	11,510.07	39,484.89

VI. CONCLUSION

This paper proposes a low carbon heating system by using borehole inter-seasonal heat storage and heat pumps to meet heating demand. A novel charging algorithm for the borehole system is developed. Through extensive demonstration, there are several key findings: i) borehole interseasonal thermal storage helps GSHP consume less electricity by charging it from PV; ii) the proposed borehole operation strategy enables the borehole to reach higher temperature with less heat loss and heat input, reducing the total operation cost via reducing the reliance on the grid electricity; iii) with less heat pump electricity consumption, this space heating system generates less CO_2 compared to the traditional boiler system. In addition, there are many important areas to be considered in the future. Reducing the simulation time step can produce more accurate and detailed simulation results, informing real-time control. Besides, weather conditions considered in the operation of the system can add the uncertainties to both PV output and heating demand. In order to examine the impact of heat accumulation over the lifetime of the borehole storage system, the charging/discharging cycles should be further increased as well.

REFERENCES

[1] M. Li, P. Li, V. Chan, and A. C. K. Lai, "Full-scale temperature response function (G-function) for heat transfer by borehole ground heat exchangers (GHEs) from sub-hour to decades," *Applied Energy,* vol. 136, pp. 197-205, 12/31/ 2014.

[2] W. Wei, H. Da, and B. Simon Le, "Borehole active recharge benefit quantification on a community level low carbon heating system," in *2016 IEEE Power and Energy Society General Meeting (PESGM)*, 2016, pp. 1-5.

[3] E. I. S. Department for Business. (31 July 2013). *Domestic energy fact file and housing surveys*. Available: https://www.gov.uk/government/collections/domestic-energy-fact-file-and-housing-surveys

[4] R. Yao and K. Steemers, "A method of formulating energy load profile for domestic buildings in the UK," *Energy and Buildings,* vol. 37, pp. 663-671, 6// 2005.

[5] H. Meier and K. Rehdanz, "Determinants of residential space heating expenditures in Great Britain," *Energy Economics,* vol. 32, pp. 949-959, 2010/09/01/ 2010.

[6] T. Kanea, S. K. Firth, D. Allinson, K. N. Irvine, and K. J. Lomas. (05/2011). *Understanding occupant heating practices in UK dwellings*. Available: http://mmmm.lboro.ac.uk/doc/wrec%20paper%20-%20final%20submission.pdf

[7] S. H. Hong, T. Oreszczyn, and I. Ridley, "The impact of energy efficient refurbishment on the space heating fuel consumption in English dwellings," *Energy and Buildings,* vol. 38, pp. 1171-1181, 2006/10/01/ 2006.

[8] E. ICAX, the University of Bath, DECC. (2015, 10/04). *Owen Square Community Energy project*. Available: http://www.cepro.co.uk/2015/04/choices-solar-district-heat-study/

[9] E. N. A. Limited. (2017, 21/06/2017). *2050 Pathways for Domestic Heat*. Available: http://www.energynetworks.org/gas/futures/2050-pathways-for-domestic-heat.html

[10] M. Li and A. C. K. Lai, "Analytical model for short-time responses of ground heat exchangers with U-shaped tubes: Model development and validation," *Applied Energy,* vol. 104, pp. 510-516, 2013.

[11] M. Li and A. C. K. Lai, "New temperature response functions (G functions) for pile and borehole ground heat exchangers based on composite-medium line-source theory," *Energy,* vol. 38, pp. 255-263, 2012/02/01/ 2012.

[12] J. Claesson and S. Javed. (2011). *An analytical method to calculate borehole fluid temperatures for time-scales from minutes to decades*. Available: http://publications.lib.chalmers.se/records/fulltext/151315/local_151315.pdf

[13] M. Li and A. C. K. Lai, "Heat-source solutions to heat conduction in anisotropic media with application to pile and borehole ground heat exchangers," *Applied Energy,* vol. 96, pp. 451-458, 2012/08/01/ 2012.

[14] N. Diao, Q. Li, and Z. Fang, "Heat transfer in ground heat exchangers with groundwater advection," *International Journal of Thermal Sciences,* vol. 43, pp. 1203-1211, 2004/12/01/ 2004.

[15] N. Molina-Giraldo, P. Blum, K. Zhu, P. Bayer, and Z. Fang, "A moving finite line source model to simulate borehole heat exchangers with groundwater advection," *International Journal of Thermal Sciences,* vol. 50, pp. 2506-2513, 2011/12/01/ 2011.

[16] H. Zeng, N. Diao, and Z. Fang, "Heat transfer analysis of boreholes in vertical ground heat exchangers," *International Journal of Heat and Mass Transfer,* vol. 46, pp. 4467-4481, 2003/11/01/ 2003.

[17] A. Zarrella, M. Scarpa, and M. D. Carli, "Short time-step performances of coaxial and double U-tube borehole heat exchangers: Modeling and measurements," *HVAC&R Research,* vol. 17, pp. 959-976, 2011/12/01 2011.

[18] Y. Nam, R. Ooka, and S. Hwang, "Development of a numerical model to predict heat exchange rates for a ground-source heat pump system," *Energy and Buildings,* vol. 40, pp. 2133-2140, 2008/01/01/ 2008.

[19] H. Su, Q. Li, X. H. Li, Y. Zhang, Y. T. Kang, Z. H. Si, *et al.*, "Fast Simulation of a Vertical U-Tube Ground Heat Exchanger by Using a One-Dimensional Transient Numerical Model," *Numerical Heat Transfer, Part A: Applications,* vol. 60, pp. 328-346, 2011/08/15 2011.

[20] C. K. Lee, "Effects of multiple ground layers on thermal response test analysis and ground-source heat pump simulation," *Applied Energy,* vol. 88, pp. 4405-4410, 2011/12/01/ 2011.

[21] R. R. F. Al-Chalabi, "Thermal resistance of U-tube borehole heat exchanger system: numerical study," 2013.

[22] Y. Zhang, Y. Zhang, and P. Zhang, "Modeling and simulation of double-boreholes vertical U-shaped pipe heat transfer," ed, 2013, pp. 1978-1983.

[23] S. L. Weihua Yang, Xiaosong Zhang, "Numerical Simulation on Heat Transfer Characteristics of Soil Around U-Tube Underground Heat Exchangers," presented at the International Refrigeration and Air Conditioning Conference, 2008.

[24] F. De Ridder, M. Diehl, G. Mulder, J. Desmedt, and J. Van Bael, "An optimal control algorithm for borehole thermal energy storage systems," *Energy and Buildings,* vol. 43, pp. 2918-2925, 2011.

[25] I. f. E. Joint Researcg Centre, Renewable Energy Unit. *Photovoltaic Geographical Information System (PVGIS)*. Available: http://re.jrc.ec.europa.eu/pvgis/

[26] C. Gu, W. Yang, Y. Song, and F. Li, "Distribution Network Pricing for Uncertain Load Growth Using Fuzzy Set Theory," 2016.

[27] B. Gas. (2018). *Comparing your energy usage*. Available: http://www.britishgas.co.uk/help-and-advice/Online-account/Comparing-your-energy-usage/How-do-you-work-out-the-CO2-values.html

5.2 Follow-up case study and results

5.2.1 Cases

In the new comparison between the cases, the PV electricity is considered as a major electricity source as well as the FIT. The following cases show the conditions under which each case is carried out.

1) Case 1 without active charging in charging season with all the PV exported to the grid

The difference between the new Case 1 and the old Case 1 is that, the PV is installed, however, all the electricity generated by PV is exported to the grid and the grid electricity supplies the whole system. In the old Case 1, the PV generation is ignored during the charging season because the focus of the study is on the discharging season. However, in the new Case 1, the exported PV is considered as an important aspect of system cost. As a result, large amount of PV electricity is exported to the grid.

Table 5-1 Old and new Case 1 comparison on electricity sources

Whole process	Case 1 (old)	Case 1 (new)
PV electricity export (kWh)	3212.09	94130.57
Grid electricity import (kWh)	16547.11	48448.54

2) Case 2 with active charging according to PV generation

The new Case 2 is the same as the old Case 2 in the paper.

3) Case 3 optimized charging strategy

There is one change from the old Case 3. In the old Case 3, because the charging strategy requires the ASHP provides the maximum heat flux during the charging time steps and the PV can only provide limited electricity to the ASHP, so that the grid electricity is imported to provide the rest of the ASHP electricity demand during the charging season. However, in the new Case 3, the PV installation stays the same, but it is assumed that the electricity generated from the PV can be allocated to any time step according the charging strategy and then the surplus electricity is exported.

Table 5-2 Old and new Case 3 comparison on charging electricity sources

Charging season	Case 3 (old)	Case 3 (new)
PV electricity export (kWh)	41332.92	13911.56
Grid electricity import (kWh)	27421.36	0

5.2.2 Results and conclusion

According to the data used in the paper, with all the PV electricity exported to the grid, new Case 1 actually earns the most money (£3,509.5) shown in Table 5-3. Because that the total PV electricity is exported to the grid, a large amount of earning can cover the electricity consumption of the system. However, the system under this condition needs the largest amount of grid electricity supply in return (£7,413.8). In the new Case 3, the charging heat flux is all from converting the free PV electricity to heat energy and is available to be allocated to the time step when the system decides to charge the borehole. In the new Case 3, the system cost reduced by 50% compared with the old Case 3.

Table 5-3 Detailed electricity cost/earn from different electricity sources and system cost comparison

£	Case 1(old)	Case 1(new)	Case 2	Case 3(old)	Case 3(new)
PV FIT	+353.3	+10354.3	+367.5	+4914.6	+1898.2
Grid electricity	-2933.0	-7413.8	-2891.6	-6928.9	-2891.6
System cost	-2579.6	+3509.5	-2524.0	-2014.3	-993.4

To conclude, the system benefits from selling PV electricity to the grid, however, the operation of the proposed space heating system benefits more from the active charging especially using renewable energy and the active charging reduces the reliance on the grid electricity.

5.3 Chapter summary

In this chapter, the optimized short-term charging strategy is presented in the paper with a follow-up analysis on the system cost. With the optimized charging strategy, the system makes the most of the thermal storage and the efficiency can be increase. In this borehole coupled with heat pumps space heating system, the installation of PV can largely affect the system, and with high involvement of renewable energy, the system operational cost can be reduces.

6 Long term charging optimization

6.1 Introduction

The previous chapter discussed the charging strategy simulation which only contains one charging/discharging cycle and found out the most efficient method to use the borehole combined with the heat pumps. However, the borehole heat energy storage is built for its lifetime usage. As a result, in this chapter, the optimization is carried out on the several charging/discharging cycles to see how to make the best use of the heating system during long term simulation to see how heat accumulation affect the system in the long-term operation.

6.2 Case set up and explanation

In this section, the optimization is carried under 2 and 5 years for long term study. In this optimization process, it is assumed that the total charging heat flux is the fixed amount during the whole simulation and the aim is to find how to maximise the benefit from charging the borehole during the charging periods.

The objective function is in Equation (6.1). The optimization is to minimise the GSHP electricity consumption during the discharging season. The total heat flux injected into the borehole during the charging season is a fixed value as shown in Equation (6.2a) which is the constraint. Equation 6.2b describes the boundary of the variables at each time step. Equation 6.3 and 6.4 shows how electricity and heat flux converted by the heat pumps in this system.

$$\text{Obj} = \min \sum E_{GSHP(n)} \tag{6.1}$$

$$0 = Heatflux_{fixed} - \sum x_{(charging)} \tag{6.2a}$$

$$\begin{cases} 0 \leq x_{(charging)} \leq 4541 \\ x_{(discharging)} = heating\ load \end{cases} \tag{6.2b}$$

$$E_{HP} = \frac{H_{HP}}{\text{CoP}} = \frac{x}{a \cdot \text{temperature} + b} \tag{6.3}$$

$$x_{(charging/discharging)} = \frac{1000 \times E_{HP} \times \text{CoP}}{hours \times N_{borehole} \times V_{borehole}} = \frac{1000 \times E_{HP} \times (a \cdot temperature + b)}{24 \times 7 \times N_{borehole} \times V_{borehole}} \tag{6.4}$$

- E_{HP} is heat pump electricity consumption (kWh)
- $Heatflux_{fixed}$ fixed total heat flux injection during the charging season.
- CoP is the heat pumps' CoP at step
- $x_{(charge)}$ and $x_{(discharge)}$ are the heat flux injection and extraction (W/m^3).
- $N_{borehole}$ is the borehole number.
- $V_{borehole}$ is the single borehole volume (m^3).
- H_{HP} is the heat energy generated by heat pumps.

Figure 6-1 is the optimization flow chart. The optimization method used in this chapter is the numerical optimization pattern search to find the minimum electricity consumption as is shown in equation (6.1). The pattern search was introduced by Hooke and Jeeves in 1961. The pattern search starts with a current point and searches in a predetermined direction. If a better point is found, this point becomes the new start and the search keeps going on.

The process starts with a given heat flux applying to the borehole model and with the GSHP technical data, the electricity used during the heating season can be calculated. If the result is not the minimum electricity consumption, the control variable is altered and applied to the system until the constraints are fulfilled. When the objective function is satisfied, the system generates the optimized x (heat flux) and temperature file.

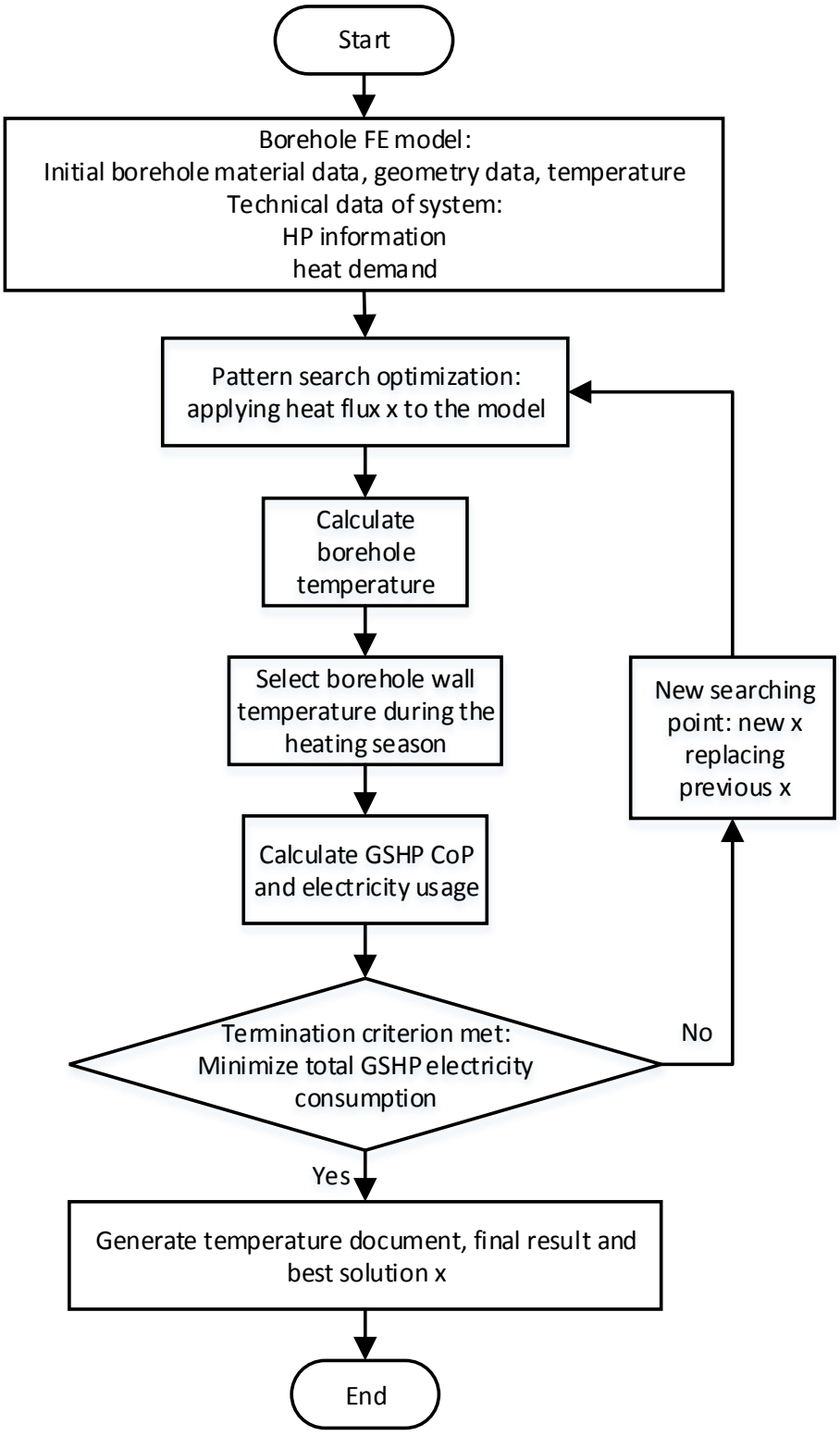

Figure 6-1 Optimization process

6.3 System inputs

The PV electricity generation data is obtained from G.B. National Grid Status [86] and PVGIS [83]. During the charging season, the PV weekly generation data is shown in Figure 6-2. The charging season starts from April to September and the electricity generation is relatively high during June, July, and August. During the charging season, the electricity generated from installed PV will provide the ASHP to charge the borehole. The space heating weekly demand is shown in Figure 6-3. The data is estimated from the historical data [87]. It is assumed that during the long term simulation, each year, the PV and heat demand has the same weekly profile. From each figure, the electricity generation and the space heating demand vary largely each week. In this PV historical generation figure, most electricity is generated around the summer time as shown in week 9 to week 20. In the space heating figure, the coldest time is around the end of December to March. However, the data used in this simulation is based on the historical analysis and depending on the weather condition and there will be exceptions in the figures which can be ignored considering the operation of the system.

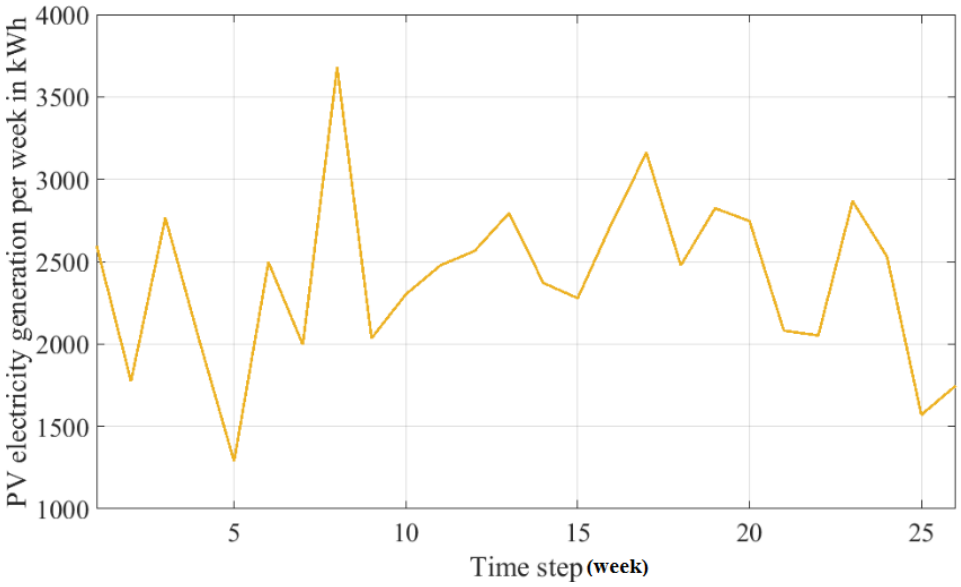

Figure 6-2 PV electricity generation during the charging season (April to September)

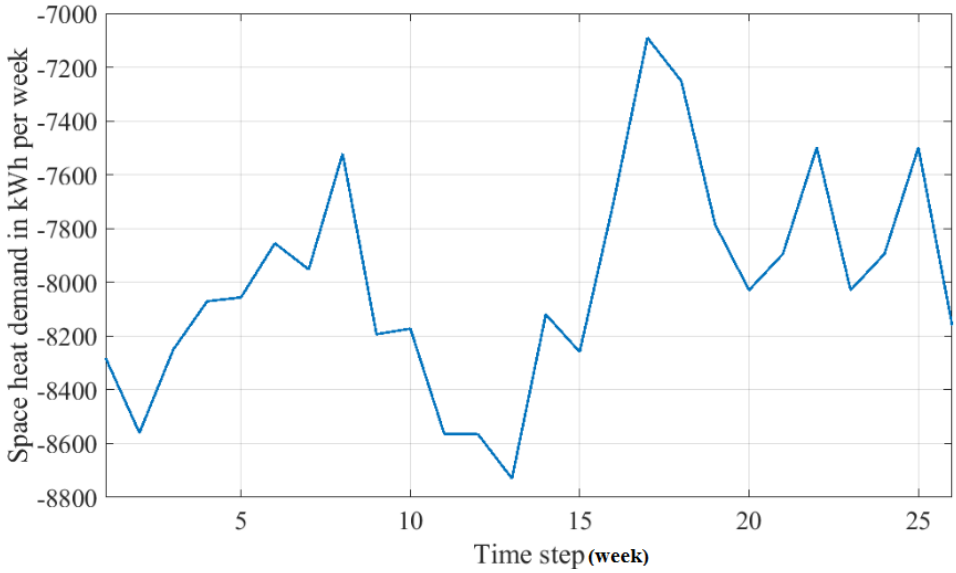

Figure 6-3 Space heat demand during the heating season (October to March)

Besides the heat demand and PV generation input, the heat pump information is shown in previous chapters.

6.4 Case explanation and comparison

In the long term simulation, in order to shorten the optimization time, the time step length is set to one week and the total time step number for 2 years, and 5 years will be 104, and 260 respectively. In every single charging/discharging cycle, it is assumed that the system uses halftime to charge and discharge.

- Case 1 operation according to PV generation

This is the base case and the borehole is charged according to the electricity generated by the installed PV. Figure 6-4 and 6-5 are the temperature response to the heat flux injection and extraction during 2 years and 5 years operation. In the charging seasons, the temperature increases with the constant heat flux injection. Due to the limitation on PV electricity generation, the heat flux amount fluctuates over the time. Compared to the ASHP maximum heat flux in equation 6.2b, the amount of heat flux under this condition is much lower. With higher heat flux injection, the temperature goes up quickly, with lower heat flux injection the temperature increases slow and sometimes decreases because of the heat loss. During the heating season, with the space heat demand, the borehole temperature decreases with the

constant heat extraction. It is obvious that at the beginning of the charging or discharging season, the temperature increases or decreases fast due to the massive temperature difference between each borehole layers. In this case, borehole temperature stays between 11°C and 15°C.

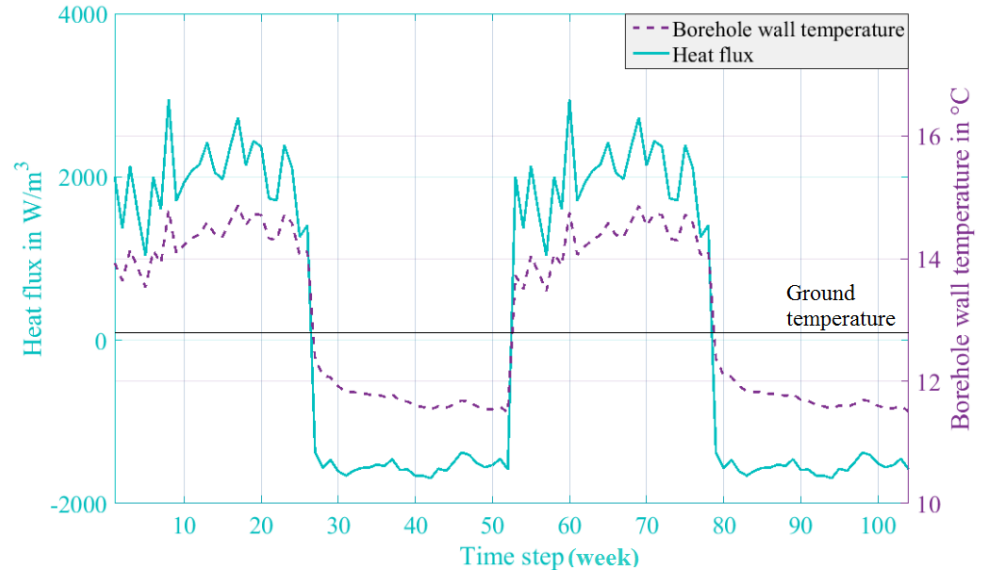

Figure 6-4 Temperature response to heat flux during 2 years' operation

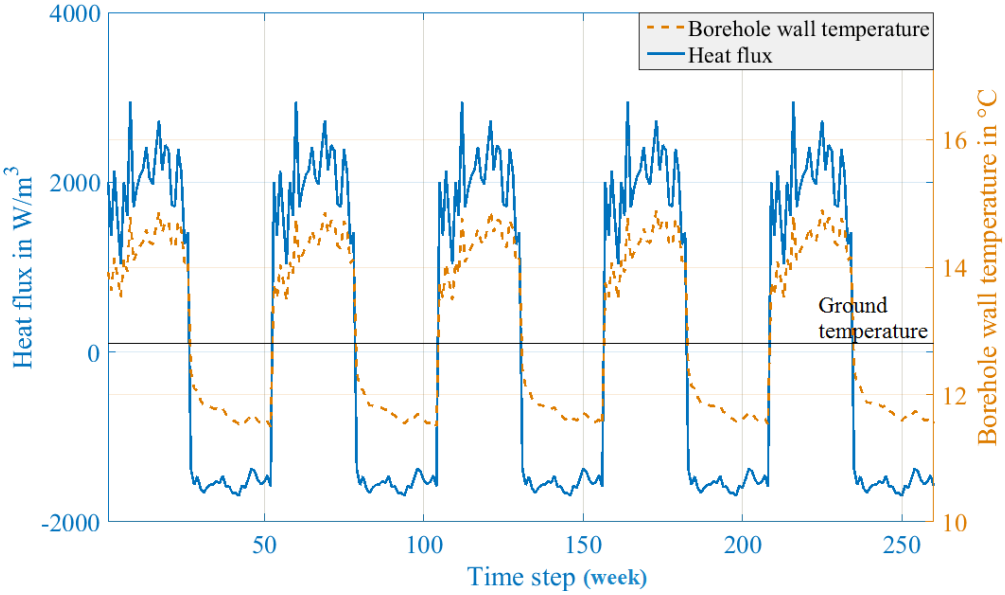

Figure 6-5 Temperature response to heat flux during 5 years' operation

- Case 2 operation using single-cycle charging strategy

In this case, the charging strategy from chapter 5 is used. In Chapter 5, the study shows that the proposed heating system benefits more from a concentrated charging strategy in a single charging/discharging cycle. As a result, the total charging heat flux remains the same and the concentrated charging strategy is used in each year. Figure 6-6 and 6-7 are the borehole wall temperature response to this charging strategy. In each charging season, the borehole is charged close to the beginning of the heating season with the available maximum heat flux from ASHP. In the charging seasons with no active charging, the surrounding ground increases the borehole temperature due to the temperature difference after the last heating season. Under this condition, borehole temperature stays between 11°C and 17°C.

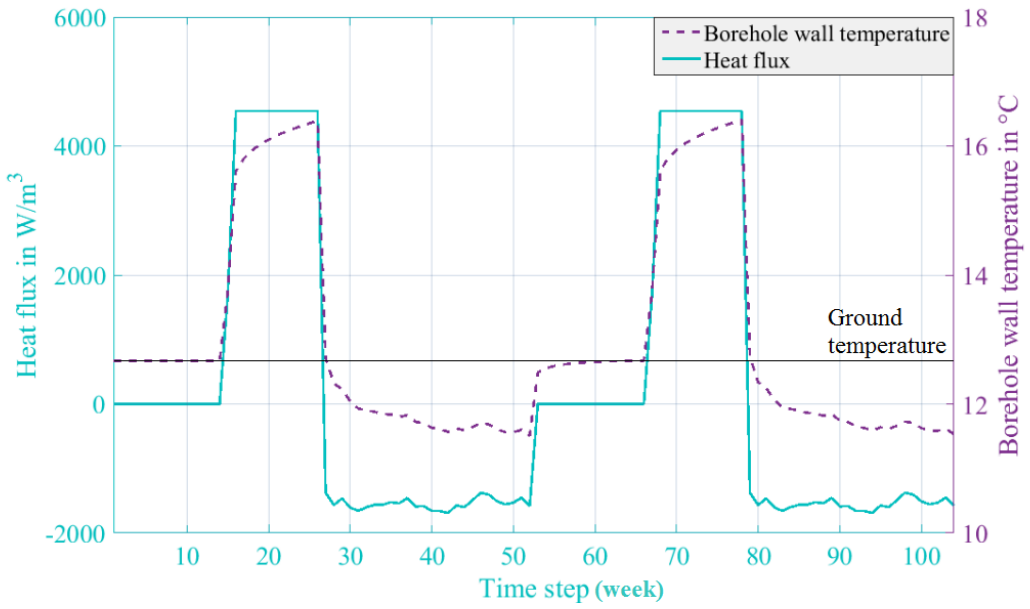

Figure 6-6 Temperature response to heat flux during 2 years' operation

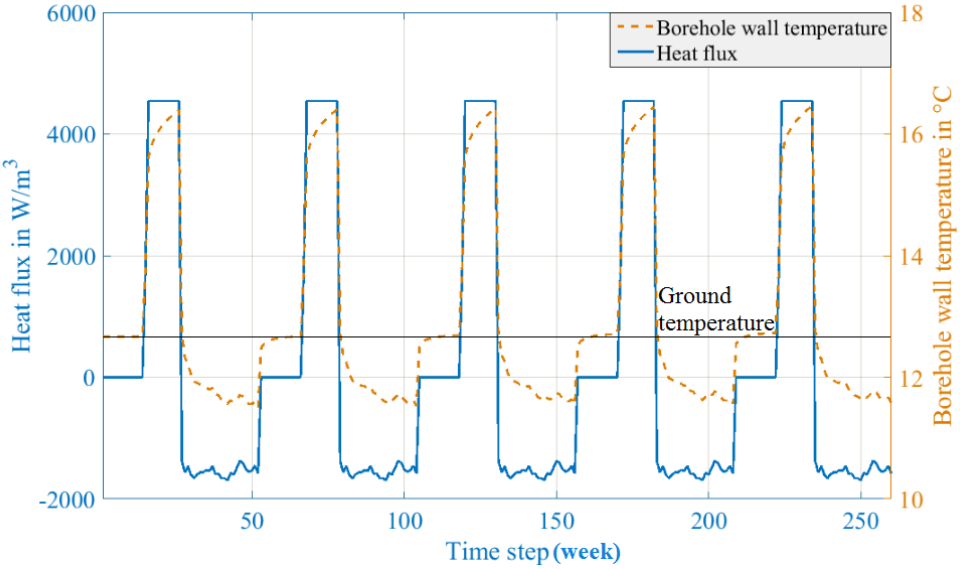

Figure 6-7 Temperature response to heat flux during 5 years' operation

- Case 3 optimized long-term optimization

In this case, the charging strategy is optimized using the method presented in section 6.2.1. The optimized strategy allocates the maximum heat injection, which is called supercharging, during the early charging seasons and the borehole wall temperature increases fast. The charging strategy used in the 2-year and 5 year is directly from the pattern search optimization result.

For the case in 2-year simulation in Figure 6-8, in the second charging season, no heat flux is injected, however, due to the temperature difference between the borehole and the surrounding ground, the surrounding ground increases the borehole temperature before the start of the heating season due to natural heat replenishment.

For the case in 5-year simulation in Figure 6-9, ASHP provides the maximum heat flux covering the first two charging seasons and obtain the single cycle charging strategy in the third charging season. In the last two charging season, there is no active charging happening. Because of the supercharging, the borehole temperature increases very fast.

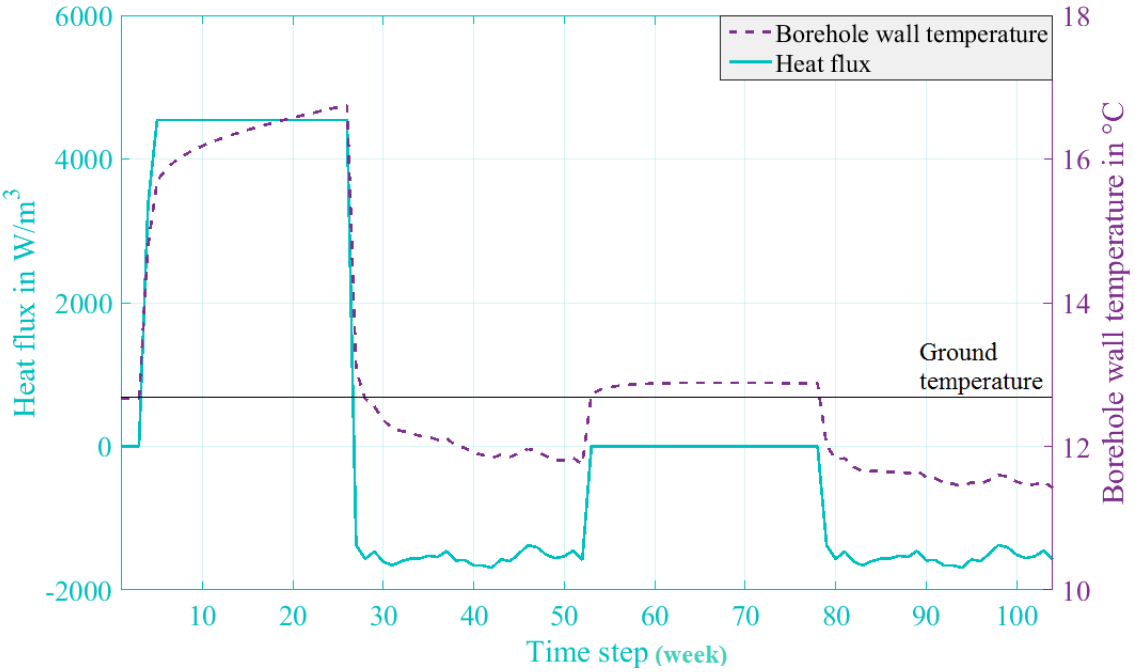

Figure 6-8 Temperature response to heat flux during 2 years' operation

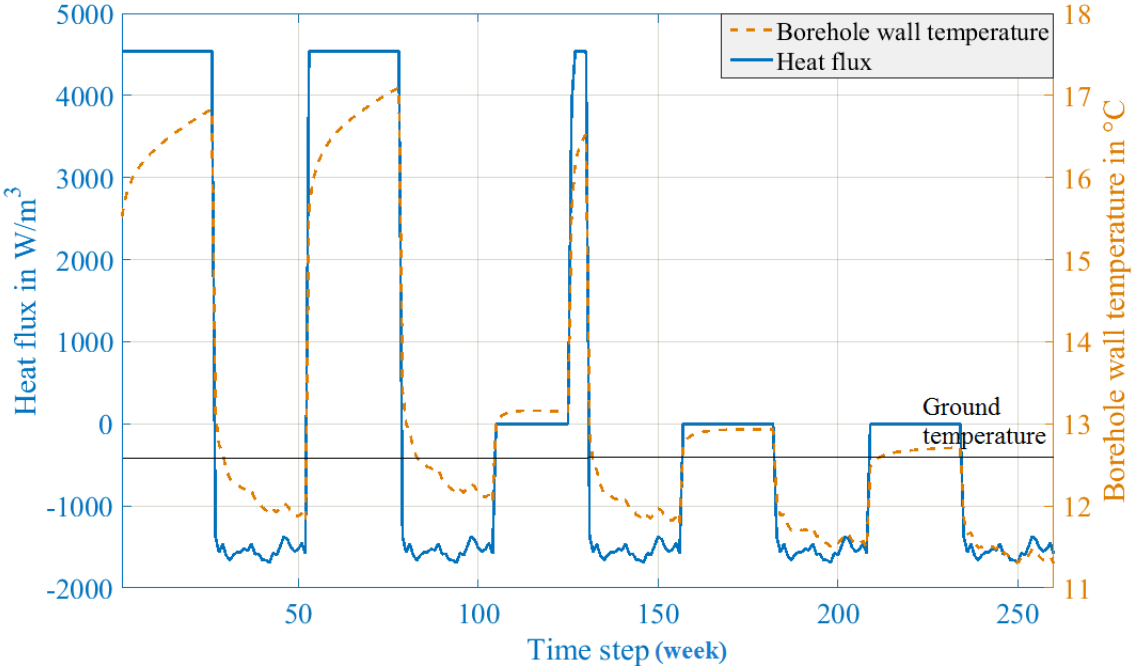

Figure 6-9 Temperature response to heat flux during 5 years' operation

From the temperature response figures in these three cases, a massive temperature change occurs between the charging and discharging seasons. In Chapter 4 borehole temperature behaviour study, the one of the characteristics of the borehole temperature changing pattern

shows that with the constant heat injection/extraction, the borehole temperature changes fast in the early time and slowly reaches a saturated level. During the operation of the borehole system in this chapter, heat loss happens when there is a temperature difference, adding the heat extraction from the borehole, the temperature drops dramatically between each season.

6.5 Result analysis

- GSHP electricity consumption

The optimization is to find the minimum GSHP electricity usage during the heating season with limited heat storage during the charging seasons. For 2-year optimization, Case 1 is the base case in which GSHP consumes the most electricity. Case 2 obtains the single charging/discharging cycle strategy and it helps to save 436.39kWh electricity compared to case one. GSHP uses the least electricity in Case 3 which is operated under the most optimal charging strategy. In case 3, the saved electricity is 505.91kWh compared to Case 1.

For 5-year optimization, the cases show the same characteristic. Compared to Case 1, GSHP electricity consumption in Case 2 and Case 3 are reduced by 1,126.73kWh and 1,679.70kWh.

From Figure 6-10 and 6-11, it is clear that with an optimized charging strategy allocating the heat input during appropriate time intervals, the electricity consumptions are reduced in Case 2 and 3 compared with Case 3.

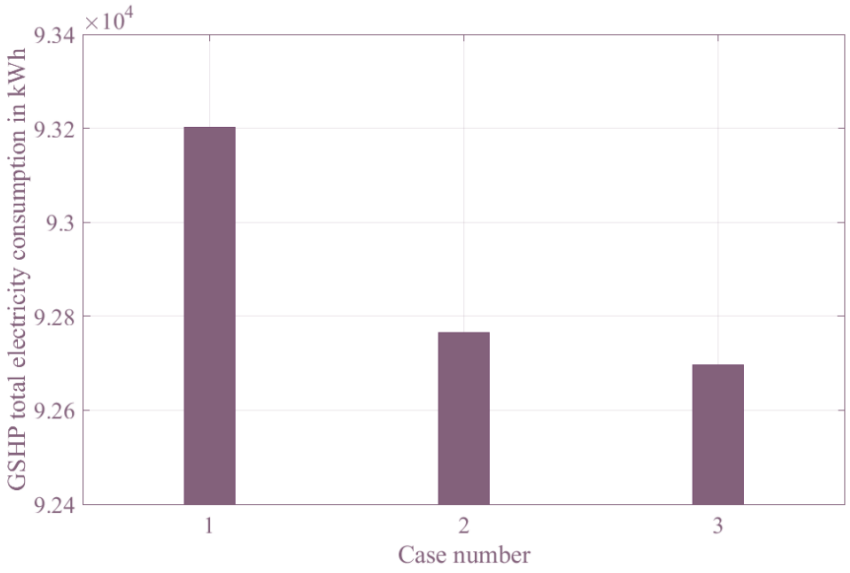

Figure 6-10 GSHP electricity consumption in 2 years

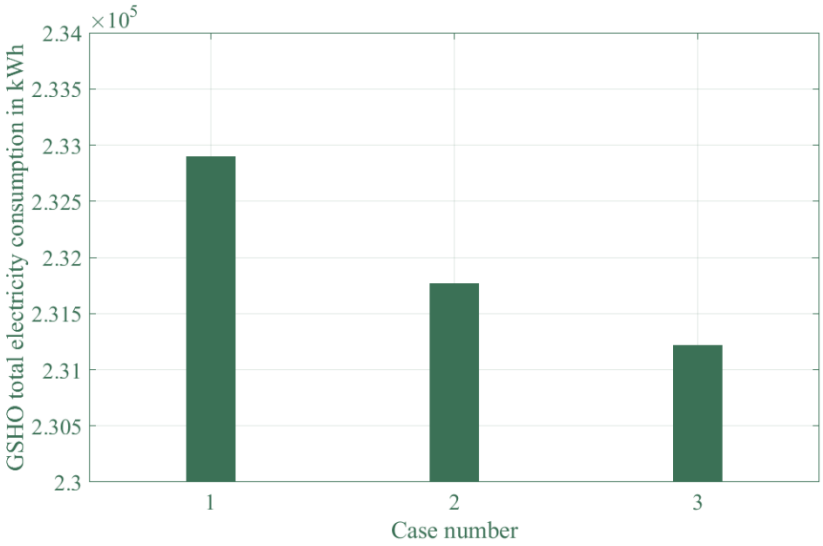

Figure 6-11 GSHP electricity consumption in 5 years

- Temperature difference

Figure 6-12 is the temperature comparison between these three cases in the 2-year simulation. With the supper charge in the first charging season in Case 3, borehole temperature increases very fast and slowly reaches a saturated level around 17 °C. After the first discharging season, the borehole wall temperature in Case 3 is higher than the other 2 cases. Without the heat flux input in the second charging season, Although in second charging season, the temperature in Case 3 is lower than Case1 and 2, the heat loss is much less than in Case 1 and 2. Overall, Case 3 uses the most of the stored heat in the borehole.

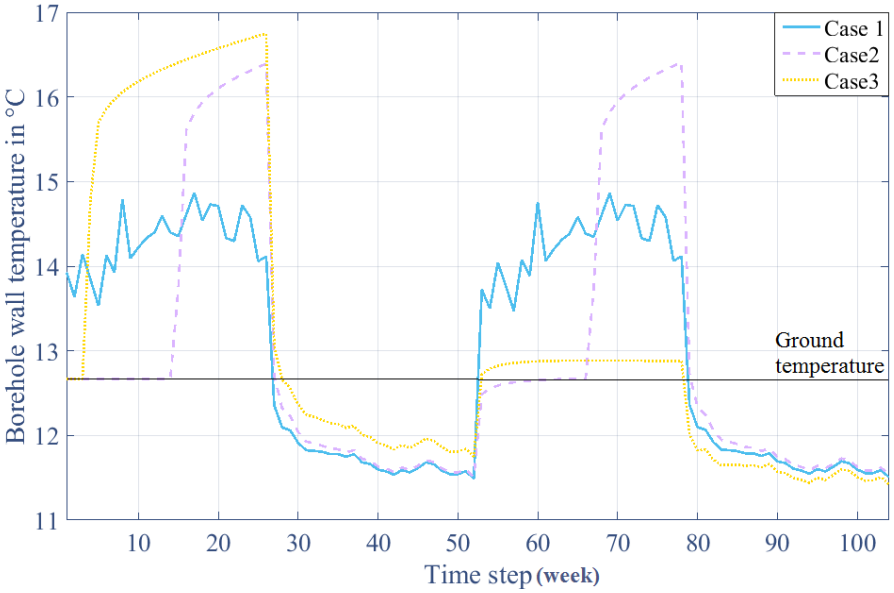

Figure 6-12 Borehole temperature comparison in 2 years

Figure 6-13 is the temperature comparison between these 3 cases in the 5-year situation. The first two supercharging seasons in Case 3 lifts the borehole wall temperature fast as well as the surround ground temperature which helps to decrease heat loss in the future, and the temperature in the first two charging seasons are increasing. In Case 1 and 2, because the charging is very even in each season, the temperature changing pattern is the same in each year. Although in the later cycles, the borehole temperature is higher than Case 3, the heat loss is higher than Case 3 and less heat is stored.

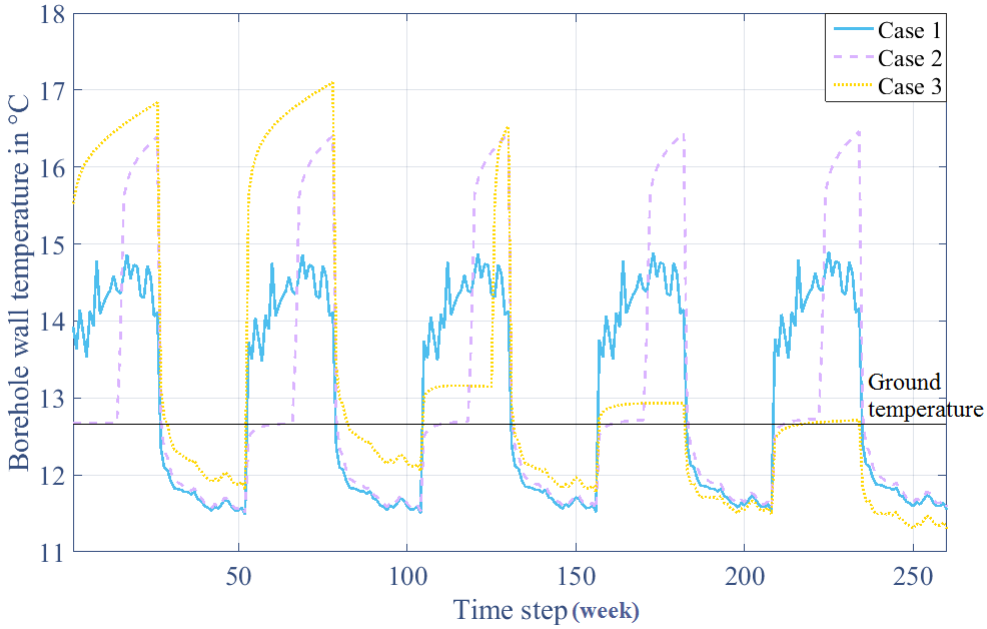

Figure 6-13 borehole temperature comparison in 5 years

- Heat accumulation affect

The installation the borehole inter-seasonal heat storage is for long term usage and by obtaining the optimized charging strategy over the long term simulation, the space heating system uses the best of the total available active recharge. The optimization is only carried on 2 years which is to tell the difference from 1 year and 5 years which is close to lifetime situation. Due to the long process time, optimization is not performing on lifetime simulation and instead, the simulation is carried out to show the result.

The previous optimization is based on the concept of each single year operation and the result shows that with the optimized charging strategy, less heat input is needed to provide the heat

demand. In this chapter, the optimization is to illustrate how charging affects the proposed heating system over a long term operation. Two base cases are set up for comparison:

- Case 1 charging according to the PV generation
- Case 2 charging using the single cycle optimized method

Case 3 uses the optimized charging method. Figure 6-14 is the results comparison. The x-axe represents a different year's simulation from 2 years to 10 years. In different year's simulation, Case 3 always has the lowest GSHP electricity consumption according to the bar chart. Case 2 has the second lowest GSHP electricity consumption and in Case 1 GSHP consumes the most electricity during the whole heating season.

The red dotted line and the blue solid line are the electricity saved in Case 3 and Case 2 compared to Case 1. It is obvious that by using the optimized long term charging strategy, with the growth of operation time, more electricity is saved over the years. By using the single cycle charging strategy in each year, the saved electricity in total is increasing slowly.

Table 6-1 is the saved electricity amount in Case 2 and 3 within the whole heating seasons under each simulated time window. It is clear that the optimized charging strategy helps to save more electricity over a longer operation time.

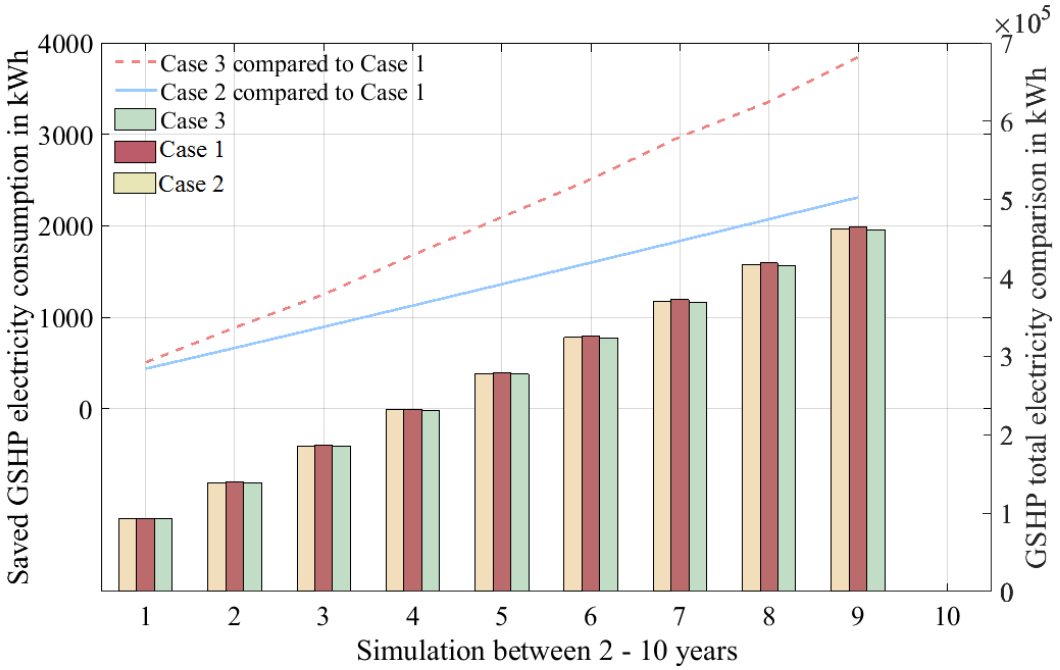

Figure 6-14 GSHP electricity consumption comparison

Table 6-1 Total save electricity (kWh) during the whole simulation time

Total saved electricity compared to Case 1	2 years	3 years	4 years	5 years	6 years	7 years	8 years	9 years	10 years
Case 2	436.39	663.63	894.08	1126.7	1360.8	1596.7	1833.6	2071.4	2310.1
Case 3	505.91	885.68	1249.7	1679.7	2093.8	2508.7	2972.5	3355.1	3844.0

From this comparison figure and table, it can be seen that, in Case 3, with supercharge in the early state, heat accumulates under the ground which benefits the most regardless of the length of the time and with the longer operation time, the saving is increasing.

6.6 Chapter summary

In this chapter, the optimization is carried out on the operation of borehole thermal storage combined with heat pumps for long term simulation.

Heat transfer in the ground is a very complicated process. The borehole FE model used in this study considers the heat transfer between the surrounding ground and different borehole materials in each part, thus, heat loss and heat accumulation under the ground are inevitable. With the efficient operation of borehole heat storage, the proposed space heating system can be operated more efficiently. With the same amount charging heat flux injected into the borehole thermal storage during the charging seasons, it is better to charge the borehole early with the maximum available heat flux that ASHP can provide which is called supercharge. Compared with the cases treating each charging/discharging cycle as an individual process, the optimized strategy reduces the most electricity consumption during the heating seasons with the same amount of charging during the summer time. With this charging strategy, it prevents borehole from more heat loss in the later stage and increases the surrounding ground temperature as soon as possible during the long term operation. By using the optimized method, the injected heat flux brings the maximum benefit to the space heating system.

7 Conclusion

This dissertation is focused on the modelling of borehole inter-seasonal thermal storage and borehole thermal storage application. This study is carried out and developed based on a practical project located in Bristol, UK, focusing on the low carbon heat network development. The project aims to operate an ASHP on hot summer days matched in PV generation and delivers the heat to an inter-seasonal borehole thermal storage array; then GSHP to extract heat from the thermal store. The process is called "active replenishment" which shift electricity-heat consumption in the heating system and enable the small borehole to supply more properties reducing the capital cost [13].

This work started with the feasibility study of the borehole storage energy chain based on the energy hub concept. In Chapter 3, the basic system process is brought up and studied. The new space heating system was later applied to a community building. With the actual system parameter applied in the simulation, the results in this section were compared with the historical space heating data from the old heating system with boilers. There are two main findings:

- An active charging to borehole during the summertime increases the borehole temperature which helps to reduce the electricity consumption of GSHP during the winter time.
- The feasibility study on the lifetime performance shows great potential on saving energy and reducing carbon emission. The heat accumulates in the borehole and brings benefit in the lifetime.

With the feasibility study on the proposed heating system, Chapter 4 develops an accurate model for the borehole arrays and studies the temperature behaviour of the heat transfer with the media of the borehole and surrounding ground. The following part introduced this 12-borehole model based on the real geometry layout. The model:

- The fluid in the borehole has a high temperature, however, the heat quickly settles down in the surrounding area especially the borehole wall. The borehole wall temperature is the key information in the heating system.

- The temperature in the borehole changes fast at the beginning of the charging or discharging due to the temperature difference between each media and gradually, the temperature reaches a saturated value. With the active charging during the charging season, the overall temperature is increasing and the efficiency of the heating system is going up.

Because the heat transfer is a very complicated process involving constant heat dissipation, injection and extraction, and for the proposed space heating system, borehole temperature is related to the heat pumps, finding the most efficient operation strategy is significant for the operation of the system. In Chapter 5, the system is optimized according to single charging/discharging process, for the same amount of electricity used to provide space heating during the heating season, the optimized borehole charging strategy is found and the main conclusions are:

- For this single charging/discharging optimization, instead of charging the borehole according to the PV generation across the whole charging season, the optimized charging strategy required less electricity consumption from ASHP to generate heat energy injected into the borehole during the charging season and remains the performance of GSHP during the discharging season.
- The proposed heating system reduces 70% of CO_2 emission compared to the traditional heating method (gas boilers). By using the optimized charging strategy, during the discharging season, the CO_2 emission is reduced compared to the normal charging strategy.

The borehole inter-seasonal heat storage has a very low maintenance cost and used not only for one single charging/discharging cycle, but it is also important to study on the performance in long term operation. In Chapter 6, the optimization of long term system operation is carried out, with the charging strategy studied, there are two main findings as listed below:

- With the limited total charging heat energy, the charging strategy is very different from the single charging/discharging cycle. Instead of using the single cycle optimized charging strategy in each cycle, it is more efficient to supercharge the borehole in the early charging seasons.

- The early heat accumulate under the ground not only helps the current heating season to benefit from high temperature due to the supercharging and the temperature is normally 2-3°C higher which increases the GSHP CoP more. The heat accumulated under the ground also benefit the future charging/discharging cycles. With higher surrounding ground temperature, it helps to preserve more heat in the later charging season reducing the heat loss and when the borehole temperature is low, the surrounding ground transfers back the heat preventing the system from low temperature.

This thesis starts with the study of high-level space heating energy chain based on a practical project followed with the operation strategy within a space heating system. The operation strategies of the inter-seasonal borehole heat energy storage presents the guide to increase the system efficiency, reduce the energy consumption and CO_2 emission on space heating system and can be used in the future with more complicated energy supply system on the community level.

8 Future work

This chapter discusses a number of opportunities that can be improved in the future based on the work presented in this thesis. This research is the initial borehole thermal storage operation study and it presents an operational guide for the thermal storage when coupled with heat pumps. Besides the benefit brought by this proposed space heating system, further research work is needed to increase the application of the low carbon heating system and with more aspects taken into account, the space heating system could possibly provide more detailed information to the end users as well as helping the energy network to improve the operation and therefore achieve the government regulation and requirement. The following bullet points are the main future research directions:

- **Increase system accuracy over timescale and model conditions**

In this thesis, work has been done on the operation of the low carbon space heating system. Due to the complexity of the borehole system, it is difficult to optimize a lifetime performance with a small time step. The optimization has been done on short timestep with short total simulation time, and long timestep with long total simulation time. With a longer time step, assumptions are made: i) the system is simulated as seasonal, during the charging and discharging season, the heat flux injection or extraction is a constant process during each time step. ii) Because that the system is simulated seasonally, the electricity price is not considered in the system. iii) the electricity used for charging the borehole is from the PV generation and is assumed that it is available at any time. iv) in each season, the weather, temperature and heat demand is assumed to be the same.

In the future work there is improvement needed to be done in terms of the performance of the space heat system:

i) **Time step length**: for the single-cycle and multi-cycle optimization, each time step length is one week and during each time step it is assumed that the borehole is constantly charging or discharging. With the renewable energy involved especially PV, the system cannot be guaranteed with the constant input from the PV during the charging season. With the borehole being an inter-seasonal heat

storage, the focus is on the heat accumulation in the borehole and the benefit in the lifetime operation and it is reasonable to make the assumption in each time step. However, the heat transfer is a complex process and the temperature changes differently which will affect the short-term simulation. This situation can be further improved by shortening the time step into an hourly simulation which can be better used with renewable energy and cooperate easily with another form of energies.

ii) **Heat pumps performance**: in this proposed heating system, the focus is on the borehole operation and delivered charging strategies on the system to increase the efficiency during the heating season. Further work needs to be done considering the more aspects of the low carbon space heating system. For instance, the operation of the heat pumps, ASHP in this system works as the input of the borehole, and it takes the advantage of the high air temperature during the summer time. However, in this research, the focus is on the borehole temperature and system efficiency over the heating season, as a result, there is a lack of study on how large the influence of ASHP can bring to the space heating system. GSHP CoP during the heating season directly gets influenced from the borehole temperature changing and provide space heating for the community. However, the output of the GSHP is set to a fixed value as the radiator temperature which can leads to over-heating or under-heating according to the room temperature and weather. In the future work, more research can be done on the relationship between GHSP and weather.

- **Improving borehole application in the multi-energy system**

This study delivered a promising operation strategy for the space heating system, however, for the domestic energy consumption, other forms of energy demand need to be considered. In order to improve the application of the heat energy storage, future work needs to be done in smart homes/grid, and understand how the borehole heating system performs and brings benefit to a multi-energy system.

Continuing with the work presented in this thesis, initial research has been done over inter-connected energy hubs on sharing energies among energy hubs. In the research, the small community consists of 11 houses and there are conventional energy forms and renewable

energies. In order to reduce the optimization time, the borehole FE model is simplified and blended in the community inter-connected energy hub system. The research concludes on the benefit from the borehole combined heat pump: 1) stable system performance 2) reduced total energy cost.

This initial research is based on daily operation and for the borehole inter-seasonal storage, however, the affection to the energy supply system from the heat accumulation in the borehole and the bedrock is not shown, as a result, in the future work, long-term optimal control for the borehole combined heat pump system will be studied.

- ## Uncertainty analysis

In the presented research, the focus is on the borehole temperature affecting the heat pump performance and how the charging strategy affects the system in the long-term simulation. However, during the charging and discharging seasons, the weather condition is not considered, assumptions are made on the operation of heat pumps and borehole storage. At the same time, because of the lack of investigation during the heating season and the historical data is used, social profiles are not considered.

As a result, the uncertainty of system input and output will be investigated in the future:

i) **Weather**: continue with the work presented in this thesis, which include the assumption on the weather condition, modelling the relationship between renewable energy generations varying along the weather condition, ASHP reacting to the air temperature during the charging season, and heat demand changes along the winter air temperature (household load forecasting) can help to improve the operation

ii) **Social profile**: model how the demand varies according to different social groups which helps to optimize the operation during the heating season and further improves cooperation between the borehole heat energy storage and other energy supply in the multi-energy system.

Appendix A

Ground Source Heat Pump

	Evaporator outlet temperature (°C)	Evaporator inlet temperature (°C)	Condenser Water Outlet Temperature (°C)			
			30			
			Cooling (kW)	Input (kW)	Heating (kW)	COP
GSHP	**-10**	**-7**	50.1	16.8	66.2	3.94
	-4	**-1**	62.8	16.9	79.1	4.68
	0	**4**	73.0	17.0	89.5	5.25
	2	**6**	78.1	17.1	94.7	5.54
	5	**10**	89.1	17.3	105.9	6.12
	6	**11**	92.1	17.4	109.0	6.28
	7	**12**	95.1	17.4	112	6.44
	10	**15**	**105.2**	**17.7**	**122.5**	**6.92**
	12	**18**	112	17.9	129.5	7.23
	15	**21**	122	18	139	7.69
	18	**24**	132	19	151	8.09
	Evaporator outlet temperature (°C)	**Evaporator inlet temperature (°C)**	**Condenser Water Outlet Temperature (°C)**			
			35			
			Cooling (kW)	**Input (kW)**	**Heating (kW)**	**COP**
GSHP	**-10**	**-7**	47.6	18.7	65.4	3.50
	-4	**-1**	59.9	18.9	78.0	4.13
	0	**4**	69.9	19.0	88.2	4.65
	2	**6**	74.9	19.0	93.3	4.91
	5	**10**	85.5	19.2	104.0	5.42
	6	**11**	88.4	19.2	107.0	5.57
	7	**12**	91.3	19.2	109.9	5.72
	10	**15**	**100.7**	**19.4**	**120.0**	**6.17**
	12	**18**	107.0	19.6	126.7	6.46

	15	**21**	116.9	19.5	136.0	6.97
	18	**24**	127.6	20.0	147.2	7.36
GSHP	**Evaporator outlet temperature (°C)**	**Evaporator inlet temperature (°C)**	**Condenser Water Outlet Temperature (°C)**			
			40			
			Cooling (kW)	**Input (kW)**	**Heating (kW)**	**COP**
	-10	**-7**	44.7	20.70	64.40	3.11
	-4	**-1**	56.8	21.00	76.90	3.66
	0	**4**	66.4	21.1	86.8	4.11
	2	**6**	71.2	21.20	91.70	4.33
	5	**10**	81.4	21.30	102.00	4.79
	6	**11**	84.2	21.4	104.8	4.91
	7	**12**	86.9	21.40	107.60	5.03
	10	**15**	**96.5**	**21.5**	**117.4**	**5.45**
	12	**18**	102.9	21.60	123.90	5.74
	15	**21**	111.9	21.40	132.70	6.20
	18	**24**	122.2	21.70	143.30	6.60
GSHP	**Evaporator outlet temperature (°C)**	**Evaporator inlet temperature (°C)**	**Condenser Water Outlet Temperature (°C)**			
			45			
			Cooling (kW)	**Input (kW)**	**Heating (kW)**	**COP**
	-10	**-7**	41.8	22.9	63.4	2.77
	-4	**-1**	53.3	23.4	75.6	3.23
	0	**4**	**62.6**	**23.6**	**85.2**	**3.61**
	2	**6**	67.2	23.7	90.0	3.80
	5	**10**	76.9	23.8	99.8	4.19
	6	**11**	79.6	23.9	102.6	4.30
	7	**12**	82.3	23.9	105.3	4.41
	10	**15**	91.6	24.0	114.7	4.79
	12	**18**	97.8	24.0	121.0	5.04
	15	**21**	106.6	23.6	129.5	5.49
	18	**24**	116.4	23.8	139.5	5.86

	Evaporator outlet temperature (°C)	Evaporator inlet temperature (°C)	Condenser Water Outlet Temperature (°C)			
			50			
			Cooling (kW)	Input (kW)	Heating (kW)	COP
GSHP	-10	-7	N/A			
	-4	-1	49.3	26	74	2.85
	0	4	58.2	26.3	83.3	3.16
	2	6	62.7	26.5	88	3.32
	5	10	72	26.6	97.5	3.67
	6	11	74.6	26.6	100.1	3.76
	7	12	77.1	26.6	102.7	3.86
	10	15	85.9	26.7	111.6	4.18
	12	18	91.7	26.8	117.6	4.39
	15	21	100	26	126	4.80
	18	24	109	26	135	5.10
	Evaporator outlet temperature (°C)	Evaporator inlet temperature (°C)	Condenser Water Outlet Temperature (°C)			
			55			
			Cooling (kW)	Input (kW)	Heating (kW)	COP
GSHP	-10	-7	N/A			
	-4	-1				
	0	4				
	2	6	57.6	29.5	85.7	2.91
	5	10	66.6	29.7	94.9	3.20
	6	11	69.0	29.8	97.4	3.27
	7	12	71.4	29.8	99.8	3.35
	10	15	79.7	29.9	108.4	3.63
	12	18	85.3	29.9	114.1	3.82
	15	21	93	30	121	4.10
	18	24	103	29	131	4.46

Air Source Heat Pump

	Air temperature (°C)	Condenser Water Outlet Temperature (°C)		
		30		
		Input (kW)	Heating (kW)	COP
ASHP	-20	11.39	27.36	2.40
	-17	11.54	29.82	2.58
	-15	11.68	31.7	2.71
	-13	11.81	33.51	2.84
	-12	11.88	34.42	2.90
	-10	12.02	36.48	3.03
	-5	12.49	41.89	3.35
	0	12.93	47.92	3.71
	5	13.42	54.33	4.05
	7	13.62	57.07	4.19
	10	13.88	61.17	4.41
	15	14.29	68.02	4.76
	20	14.66	75.01	5.12
	Air temperature (°C)	Condenser Water Outlet Temperature (°C)		
		35		
		Input (kW)	Heating (kW)	COP
ASHP	-20	12.44	27.36	2.20
	-17	12.58	29.79	2.37
	-15	12.67	31.5	2.49
	-13	12.8	33.28	2.60
	-12	12.86	34.16	2.66
	-10	13.02	36.14	2.78
	-5	13.42	41.36	3.08
	0	13.88	47.12	3.39
	5	14.38	53.38	3.71
	7	14.58	55.95	3.84
	10	14.86	59.87	4.03
	15	15.3	66.71	4.36

	20	15.68	73.36	4.68
ASHP	**Air temperature (°C)**	**Condenser Water Outlet Temperature (°C)**		
		40		
		Input (kW)	**Heating (kW)**	**COP**
	-20	N/A		
	-17	13.7	29.69	2.17
	-15	13.79	31.33	2.27
	-13	13.89	33.05	2.38
	-12	13.96	33.92	2.43
	-10	14.08	35.8	2.54
	-5	14.46	40.88	2.83
	0	14.9	46.46	3.12
	5	15.38	52.27	3.40
	7	15.59	54.67	3.51
	10	15.9	58.62	3.69
	15	16.35	65.12	3.98
	20	16.76	71.57	4.27
ASHP	**Air temperature (°C)**	**45**		
		Input (kW)	**Heating (kW)**	**COP**
	-20	N/A		
	-17			
	-15			
	-13	15.1	32.85	2.18
	-12	15.15	33.71	2.23
	-10	15.26	35.44	2.32
	-5	15.61	40.3	2.58
	0	16.05	45.66	2.84
	5	16.57	51.2	3.09
	7	16.73	53.49	3.20
	10	17.02	57.28	3.37
	15	17.49	63.43	3.63

	20	17.9	69.46	3.88
ASHP	**Air temperature (°C)**	**Condenser Water Outlet Temperature (°C)**		
		50		
		Input (kW)	**Heating (kW)**	**COP**
	-20	N/A		
	-17			
	-15			
	-13			
	-12			
	-10			
	-5	16.91	39.74	2.35
	0	17.31	44.83	2.59
	5	17.75	50.05	2.82
	7	17.96	52.37	2.92
	10	18.27	55.91	3.06
	15	18.72	61.62	3.29
	20	19.17	67.28	3.51
ASHP	**Air temperature (°C)**	**Condenser Water Outlet Temperature (°C)**		
		55		
		Input (kW)	**Heating (kW)**	**COP**
	-20	N/A		
	-17			
	-15			
	-13			
	-12			
	-10			
	-5			
	0	18.72	44.02	2.35
	5	19.16	48.89	2.55
	7	19.34	51.06	2.64
	10	19.64	54.42	2.77

	15	20.09	59.98	2.99
	20	20.48	65.23	3.19
ASHP	**Air temperature (°C)**	**Condenser Water Outlet Temperature (°C)**		
		58		
		Input (kW)	**Heating (kW)**	**COP**
	-20	N/A		
	-17			
	-15			
	-13			
	-12			
	-10			
	-5			
	0	19.64	43.48	2.21
	5	20.05	48.26	2.41
	7	20.25	50.34	2.49
	10	20.52	53.48	2.61
	15	20.96	58.8	2.81
	20	21.35	64.01	3.00

Appendix B

			kWh		**KWh**	**kg**	**£**
	Days	**Time step**	**Boiler operation**				
			Input energy	**Efficiency**	**Output energy (Heat)**	**CO2 emission**	**Cost**
	starting point		0.0	0.0	0.0	0.0	0.0
October	Day 1	07:00-19:00	484.8	0.9	412.1	84.2	41.4
		19:00-07:00	484.8	0.9	412.1	84.2	41.4
	Day 2	07:00-19:00	484.8	0.9	412.1	84.2	41.4

		19:00-07:00	484.8	0.9	412.1	84.2	41.4
	Day 3	07:00-19:00	484.8	0.9	412.1	84.2	41.4
		19:00-07:00	484.8	0.9	412.1	84.2	41.4
	Day 4	07:00-19:00	484.8	0.9	412.1	84.2	41.4
		19:00-07:00	484.8	0.9	412.1	84.2	41.4
	Day 5	07:00-19:00	484.8	0.9	412.1	84.2	41.4
		19:00-07:00	484.8	0.9	412.1	84.2	41.4
	Day 6	07:00-19:00	484.8	0.9	412.1	84.2	41.4
		19:00-07:00	484.8	0.9	412.1	84.2	41.4
	Day 7	07:00-19:00	484.8	0.9	412.1	84.2	41.4
		19:00-07:00	484.8	0.9	412.1	84.2	41.4
	Day 8	07:00-19:00	484.8	0.9	412.1	84.2	41.4
		19:00-07:00	484.8	0.9	412.1	84.2	41.4
	Day 9	07:00-19:00	484.8	0.9	412.1	84.2	41.4
		19:00-07:00	484.8	0.9	412.1	84.2	41.4
	Day 10	07:00-19:00	484.8	0.9	412.1	84.2	41.4
		19:00-07:00	484.8	0.9	412.1	84.2	41.4
	Day 11	07:00-19:00	484.8	0.9	412.1	84.2	41.4
		19:00-07:00	484.8	0.9	412.1	84.2	41.4
	Day 12	07:00-19:00	484.8	0.9	412.1	84.2	41.4
		19:00-07:00	484.8	0.9	412.1	84.2	41.4
	Day 13	07:00-19:00	484.8	0.9	412.1	84.2	41.4
		19:00-07:00	484.8	0.9	412.1	84.2	41.4
	Day 14	07:00-19:00	484.8	0.9	412.1	84.2	41.4
		19:00-07:00	484.8	0.9	412.1	84.2	41.4

	Day 15	07:00-19:00	484.8	0.9	412.1	84.2	41.4
		19:00-07:00	484.8	0.9	412.1	84.2	41.4
	Day 16	07:00-19:00	484.8	0.9	412.1	84.2	41.4
		19:00-07:00	484.8	0.9	412.1	84.2	41.4
	Day 17	07:00-19:00	484.8	0.9	412.1	84.2	41.4
		19:00-07:00	484.8	0.9	412.1	84.2	41.4
	Day 18	07:00-19:00	484.8	0.9	412.1	84.2	41.4
		19:00-07:00	484.8	0.9	412.1	84.2	41.4
	Day 19	07:00-19:00	484.8	0.9	412.1	84.2	41.4
		19:00-07:00	484.8	0.9	412.1	84.2	41.4
	Day 20	07:00-19:00	484.8	0.9	412.1	84.2	41.4
		19:00-07:00	484.8	0.9	412.1	84.2	41.4
	Day 21	07:00-19:00	484.8	0.9	412.1	84.2	41.4
		19:00-07:00	484.8	0.9	412.1	84.2	41.4
	Day 22	07:00-19:00	484.8	0.9	412.1	84.2	41.4
		19:00-07:00	484.8	0.9	412.1	84.2	41.4
	Day 23	07:00-19:00	484.8	0.9	412.1	84.2	41.4
		19:00-07:00	484.8	0.9	412.1	84.2	41.4
	Day 24	07:00-19:00	484.8	0.9	412.1	84.2	41.4
		19:00-07:00	484.8	0.9	412.1	84.2	41.4
	Day 25	07:00-19:00	484.8	0.9	412.1	84.2	41.4
		19:00-07:00	484.8	0.9	412.1	84.2	41.4
	Day 26	07:00-19:00	484.8	0.9	412.1	84.2	41.4
		19:00-07:00	484.8	0.9	412.1	84.2	41.4
	Day 27	07:00-19:00	484.8	0.9	412.1	84.2	41.4

		19:00-07:00	484.8	0.9	412.1	84.2	41.4
	Day 28	07:00-19:00	484.8	0.9	412.1	84.2	41.4
		19:00-07:00	484.8	0.9	412.1	84.2	41.4
	Day 29	07:00-19:00	484.8	0.9	412.1	84.2	41.4
		19:00-07:00	484.8	0.9	412.1	84.2	41.4
	Day 30	07:00-19:00	484.8	0.9	412.1	84.2	41.4
		19:00-07:00	484.8	0.9	412.1	84.2	41.4
	Day 31	07:00-19:00	484.8	0.9	412.1	84.2	41.4
		19:00-07:00	484.8	0.9	412.1	84.2	41.4
November	Day 32	07:00-19:00	484.8	0.9	412.1	84.2	41.4
		19:00-07:00	484.8	0.9	412.1	84.2	41.4
	Day 33	07:00-19:00	484.8	0.9	412.1	84.2	41.4
		19:00-07:00	484.8	0.9	412.1	84.2	41.4
	Day 34	07:00-19:00	484.8	0.9	412.1	84.2	41.4
		19:00-07:00	484.8	0.9	412.1	84.2	41.4
	Day 35	07:00-19:00	484.8	0.9	412.1	84.2	41.4
		19:00-07:00	484.8	0.9	412.1	84.2	41.4
	Day 36	07:00-19:00	484.8	0.9	412.1	84.2	41.4
		19:00-07:00	484.8	0.9	412.1	84.2	41.4
	Day 37	07:00-19:00	484.8	0.9	412.1	84.2	41.4
		19:00-07:00	484.8	0.9	412.1	84.2	41.4
	Day 38	07:00-19:00	484.8	0.9	412.1	84.2	41.4
		19:00-07:00	484.8	0.9	412.1	84.2	41.4
	Day 39	07:00-19:00	484.8	0.9	412.1	84.2	41.4
		19:00-07:00	484.8	0.9	412.1	84.2	41.4

	Day 40	07:00-19:00	484.8	0.9	412.1	84.2	41.4
		19:00-07:00	484.8	0.9	412.1	84.2	41.4
	Day 41	07:00-19:00	484.8	0.9	412.1	84.2	41.4
		19:00-07:00	484.8	0.9	412.1	84.2	41.4
	Day 42	07:00-19:00	484.8	0.9	412.1	84.2	41.4
		19:00-07:00	484.8	0.9	412.1	84.2	41.4
	Day 43	07:00-19:00	484.8	0.9	412.1	84.2	41.4
		19:00-07:00	484.8	0.9	412.1	84.2	41.4
	Day 44	07:00-19:00	484.8	0.9	412.1	84.2	41.4
		19:00-07:00	484.8	0.9	412.1	84.2	41.4
	Day 45	07:00-19:00	484.8	0.9	412.1	84.2	41.4
		19:00-07:00	484.8	0.9	412.1	84.2	41.4
	Day 46	07:00-19:00	484.8	0.9	412.1	84.2	41.4
		19:00-07:00	484.8	0.9	412.1	84.2	41.4
	Day 47	07:00-19:00	484.8	0.9	412.1	84.2	41.4
		19:00-07:00	484.8	0.9	412.1	84.2	41.4
	Day 48	07:00-19:00	484.8	0.9	412.1	84.2	41.4
		19:00-07:00	484.8	0.9	412.1	84.2	41.4
	Day 49	07:00-19:00	484.8	0.9	412.1	84.2	41.4
		19:00-07:00	484.8	0.9	412.1	84.2	41.4
	Day 50	07:00-19:00	484.8	0.9	412.1	84.2	41.4
		19:00-07:00	484.8	0.9	412.1	84.2	41.4
	Day 51	07:00-19:00	484.8	0.9	412.1	84.2	41.4
		19:00-07:00	484.8	0.9	412.1	84.2	41.4
	Day 52	07:00-19:00	484.8	0.9	412.1	84.2	41.4

		19:00-07:00	484.8	0.9	412.1	84.2	41.4
	Day 53	07:00-19:00	484.8	0.9	412.1	84.2	41.4
		19:00-07:00	484.8	0.9	412.1	84.2	41.4
	Day 54	07:00-19:00	484.8	0.9	412.1	84.2	41.4
		19:00-07:00	484.8	0.9	412.1	84.2	41.4
	Day 55	07:00-19:00	484.8	0.9	412.1	84.2	41.4
		19:00-07:00	484.8	0.9	412.1	84.2	41.4
	Day 56	07:00-19:00	484.8	0.9	412.1	84.2	41.4
		19:00-07:00	484.8	0.9	412.1	84.2	41.4
	Day 57	07:00-19:00	484.8	0.9	412.1	84.2	41.4
		19:00-07:00	484.8	0.9	412.1	84.2	41.4
	Day 58	07:00-19:00	484.8	0.9	412.1	84.2	41.4
		19:00-07:00	484.8	0.9	412.1	84.2	41.4
	Day 59	07:00-19:00	484.8	0.9	412.1	84.2	41.4
		19:00-07:00	484.8	0.9	412.1	84.2	41.4
	Day 60	07:00-19:00	484.8	0.9	412.1	84.2	41.4
		19:00-07:00	484.8	0.9	412.1	84.2	41.4
	Day 61	07:00-19:00	484.8	0.9	412.1	84.2	41.4
		19:00-07:00	484.8	0.9	412.1	84.2	41.4
December	Day 62	07:00-19:00	484.8	0.9	412.1	84.2	41.4
		19:00-07:00	484.8	0.9	412.1	84.2	41.4
	Day 63	07:00-19:00	484.8	0.9	412.1	84.2	41.4
		19:00-07:00	484.8	0.9	412.1	84.2	41.4
	Day 64	07:00-19:00	484.8	0.9	412.1	84.2	41.4
		19:00-07:00	484.8	0.9	412.1	84.2	41.4

	Day 65	07:00-19:00	484.8	0.9	412.1	84.2	41.4
		19:00-07:00	484.8	0.9	412.1	84.2	41.4
	Day 66	07:00-19:00	484.8	0.9	412.1	84.2	41.4
		19:00-07:00	484.8	0.9	412.1	84.2	41.4
	Day 67	07:00-19:00	484.8	0.9	412.1	84.2	41.4
		19:00-07:00	484.8	0.9	412.1	84.2	41.4
	Day 68	07:00-19:00	484.8	0.9	412.1	84.2	41.4
		19:00-07:00	484.8	0.9	412.1	84.2	41.4
	Day 69	07:00-19:00	484.8	0.9	412.1	84.2	41.4
		19:00-07:00	484.8	0.9	412.1	84.2	41.4
	Day 70	07:00-19:00	484.8	0.9	412.1	84.2	41.4
		19:00-07:00	484.8	0.9	412.1	84.2	41.4
	Day 71	07:00-19:00	484.8	0.9	412.1	84.2	41.4
		19:00-07:00	484.8	0.9	412.1	84.2	41.4
	Day 72	07:00-19:00	484.8	0.9	412.1	84.2	41.4
		19:00-07:00	484.8	0.9	412.1	84.2	41.4
	Day 73	07:00-19:00	484.8	0.9	412.1	84.2	41.4
		19:00-07:00	484.8	0.9	412.1	84.2	41.4
	Day 74	07:00-19:00	484.8	0.9	412.1	84.2	41.4
		19:00-07:00	484.8	0.9	412.1	84.2	41.4
	Day 75	07:00-19:00	484.8	0.9	412.1	84.2	41.4
		19:00-07:00	484.8	0.9	412.1	84.2	41.4
	Day 76	07:00-19:00	484.8	0.9	412.1	84.2	41.4
		19:00-07:00	484.8	0.9	412.1	84.2	41.4
	Day 77	07:00-19:00	484.8	0.9	412.1	84.2	41.4

		19:00-07:00	484.8	0.9	412.1	84.2	41.4
	Day 78	07:00-19:00	484.8	0.9	412.1	84.2	41.4
		19:00-07:00	484.8	0.9	412.1	84.2	41.4
	Day 79	07:00-19:00	484.8	0.9	412.1	84.2	41.4
		19:00-07:00	484.8	0.9	412.1	84.2	41.4
	Day 80	07:00-19:00	484.8	0.9	412.1	84.2	41.4
		19:00-07:00	484.8	0.9	412.1	84.2	41.4
	Day 81	07:00-19:00	484.8	0.9	412.1	84.2	41.4
		19:00-07:00	484.8	0.9	412.1	84.2	41.4
	Day 82	07:00-19:00	484.8	0.9	412.1	84.2	41.4
		19:00-07:00	484.8	0.9	412.1	84.2	41.4
	Day 83	07:00-19:00	484.8	0.9	412.1	84.2	41.4
		19:00-07:00	484.8	0.9	412.1	84.2	41.4
	Day 84	07:00-19:00	484.8	0.9	412.1	84.2	41.4
		19:00-07:00	484.8	0.9	412.1	84.2	41.4
	Day 85	07:00-19:00	484.8	0.9	412.1	84.2	41.4
		19:00-07:00	484.8	0.9	412.1	84.2	41.4
	Day 86	07:00-19:00	484.8	0.9	412.1	84.2	41.4
		19:00-07:00	484.8	0.9	412.1	84.2	41.4
	Day 87	07:00-19:00	484.8	0.9	412.1	84.2	41.4
		19:00-07:00	484.8	0.9	412.1	84.2	41.4
	Day 88	07:00-19:00	484.8	0.9	412.1	84.2	41.4
		19:00-07:00	484.8	0.9	412.1	84.2	41.4
	Day 89	07:00-19:00	484.8	0.9	412.1	84.2	41.4
		19:00-07:00	484.8	0.9	412.1	84.2	41.4

	Day 90	07:00-19:00	484.8	0.9	412.1	84.2	41.4
		19:00-07:00	484.8	0.9	412.1	84.2	41.4
	Day 91	07:00-19:00	484.8	0.9	412.1	84.2	41.4
		19:00-07:00	484.8	0.9	412.1	84.2	41.4
	Day 92	07:00-19:00	484.8	0.9	412.1	84.2	41.4
		19:00-07:00	484.8	0.9	412.1	84.2	41.4
January	Day 93	07:00-19:00	484.8	0.9	412.1	84.2	41.4
		19:00-07:00	484.8	0.9	412.1	84.2	41.4
	Day 94	07:00-19:00	484.8	0.9	412.1	84.2	41.4
		19:00-07:00	484.8	0.9	412.1	84.2	41.4
	Day 95	07:00-19:00	484.8	0.9	412.1	84.2	41.4
		19:00-07:00	484.8	0.9	412.1	84.2	41.4
	Day 96	07:00-19:00	484.8	0.9	412.1	84.2	41.4
		19:00-07:00	484.8	0.9	412.1	84.2	41.4
	Day 97	07:00-19:00	484.8	0.9	412.1	84.2	41.4
		19:00-07:00	484.8	0.9	412.1	84.2	41.4
	Day 98	07:00-19:00	484.8	0.9	412.1	84.2	41.4
		19:00-07:00	484.8	0.9	412.1	84.2	41.4
	Day 99	07:00-19:00	484.8	0.9	412.1	84.2	41.4
		19:00-07:00	484.8	0.9	412.1	84.2	41.4
	Day 100	07:00-19:00	484.8	0.9	412.1	84.2	41.4
		19:00-07:00	484.8	0.9	412.1	84.2	41.4
	Day 101	07:00-19:00	484.8	0.9	412.1	84.2	41.4
		19:00-07:00	484.8	0.9	412.1	84.2	41.4
	Day 102	07:00-19:00	484.8	0.9	412.1	84.2	41.4

		19:00-07:00	484.8	0.9	412.1	84.2	41.4
	Day 103	07:00-19:00	484.8	0.9	412.1	84.2	41.4
		19:00-07:00	484.8	0.9	412.1	84.2	41.4
	Day 104	07:00-19:00	484.8	0.9	412.1	84.2	41.4
		19:00-07:00	484.8	0.9	412.1	84.2	41.4
	Day 105	07:00-19:00	484.8	0.9	412.1	84.2	41.4
		19:00-07:00	484.8	0.9	412.1	84.2	41.4
	Day 106	07:00-19:00	484.8	0.9	412.1	84.2	41.4
		19:00-07:00	484.8	0.9	412.1	84.2	41.4
	Day 107	07:00-19:00	484.8	0.9	412.1	84.2	41.4
		19:00-07:00	484.8	0.9	412.1	84.2	41.4
	Day 108	07:00-19:00	484.8	0.9	412.1	84.2	41.4
		19:00-07:00	484.8	0.9	412.1	84.2	41.4
	Day 109	07:00-19:00	484.8	0.9	412.1	84.2	41.4
		19:00-07:00	484.8	0.9	412.1	84.2	41.4
	Day 110	07:00-19:00	484.8	0.9	412.1	84.2	41.4
		19:00-07:00	484.8	0.9	412.1	84.2	41.4
	Day 111	07:00-19:00	484.8	0.9	412.1	84.2	41.4
		19:00-07:00	484.8	0.9	412.1	84.2	41.4
	Day 112	07:00-19:00	484.8	0.9	412.1	84.2	41.4
		19:00-07:00	484.8	0.9	412.1	84.2	41.4
	Day 113	07:00-19:00	484.8	0.9	412.1	84.2	41.4
		19:00-07:00	484.8	0.9	412.1	84.2	41.4
	Day 114	07:00-19:00	484.8	0.9	412.1	84.2	41.4
		19:00-07:00	484.8	0.9	412.1	84.2	41.4

	Day 115	07:00-19:00	484.8	0.9	412.1	84.2	41.4
		19:00-07:00	484.8	0.9	412.1	84.2	41.4
	Day 116	07:00-19:00	484.8	0.9	412.1	84.2	41.4
		19:00-07:00	484.8	0.9	412.1	84.2	41.4
	Day 117	07:00-19:00	484.8	0.9	412.1	84.2	41.4
		19:00-07:00	484.8	0.9	412.1	84.2	41.4
	Day 118	07:00-19:00	484.8	0.9	412.1	84.2	41.4
		19:00-07:00	484.8	0.9	412.1	84.2	41.4
	Day 119	07:00-19:00	484.8	0.9	412.1	84.2	41.4
		19:00-07:00	484.8	0.9	412.1	84.2	41.4
	Day 120	07:00-19:00	484.8	0.9	412.1	84.2	41.4
		19:00-07:00	484.8	0.9	412.1	84.2	41.4
	Day 121	07:00-19:00	484.8	0.9	412.1	84.2	41.4
		19:00-07:00	484.8	0.9	412.1	84.2	41.4
	Day 122	07:00-19:00	484.8	0.9	412.1	84.2	41.4
		19:00-07:00	484.8	0.9	412.1	84.2	41.4
	Day 123	07:00-19:00	484.8	0.9	412.1	84.2	41.4
		19:00-07:00	484.8	0.9	412.1	84.2	41.4
February	Day 124	07:00-19:00	484.8	0.9	412.1	84.2	41.4
		19:00-07:00	484.8	0.9	412.1	84.2	41.4
	Day 125	07:00-19:00	484.8	0.9	412.1	84.2	41.4
		19:00-07:00	484.8	0.9	412.1	84.2	41.4
	Day 126	07:00-19:00	484.8	0.9	412.1	84.2	41.4
		19:00-07:00	484.8	0.9	412.1	84.2	41.4
	Day 127	07:00-19:00	484.8	0.9	412.1	84.2	41.4

		19:00-07:00	484.8	0.9	412.1	84.2	41.4
	Day 128	07:00-19:00	484.8	0.9	412.1	84.2	41.4
		19:00-07:00	484.8	0.9	412.1	84.2	41.4
	Day 129	07:00-19:00	484.8	0.9	412.1	84.2	41.4
		19:00-07:00	484.8	0.9	412.1	84.2	41.4
	Day 130	07:00-19:00	484.8	0.9	412.1	84.2	41.4
		19:00-07:00	484.8	0.9	412.1	84.2	41.4
	Day 131	07:00-19:00	484.8	0.9	412.1	84.2	41.4
		19:00-07:00	484.8	0.9	412.1	84.2	41.4
	Day 132	07:00-19:00	484.8	0.9	412.1	84.2	41.4
		19:00-07:00	484.8	0.9	412.1	84.2	41.4
	Day 133	07:00-19:00	484.8	0.9	412.1	84.2	41.4
		19:00-07:00	484.8	0.9	412.1	84.2	41.4
	Day 134	07:00-19:00	484.8	0.9	412.1	84.2	41.4
		19:00-07:00	484.8	0.9	412.1	84.2	41.4
	Day 135	07:00-19:00	484.8	0.9	412.1	84.2	41.4
		19:00-07:00	484.8	0.9	412.1	84.2	41.4
	Day 136	07:00-19:00	484.8	0.9	412.1	84.2	41.4
		19:00-07:00	484.8	0.9	412.1	84.2	41.4
	Day 137	07:00-19:00	484.8	0.9	412.1	84.2	41.4
		19:00-07:00	484.8	0.9	412.1	84.2	41.4
	Day 138	07:00-19:00	484.8	0.9	412.1	84.2	41.4
		19:00-07:00	484.8	0.9	412.1	84.2	41.4
	Day 139	07:00-19:00	484.8	0.9	412.1	84.2	41.4
		19:00-07:00	484.8	0.9	412.1	84.2	41.4

	Day 140	07:00-19:00	484.8	0.9	412.1	84.2	41.4
		19:00-07:00	484.8	0.9	412.1	84.2	41.4
	Day 141	07:00-19:00	484.8	0.9	412.1	84.2	41.4
		19:00-07:00	484.8	0.9	412.1	84.2	41.4
	Day 142	07:00-19:00	484.8	0.9	412.1	84.2	41.4
		19:00-07:00	484.8	0.9	412.1	84.2	41.4
	Day 143	07:00-19:00	484.8	0.9	412.1	84.2	41.4
		19:00-07:00	484.8	0.9	412.1	84.2	41.4
	Day 144	07:00-19:00	484.8	0.9	412.1	84.2	41.4
		19:00-07:00	484.8	0.9	412.1	84.2	41.4
	Day 145	07:00-19:00	484.8	0.9	412.1	84.2	41.4
		19:00-07:00	484.8	0.9	412.1	84.2	41.4
	Day 146	07:00-19:00	484.8	0.9	412.1	84.2	41.4
		19:00-07:00	484.8	0.9	412.1	84.2	41.4
	Day 147	07:00-19:00	484.8	0.9	412.1	84.2	41.4
		19:00-07:00	484.8	0.9	412.1	84.2	41.4
	Day 148	07:00-19:00	484.8	0.9	412.1	84.2	41.4
		19:00-07:00	484.8	0.9	412.1	84.2	41.4
	Day 149	07:00-19:00	484.8	0.9	412.1	84.2	41.4
		19:00-07:00	484.8	0.9	412.1	84.2	41.4
	Day 150	07:00-19:00	484.8	0.9	412.1	84.2	41.4
		19:00-07:00	484.8	0.9	412.1	84.2	41.4
	Day 151	07:00-19:00	484.8	0.9	412.1	84.2	41.4
		19:00-07:00	484.8	0.9	412.1	84.2	41.4
March	Day 152	07:00-19:00	484.8	0.9	412.1	84.2	41.4

		19:00-07:00	484.8	0.9	412.1	84.2	41.4
	Day 153	07:00-19:00	484.8	0.9	412.1	84.2	41.4
		19:00-07:00	484.8	0.9	412.1	84.2	41.4
	Day 154	07:00-19:00	484.8	0.9	412.1	84.2	41.4
		19:00-07:00	484.8	0.9	412.1	84.2	41.4
	Day 155	07:00-19:00	484.8	0.9	412.1	84.2	41.4
		19:00-07:00	484.8	0.9	412.1	84.2	41.4
	Day 156	07:00-19:00	484.8	0.9	412.1	84.2	41.4
		19:00-07:00	484.8	0.9	412.1	84.2	41.4
	Day 157	07:00-19:00	484.8	0.9	412.1	84.2	41.4
		19:00-07:00	484.8	0.9	412.1	84.2	41.4
	Day 158	07:00-19:00	484.8	0.9	412.1	84.2	41.4
		19:00-07:00	484.8	0.9	412.1	84.2	41.4
	Day 159	07:00-19:00	484.8	0.9	412.1	84.2	41.4
		19:00-07:00	484.8	0.9	412.1	84.2	41.4
	Day 160	07:00-19:00	484.8	0.9	412.1	84.2	41.4
		19:00-07:00	484.8	0.9	412.1	84.2	41.4
	Day 161	07:00-19:00	484.8	0.9	412.1	84.2	41.4
		19:00-07:00	484.8	0.9	412.1	84.2	41.4
	Day 162	07:00-19:00	484.8	0.9	412.1	84.2	41.4
		19:00-07:00	484.8	0.9	412.1	84.2	41.4
	Day 163	07:00-19:00	484.8	0.9	412.1	84.2	41.4
		19:00-07:00	484.8	0.9	412.1	84.2	41.4
	Day 164	07:00-19:00	484.8	0.9	412.1	84.2	41.4
		19:00-07:00	484.8	0.9	412.1	84.2	41.4

	Day 165	07:00-19:00	484.8	0.9	412.1	84.2	41.4
		19:00-07:00	484.8	0.9	412.1	84.2	41.4
	Day 166	07:00-19:00	484.8	0.9	412.1	84.2	41.4
		19:00-07:00	484.8	0.9	412.1	84.2	41.4
	Day 167	07:00-19:00	484.8	0.9	412.1	84.2	41.4
		19:00-07:00	484.8	0.9	412.1	84.2	41.4
	Day 168	07:00-19:00	484.8	0.9	412.1	84.2	41.4
		19:00-07:00	484.8	0.9	412.1	84.2	41.4
	Day 169	07:00-19:00	484.8	0.9	412.1	84.2	41.4
		19:00-07:00	484.8	0.9	412.1	84.2	41.4
	Day 170	07:00-19:00	484.8	0.9	412.1	84.2	41.4
		19:00-07:00	484.8	0.9	412.1	84.2	41.4
	Day 171	07:00-19:00	484.8	0.9	412.1	84.2	41.4
		19:00-07:00	484.8	0.9	412.1	84.2	41.4
	Day 172	07:00-19:00	484.8	0.9	412.1	84.2	41.4
		19:00-07:00	484.8	0.9	412.1	84.2	41.4
	Day 173	07:00-19:00	484.8	0.9	412.1	84.2	41.4
		19:00-07:00	484.8	0.9	412.1	84.2	41.4
	Day 174	07:00-19:00	484.8	0.9	412.1	84.2	41.4
		19:00-07:00	484.8	0.9	412.1	84.2	41.4
	Day 175	07:00-19:00	484.8	0.9	412.1	84.2	41.4
		19:00-07:00	484.8	0.9	412.1	84.2	41.4
	Day 176	07:00-19:00	484.8	0.9	412.1	84.2	41.4
		19:00-07:00	484.8	0.9	412.1	84.2	41.4
	Day 177	07:00-19:00	484.8	0.9	412.1	84.2	41.4

		19:00-07:00	484.8	0.9	412.1	84.2	41.4
	Day 178	07:00-19:00	484.8	0.9	412.1	84.2	41.4
		19:00-07:00	484.8	0.9	412.1	84.2	41.4
	Day 179	07:00-19:00	484.8	0.9	412.1	84.2	41.4
		19:00-07:00	484.8	0.9	412.1	84.2	41.4
	Day 180	07:00-19:00	484.8	0.9	412.1	84.2	41.4
		19:00-07:00	484.8	0.9	412.1	84.2	41.4
	Day 181	07:00-19:00	484.8	0.9	412.1	84.2	41.4
		19:00-07:00	484.8	0.9	412.1	84.2	41.4

Appendix C

```
model=createpde(1);
C1=[1     0    0    40];
C2=[1    -24.3    -3.4    0.075];
C3=[1     -11.4     -8.1     0.075];
C4=[1    3.5    5.2    0.075];
C5=[1    -17.1    4.1    0.075];
C6=[1    -6.6    3.8    0.075];
C7=[1    -6.6    11.8    0.075];
C8=[1    7.5    1.7    0.075];
C9=[1    16.7    1.7    0.075];
C10=[1    23.9    10.5    0.075];
C11=[1    23.9    19.3    0.075];
C12=[1    26.5    1.7    0.075];
C13=[1    33.4    7.9    0.075];
C14=[1    -24.3    -3.4    0.0326];
C15=[1     -11.4     -8.1     0.0326];
C16=[1    3.5    5.2    0.0326];
C17=[1    -17.1    4.1    0.0326];
C18=[1    -6.6    3.8    0.0326];
C19=[1    -6.6    11.8    0.0326];
C20=[1    7.5    1.7    0.0326];
C21=[1    16.7    1.7    0.0326];
C22=[1    23.9    10.5    0.0326];
C23=[1    23.9    19.3    0.0326];
C24=[1    26.5    1.7    0.0326];
C25=[1    33.4    7.9    0.0326];

C2=[C2;zeros(length(C1) - length(C2),1)];
C3=[C3;zeros(length(C1) - length(C3),1)];
C4=[C4;zeros(length(C1) - length(C4),1)];
C5=[C5;zeros(length(C1) - length(C5),1)];
C6=[C6;zeros(length(C1) - length(C6),1)];
C7=[C7;zeros(length(C1) - length(C7),1)];
C8=[C8;zeros(length(C1) - length(C8),1)];
C9=[C9;zeros(length(C1) - length(C9),1)];
C10=[C10;zeros(length(C1) - length(C10),1)];
C11=[C11;zeros(length(C1) - length(C11),1)];
C12=[C12;zeros(length(C1) - length(C12),1)];
C13=[C13;zeros(length(C1) - length(C13),1)];

C14=[C14;zeros(length(C1) - length(C14),1)];
C15=[C15;zeros(length(C1) - length(C15),1)];
C16=[C16;zeros(length(C1) - length(C16),1)];
C17=[C17;zeros(length(C1) - length(C17),1)];
C18=[C18;zeros(length(C1) - length(C18),1)];
C19=[C19;zeros(length(C1) - length(C19),1)];
C20=[C20;zeros(length(C1) - length(C20),1)];
C21=[C21;zeros(length(C1) - length(C21),1)];
C22=[C22;zeros(length(C1) - length(C22),1)];
C23=[C23;zeros(length(C1) - length(C23),1)];
C24=[C24;zeros(length(C1) - length(C24),1)];
C25=[C25;zeros(length(C1) - length(C25),1)];
```

```
gd=[C1,C2,C3,C4,C5,C6,C7,C8,C9,C10,C11,C12,C13,C14,C15,C16,C17,C18,C19,C20,C21,C22,C23,C2
4,C25];
ns=char('C1','C2','C3','C4','C5','C6','C7','C8','C9','C10','C11','C12','C13','C14','C15','C16','C17','C18','C19','
C20','C21','C22','C23','C24','C25');
ns=ns';

% Set formula
sf='C1-C2-C3-C4-C5-C6-C7-C8-C9-C10-C11-C12-C13-C14-C15-C16-C17-C18-C19-C20-C21-C22-
C23-C24-
C25+(C1*C2)+(C1*C3)+(C1*C4)+(C1*C5)+(C1*C6)+(C1*C7)+(C1*C8)+(C1*C9)+(C1*C10)+(C1*C1
1)+(C1*C12)+(C1*C13)+(C1*C14)+(C1*C15)+(C1*C16)+(C1*C17)+(C1*C18)+(C1*C19)+(C1*C20)+(
C1*C21)+(C1*C22)+(C1*C23)+(C1*C24)+(C1*C25)';
g=decsg(gd,sf,ns);
geometryFromEdges(model,g);
pdegplot(model,'EdgeLabels','on','SubdomainLabels','on')
xlim([-40 40]);
axis equal;

% Generate mesh
generateMesh(model,'Hgrad',1.999999999);   % Must have geometry From Edges
figure(1)
pdeplot(model)

% Mesh to [p,e,t} form
[p,e,t] = meshToPet(model.Mesh);
%                                           Ground        Fluid          Backfilling(Grout)
% Density (kg/m^3)                          dg=2770     df=1052       db=1550
% Heat capacity (j/(kg.K))                  hcg=829     hcf=3795      hcb=1000
% Thermal conductivity (W/(m.K))      ccg=2.61     ccf=0.5        ccb=2.1
dg=2770;    df=1052;    db=1550;     hcg=829;    hcf=3795;    hcb=1000;    ccg=2.88;    ccf=0.5;    ccb=2.1;

% PDE coefficient
% d is density and capacity
d=sprintf('(%f).*(%f)!(%f).*(%f)!(%f).*(%f)!(%f).*(%f)!(%f).*(%f)!(%f).*(%f)!(%f).*(%f)!(%f).*(%f)!(
%f).*(%f)!(%f).*(%f)!(%f).*(%f)!(%f).*(%f)!(%f).*(%f)!(%f).*(%f)!(%f).*(%f)!(%f).*(%f)!(%f).*(%f)!(
%f).*(%f)!(%f).*(%f)!(%f).*(%f)!(%f).*(%f)!(%f).*(%f)!(%f).*(%f)!(%f).*(%f)!(%f).*(%f)',dg,hcg,db,h
cb,db,hcb,db,hcb,db,hcb,db,hcb,db,hcb,db,hcb,df,hcf,db,hcb,df,hcf,db,hcb,db,hcb,df,hcf,db,hcb,db,hcb,df,
hcf,df,hcf,df,hcf,df,hcf,df,hcf,df,hcf,df,hcf,df,hcf,df,hcf);
a='0!0!0!0!0!0!0!0!0!0!0!0!0!0!0!0!0!0!0!0!0!0!0!0!0';

% c is thermal conductivity
c=sprintf('%f!%f!%f!%f!%f!%f!%f!%f!%f!%f!%f!%f!%f!%f!%f!%f!%f!%f!%f!%f!%f!%f!%f!%f!%f',cc
g,ccb,ccb,ccb,ccb,ccb,ccb,ccb,ccf,ccb,ccf,ccb,ccb,ccf,ccb,ccb,ccf,ccf,ccf,ccf,ccf,ccf,ccf,ccf,ccf);

% Apply initial boundary condition
applyBoundaryCondition(model,'Edge',1:4,'u',13);

% Initial ground temperature
U0=12.67;

% Timelist (tlist)
time{1}=[1,2592000];
% External temperature
ext=0;
% Convection heat coefficient
con=0;
```

Publications

W. Wei, H. Da, and B. Simon Le, "Borehole active recharge benefit quantification on a community level low carbon heating system," in *2016 IEEE Power and Energy Society General Meeting (PESGM)*, 2016, pp. 1-5.

W. Wei, H. Da and B. Simon Le, "Comparison between FE Model and Transfer Function for Short-term Borehole Charging Optimization," in *2017 IEEE Power and Energy Society General Meeting (PESGM)*, 2017, pp. 1-5.

W. Wei, C. Gu, D. Huo, S. LeBlond, and X. Yan, "Optimal Borehole Energy Storage Charging Strategy in a Low Carbon Space Heat System," *IEEE Access*, pp. 1-1, 2018.

D. Huo, W. Wei, and S. Le Blond, "Optimisation for interconnected energy hub system with combined ground source heat pump and borehole thermal storage," *Frontiers in Energy*, pp. 1-11, 2018.

D. Huo, S. Le Blond, C. Gu, W. Wei, and D. Yu, "Optimal operation of interconnected energy hubs by using decomposed hybrid particle swarm and interior-point approach," *International Journal of Electrical Power & Energy Systems*, vol. 95, pp. 36-46, 2018.

D. Huo, C. Gu, K. Ma, W. Wei, Y. Xiang, and S. Le Blond, "Chance-Constrained Optimization for Multi Energy Hub Systems in a Smart City," *IEEE Transactions on Industrial Electronics*, 2018.

References

[1] W. Wei, H. Da, and B. Simon Le, "Borehole active recharge benefit quantification on a community level low carbon heating system," in *2016 IEEE Power and Energy Society General Meeting (PESGM)*, 2016, pp. 1-5.

[2] H. Zhang, J. Baeyens, G. Cáceres, J. Degrève, and Y. Lv, "Thermal energy storage: Recent developments and practical aspects," *Progress in Energy and Combustion Science*, vol. 53, pp. 1-40, 2016/03/01/ 2016.

[3] M. Asif and T. Muneer, "Energy supply, its demand and security issues for developed and emerging economies," *Renewable and Sustainable Energy Reviews*, vol. 11, pp. 1388-1413, 2007.

[4] Department of Energy and Climate Change. (05/11). *Climate change and energy – guidance 2050 pathways*. Available: https://www.gov.uk/guidance/2050-pathways-analysis

[5] Department for Business, Energy and Industrial Strategy. (31 July 2013). *Domestic energy fact file and housing surveys*. Available: https://www.gov.uk/government/collections/domestic-energy-fact-file-and-housing-surveys

[6] R. Yao and K. Steemers, "A method of formulating energy load profile for domestic buildings in the UK," *Energy and Buildings*, vol. 37, pp. 663-671, 2005/06/01/ 2005.

[7] H. Meier and K. Rehdanz, "Determinants of residential space heating expenditures in Great Britain," *Energy Economics*, vol. 32, pp. 949-959, 2010/09/01/ 2010.

[8] T. Kanea, S. K. Firth, D. Allinson, K. N. Irvine, and K. J. Lomas. (05/2011). *Understanding occupant heating practices in UK dwellings*. Available: http://mmmm.lboro.ac.uk/doc/wrec%20paper%20-%20final%20submission.pdf

[9] S. Hong, T. Oreszczyn, and I. Ridley, "The impact of energy efficient refurbishment on the space heating fuel consumption in English dwellings," *Energy and Buildings*, vol. 38, pp. 1171-1181, 2006/10/01/ 2006.

[10] J. Lopes, N. Hatziargyriou, J. Mutale, P. Djapic, and N. Jenkins, "Integrating distributed generation into electric power systems: A review of drivers, challenges and opportunities," *Electric Power Systems Research*, vol. 77, pp. 1189-1203, Jul 2007.

[11] Department for Business, Energy and Industrial Strategy. (2016). *Combined Heat and Power Incentives*. Available: https://www.gov.uk/guidance/combined-heat-and-power-incentives

[12] Energy Networks Association Limited. (2017, 21/06/2017). *2050 Pathways for Domestic Heat*. Available: http://www.energynetworks.org/gas/futures/2050-pathways-for-domestic-heat.html

[13] Eunomia, ICAX, University of Bath, Department of Energy and Climate Change. (2015, 10/04). *Owen Square Community Energy project*. Available: http://www.cepro.co.uk/2015/04/choices-solar-district-heat-study/

[14] Ofgem. (2017, 20/06/2017). *Non-domestic Renewable Heat Incentive (RHI)*. Available: https://www.ofgem.gov.uk/environmental-programmes/non-domestic-rhi

[15] Ofgem. (20/06/2017). *Feed-In Tariff (FIT) rates*. Available: https://www.ofgem.gov.uk/environmental-programmes/fit/fit-tariff-rates

[16] M. Geidl and G. Andersson, "A modelling and optimization approach for multiple energy carrier power flow," pp. 1-7, 2005.

[17] M. Geidl, "Integrated Modeling and Optimization of Multi-Carrier Energy Systems," Doctor of Sciences, 2007.

[18] N. J. Kelly and J. Cockroft, "Analysis of retrofit air source heat pump performance Results from detailed simulations and comparison to field trial data," *Energy Build.*, vol. 43, pp. 239-245, 2011.

[19] T. Fawcett, "The future role of heat pumps in the domestic sector," *Proceedings of ECEEE 2011 Summer Study, Energy efficiency first: The Foundation of a Low-Carbon Society*, pp. 1547-1557, 2011.

[20] L. Cabrol and P. Rowley, "Towards low carbon homes - A simulation analysis of building-integrated air-source heat pump systems," *Energy Build.*, vol. 48, pp. 127-136, 2012.

[21] Y. Zhang, Y. Zhang, and P. Zhang, "Modeling and simulation of double-boreholes vertical U-shaped pipe heat transfer," in *Control Conference (CCC), 2013 32nd Chinese*, 2013, pp. 1978-1983.

[22] P. Bayer, M. de Paly, and M. Beck, "Strategic optimization of borehole heat exchanger field for seasonal geothermal heating and cooling," *Applied Energy*, vol. 136, pp. 445-453, 2014/12/31/ 2014.

[23] P. Bayer, D. Saner, S. Bolay, L. Rybach, and P. Blum, "Greenhouse gas emission savings of ground source heat pump systems in Europe: A review," *Renewable and Sustainable Energy Reviews,* vol. 16, pp. 1256-1267, 2012/02/01/ 2012.

[24] S. J. Self, B. V. Reddy, and M. A. Rosen, "Geothermal heat pump systems: Status review and comparison with other heating options," *Applied Energy,* vol. 101, pp. 341-348, 2013/01/01/ 2013.

[25] G. A. Florides, P. Christodoulides, and P. Pouloupatis, "An analysis of heat flow through a borehole heat exchanger validated model," *Applied Energy,* vol. 92, pp. 523-533, 2012/04/01/ 2012.

[26] B. Bouhacina, R. Saim, and H. F. Oztop, "Numerical investigation of a novel tube design for the geothermal borehole heat exchanger," *Applied Thermal Engineering,* vol. 79, pp. 153-162, 2015/03/25/ 2015.

[27] International Renewable Energy Agency. (2013). *Thermal Energy Storage Technology Brief.* Available: https://www.irena.org/DocumentDownloads/Publications/IRENA-ETSAP%20Tech%20Brief%20E17%20Thermal%20Energy%20Storage.pdf

[28] L. Gao, J. Zhao, and Z. Tang, "A Review on Borehole Seasonal Solar Thermal Energy Storage," *Energy Procedia,* vol. 70, pp. 209-218, 2015/05/01/ 2015.

[29] ICAX. (27/06/2017). *Seasonal Thermal Energy Storage using ThermalBanks*. Available: http://www.icax.co.uk/thermal_energy_storage.html

[30] R. Yumrutaş and M. Ünsal, "Analysis of solar aided heat pump systems with seasonal thermal energy storage in surface tanks," *Energy,* vol. 25, pp. 1231-1243, 2000/12/01/ 2000.

[31] N. Mendis, K. M. Muttaqi, S. Sayeef, and S. Perera, "Application of a hybrid energy storage in a remote area power supply system," *Energy Conference and Exhibition (EnergyCon), 2010 IEEE International,* pp. 576-581, 18-22 Dec. 2010 2010.

[32] D. Fernandes, F. Pitié, G. Cáceres, and J. Baeyens, "Thermal energy storage: "How previous findings determine current research priorities"," *Energy,* vol. 39, pp. 246-257, 2012/03/01/ 2012.

[33] Ibrahim Dincer, *Thermal Energy Storage: Systems and Applications, 2nd Edition*, 2010.

[34] K. S. Lee, "Borehole Thermal Energy Storage," pp. 95-123, 2013.

[35] M. Li and A. C. K. Lai, "Analytical model for short-time responses of ground heat exchangers with U-shaped tubes: Model development and validation," *Applied Energy,* vol. 104, pp. 510-516, 2013.

[36] M. Li and A. C. K. Lai, "New temperature response functions (G functions) for pile and borehole ground heat exchangers based on composite-medium line-source theory," *Energy,* vol. 38, pp. 255-263, 2012/02/01/ 2012.

[37] J. Claesson and S. Javed. (2011). *An analytical method to calculate borehole fluid temperatures for time-scales from minutes to decades*. Available: http://publications.lib.chalmers.se/records/fulltext/151315/local_151315.pdf

[38] M. Li and A. C. K. Lai, "Heat-source solutions to heat conduction in anisotropic media with application to pile and borehole ground heat exchangers," *Applied Energy,* vol. 96, pp. 451-458, 2012/08/01/ 2012.

[39] N. Diao, Q. Li, and Z. Fang, "Heat transfer in ground heat exchangers with groundwater advection," *International Journal of Thermal Sciences,* vol. 43, pp. 1203-1211, 2004/12/01/ 2004.

[40] N. Molina-Giraldo, P. Blum, K. Zhu, P. Bayer, and Z. Fang, "A moving finite line source model to simulate borehole heat exchangers with groundwater advection," *International Journal of Thermal Sciences,* vol. 50, pp. 2506-2513, 2011/12/01/ 2011.

[41] H. Zeng, N. Diao, and Z. Fang, "Heat transfer analysis of boreholes in vertical ground heat exchangers," *International Journal of Heat and Mass Transfer,* vol. 46, pp. 4467-4481, 2003/11/01/ 2003.

[42] A. Zarrella, M. Scarpa, and M. D. Carli, "Short time-step performances of coaxial and double U-tube borehole heat exchangers: Modeling and measurements," *HVAC&R Research,* vol. 17, pp. 959-976, 2011/12/01 2011.

[43] Y. Nam, R. Ooka, and S. Hwang, "Development of a numerical model to predict heat exchange rates for a ground-source heat pump system," *Energy and Buildings,* vol. 40, pp. 2133-2140, 2008/01/01/ 2008.

[44] H. Su, Q. Li, X. H. Li, Y. Zhang, Y. T. Kang, Z. H. Si, *et al.*, "Fast Simulation of a Vertical U-Tube Ground Heat Exchanger by Using a One-Dimensional Transient Numerical Model," *Numerical Heat Transfer, Part A: Applications,* vol. 60, pp. 328-346, 2011/08/15 2011.

[45] C. K. Lee, "Effects of multiple ground layers on thermal response test analysis and ground-source heat pump simulation," *Applied Energy,* vol. 88, pp. 4405-4410, 2011/12/01/ 2011.

[46] W. Yang, X. Liang, M. Shi, and Z. Chen, "A Numerical Model for the Simulation of a Vertical U-Bend Ground Heat Exchanger Used in a Ground-Coupled Heat Pump," *International Journal of Green Energy,* vol. 11, pp. 761-785, 2014/08/09 2014.

[47] R. A. Beier, M. D. Smith, and J. D. Spitler, "Reference data sets for vertical borehole ground heat exchanger models and thermal response test analysis," *Geothermics,* vol. 40, pp. 79-85, 2011/03/01/ 2011.

[48] J. Luo, J. Rohn, M. Bayer, A. Priess, and W. Xiang, "Analysis on performance of borehole heat exchanger in a layered subsurface," *Applied Energy,* vol. 123, pp. 55-65, 2014.

[49] R. Borinaga-Treviño, P. Pascual-Muñoz, D. Castro-Fresno, and E. Blanco-Fernandez, "Borehole thermal response and thermal resistance of four different grouting materials measured with a TRT," *Applied Thermal Engineering,* vol. 53, pp. 13-20, 2013/04/29/ 2013.

[50] M. Arnold, R. R. Negenborn, G. Andersson, and B. De Schutter, "Model-based predictive control applied to multi-carrier energy systems," ed, 2009, pp. 1-8.

[51] H. Diersch, D. Bauer, W. Heidemann, W. Rühaak, and P. Schätzl, "Finite element modelling of borehole heat exchanger systems," *Computers & Geosciences,* vol. 37, pp. 1122-1135, 2011/08/01/ 2011.

[52] M. Li, P. Li, V. Chan, and A. C. K. Lai, "Full-scale temperature response function (G-function) for heat transfer by borehole ground heat exchangers (GHEs) from sub-hour to decades," *Applied Energy,* vol. 136, pp. 197-205, 12/31/ 2014.

[53] Y. Yang and M. Li, "Short-time performance of composite-medium line-source model for predicting responses of ground heat exchangers with single U-shaped tube," *International Journal of Thermal Sciences,* vol. 82, pp. 130-137, 2014/08/01/ 2014.

[54] O. A. Ezekoye, "Conduction of Heat in Solids," in *SFPE Handbook of Fire Protection Engineering*, M. J. Hurley, D. T. Gottuk, J. R. Hall Jr, K. Harada, E. D. Kuligowski, M. Puchovsky, *et al.*, Eds., ed New York, NY: Springer New York, 2016, pp. 25-52.

[55] M. Philippe, M. Bernier, and D. Marchio, "Validity ranges of three analytical solutions to heat transfer in the vicinity of single boreholes," *Geothermics,* vol. 38, pp. 407-413, 2009/12/01/ 2009.

[56] D. Marcotte, P. Pasquier, F. Sheriff, and M. Bernier, "The importance of axial effects for borehole design of geothermal heat-pump systems," *Renewable Energy,* vol. 35, pp. 763-770, 2010/04/01/ 2010.

[57] A. D. Chiasson, S. Rees, J. D. Spitler" A preliminary assessment of the effects of groundwater flow on closed-loop ground-source heat pump systems," *ASHRAE Trans,* pp. 380-393, 2000.

[58] H. Wang, C. Qi, H. Du, and J. Gu, "Thermal performance of borehole heat exchanger under groundwater flow: A case study from Baoding," *Energy and Buildings,* vol. 41, pp. 1368-1373, 2009/12/01/ 2009.

[59] R. Fan, Y. Jiang, Y. Yao, D. Shiming, and Z. Ma, "A study on the performance of a geothermal heat exchanger under coupled heat conduction and groundwater advection," *Energy,* vol. 32, pp. 2199-2209, 2007/11/01/ 2007.

[60] J. Raymond, R. Therrien, L. Gosselin, and R. Lefebvre, "Numerical analysis of thermal response tests with a groundwater flow and heat transfer model," *Renewable Energy,* vol. 36, pp. 315-324, 2011/01/01/.

[61] P. Eskilson and J. Claesson, "Simulation model for thermally interacting heat extraction boreholes," *Numerical Heat Transfer,* vol. 13, pp. 149-165, 1988.

[62] R. R. Fekri. Al-Chalabi, "Thermal resistance of U-tube borehole heat exchanger system: numerical study," 2013.

[63] Y. Zhang, Y. Zhang, and P. Zhang, "Modeling and simulation of double-boreholes vertical U-shaped pipe heat transfer," ed, 2013, pp. 1978-1983.

[64] Y. Zhang, Y. Zhang, and P. Zhang, "Modeling and simulation of double-boreholes vertical U-shaped pipe heat transfer," in *Proceedings of the 32nd Chinese Control Conference*, 2013, pp. 1978-1983.

[65] S. L. Weihua Yang, Xiaosong Zhang, "Numerical Simulation on Heat Transfer Characteristics of Soil Around U-Tube Underground Heat Exchangers," presented at the International Refrigeration and Air Conditioning Conference, 2008.

[66] Z. Zheng, W. Wang, and C. Ji, "A Study on the Thermal Performance of Vertical U-Tube Ground Heat Exchangers," *Energy Procedia,* vol. 12, pp. 906-914, 2011/01/01 2011.

[67] P. Hein, O. Kolditz, U.-J. Görke, A. Bucher, and H. Shao, "A numerical study on the sustainability and efficiency of borehole heat exchanger coupled ground source heat pump systems," *Applied Thermal Engineering*, vol. 100, pp. 421-433, 2016/05/05/ 2016.

[68] I. Dincer and M. Rosen, *Thermal energy storage: systems and applications*: John Wiley & Sons, 2002.

[69] A. Argiriou, "CSHPSS systems in Greece: Test of simulation software and analysis of typical systems," *Solar Energy*, vol. 60, pp. 159-170, 1997.

[70] P. Pinel, C. A. Cruickshank, I. Beausoleil-Morrison, and A. Wills, "A review of available methods for seasonal storage of solar thermal energy in residential applications," *Renewable and Sustainable Energy Reviews*, vol. 15, pp. 3341-3359, 2011.

[71] D. Pahud, "Central solar heating plants with seasonal duct storage and short-term water storage: design guidelines obtained by dynamic system simulations," *Solar Energy*, vol. 69, pp. 495-509, 2000.

[72] B. Sibbitt, D. McClenahan, R. Djebbar, J. Thornton, B. Wong, J. Carriere, *et al.*, "The performance of a high solar fraction seasonal storage district heating system–five years of operation," *Energy Procedia*, vol. 30, pp. 856-865, 2012.

[73] C. A. Balaras, K. Droutsa, E. Dascalaki, and S. Kontoyiannidis, "Heating energy consumption and resulting environmental impact of European apartment buildings," *Energy and buildings*, vol. 37, pp. 429-442, 2005.

[74] R. S. Adhikari, M. Buzzetti, and S. Magelli, "Solar photovoltaic and thermal systems for electricity generation, space heating and domestic hot water in a residential building," in *2011 International Conference on Clean Electrical Power (ICCEP)*, 2011, pp. 461-465.

[75] H. Diersch, "FEFLOW reference manual," *Institute for Water Resources Planning and Systems Research Ltd*, vol. 278, 2002.

[76] R. Rink, "Optimal operation of solar heat storage with off-peak energy price incentive," *Optimal Control Applications and Methods*, vol. 15, pp. 251-266, 1994.

[77] R. Rink, V. Gourishankar, and M. Zaheeruddin, "Optimal control of heat-pump/heat-storage systems with time-of-day energy price incentive," *Journal of optimization theory and applications*, vol. 58, pp. 93-108, 1988.

[78] M. Zaheer-Uddin and P. Fazio, "A numerical model for optimal control of a heat-pump/heat-storage system," *Energy,* vol. 13, pp. 625-632, 1988.

[79] M. Zaheeruddin, V. Gourishankar, and R. Rink, "Dynamic suboptimal control of a heat pump/heat storage system," *Optimal Control Applications and Methods,* vol. 9, pp. 341-355, 1988.

[80] M. LeBreux, M. Lacroix, and G. Lachiver, "Fuzzy and feedforward control of a hybrid thermal energy storage system," *Energy and buildings,* vol. 38, pp. 1149-1155, 2006.

[81] F. De Ridder, M. Diehl, G. Mulder, J. Desmedt, and J. Van Bael, "An optimal control algorithm for borehole thermal energy storage systems," *Energy and Buildings,* vol. 43, pp. 2918-2925, 2011.

[82] J. Luo, H. Zhao, J. Jia, W. Xiang, J. Rohn, and P. Blum, "Study on operation management of borehole heat exchangers for a large-scale hybrid ground source heat pump system in China," *Energy,* vol. 123, pp. 340-352, 2017/03/15/ 2017.

[83] Istitution for Energy, Renewable Energy Unit, Joint Research Centre, Renewable Energy Unit. *Photovoltaic Geographical Information System (PVGIS)*. Available: http://re.jrc.ec.europa.eu/pvgis/

[84] British Gas. (2018). *Comparing your energy usage*. Available: http://www.britishgas.co.uk/help-and-advice/Online-account/Comparing-your-energy-usage/How-do-you-work-out-the-CO2-values.html

[85] *British Geological Survey*. Available: http://www.bgs.ac.uk/reference/gshp/gshp_report.html

[86] *G.B. National Grid Status*. Available: https://www.gridwatch.templar.co.uk/

[87] C. Gu, W. Yang, Y. Song, and F. Li, "Distribution Network Pricing for Uncertain Load Growth Using Fuzzy Set Theory," 2016.

[88] M. Kharseh, L. Altorkmany, and B. Nordell, "Global warming's impact on the performance of GSHP," *Renewable Energy,* vol. 36, pp. 1485-1491, 2011.

[89] U. Lucia, M. Simonetti, G. Chiesa, and G. Grisolia, "Ground-source pump system for heating and cooling: Review and thermodynamic approach," *Renewable and Sustainable Energy Reviews,* vol. 70, pp. 867-874, 2017/04/01/ 2017.